EARLY INTERCEPTION OF PANCREATIC DUCTAL ADENOCARCINOMA BY TARGETING THE DYNAMIC TME: MODULATION OF NOVEL MICRORNA TARGETS AND UTILIZATION OF COMBINATION IMMUNOTHERAPY

By
Nina J. Chu

A dissertation submitted to Johns Hopkins University in conformity with the requirements for the degree of Doctor of Philosophy

Baltimore, MD
March 2018

ABSTRACT

Pancreatic ductal adenocarcinoma (PDA), or pancreatic cancer, is currently the fourth leading cause of cancer deaths in the United States, and is projected to become the second leading cause surpassing those caused by breast, prostate, and colorectal cancers by the year 2030. Surgical resection is the only cure for the disease; however, only 20% of patients are eligible for surgical resection at the time of diagnosis. A hallmark of PDA that mediates its poor prognosis is the desmoplastic stroma, a major component of PDA's dynamic tumor microenvironment (TME) that renders PDA refractory to radiation and chemotherapies.

PDA tumorigenesis is initiated, propagated, and maintained by the expression of driver mutation *KRAS*, making mutant *KRAS* an ideal target for early stage disease intervention. In addition to targeting neoplastic cells that express mutant *KRAS*, we must also target the recruited stromal compartment that is essential to PDA's immunosuppressive, tumor-supportive TME. The fibro-inflammatory stromal matrix is comprised of cellular and acellular constituents that create a dense, non-permissive environment protecting the tumor from immune recognition and chemotherapeutic penetration. Therefore, combination therapies that target transformed cells and stromal components administered during early PDA development will be the most promising solution to this lethal disease.

Our studies aimed to investigate and ultimately modulate the epigenetic and immune mediated mechanisms that contribute to early PDA development in

order to intercept disease progression. By expression profiling premalignant lesions, we uncovered novel microRNAs (miRNAs) whose levels are upregulated as a result of mutant *KRAS* activation. We discovered that miR-21 and miR-224 propel epithelial cell transformation and stromal cell activation altering their functional phenotypes in the early PDA TME, and that by endogenously inhibiting these miRNAs certain WT phenotypes can be restored.

We also investigated whether administration of a mutant *KRAS*-targeting vaccine in combination with immunomodulatory agents and checkpoint blockade can alter specific inhibitory immune pathways in the early TME to impede premalignant progression. Our results demonstrated that our combination vaccine-based therapy significantly reprograms the immunosuppressive TME by reducing the population of pro-carcinogenic T regulatory cells and expression of checkpoint molecules, leading to increased effector T cell activation, cytotoxic function, and generation of memory populations. The reprogramming achieved by our combination therapy successfully delayed the progression of premalignant lesions in our endogenous mouse model of PDA. Taken altogether, these studies reveal that the early PDA TME can be targeted on multiple levels, epigenetically and immunologically, in combination to intercept early disease development.

Advisor:	Dr. Elizabeth M. Jaffee
Reader:	Dr. Robert Anders
Thesis Committee:	Dr. Elizabeth M. Jaffee
	Dr. Robert Anders
	Dr. Douglas Robinson
	Dr. Michael Goggins

ACKNOWLEDGEMENTS

Scientific advancement is a team effort, achieved by building on what is known and drawing from the expertise of your colleagues. My journey through graduate school is no different. I would like to dedicate this thesis to my amazing team, both in the lab and out, past and present that has supported me up until this point. None of the work documented here is result of individual effort, rather, it is an encapsulation of all those who have impacted my life both scientifically and personally.

First and foremost, I would like to thank my mentor Dr. Elizabeth Jaffee, from whom I have received so much encouragement, support, and guidance since day one. Thank you for your direction in navigating these projects as we delved into the unknown and especially for your reassurance when I experienced setbacks that things will be ok and work out in the end. I am so grateful for the scientific freedom you gave me to pursue and investigate the questions that I was passionate about.

I would also like to thank my committee members Dr. Robert Anders, Dr. Michael Goggins, and Dr. Douglas Robinson for their wealth of knowledge that was always at my fingertips. Thank you for your fresh eyes and diverse scientific insight that each of you brought to this project. Bob, thank you for your expertise in cancer pathology, without which this project would not have happened. Not once did you roll your eyes when I came to you with a giant stack of slides to grade. I thoroughly enjoyed learning from you.

Next I would like to thank my labmates and classmates who have persevered by my side through this long journey. I would like to thank all those in the Jaffee lab, but especially Heather Kinkead, Kim Yang, and Brian Christmas whose scientific conversations and friendships in and outside of the lab I couldn't have done without. Additionally, I would like to thank my pharmacology classmates Dominique Figueroa, Michael Noback, Alyssa Martin, Matthew Arwood, and Oliver Rogers for the years of friendships that persist until this day, especially Dom and Michael who I now consider family.

I would like to especially thank Richard who I met in Los Angeles before starting this crazy journey, and now six years later, is with me in Baltimore. I am so grateful for the continuous love and support that you have provided both far and now near. After many long, stressful days in lab, I look forward to coming home to you and I look forward to the years to come.

And finally, I would like to thank my family, who have been there for me since the beginning. Mom, dad, Julia, Yeh Yeh, and Ni Ni. None of this would be possible without your unconditional love, support, faith, patience, comfort, enthusiasm, and confidence. The list goes on and on, but most importantly your belief in me made me believe in myself, which was and always will be invaluable. I could not have done this without you; you guys are my foundation. And to Matthew, thank you for being my first best friend. Thank you team, this one's for you.

TABLE OF CONTENTS

LIST OF TABLES

CHAPTER ONE: Novel miRNA regulation in an early progression model of PDA

CHAPTER TWO: Combination immunotherapy intercepts murine pancreatic cancer progression

LIST OF FIGURES

CHAPTER ONE: Novel miRNA regulation in an early progression model of PDA

CHAPTER TWO: Combination immunotherapy intercepts murine pancreatic cancer progression

CHAPTER ONE: Novel miRNA regulation in an early progression model of PDA

SUMMARY

The success of current immunotherapies are dependent on infiltration and function of T cells within the tumor microenvironment (TME). However, for many cancers, inflammatory and stromal cells provide formidable barriers to T cell access. Emerging data suggests that the cellular barriers to T cell access and function are regulated by both genetic and epigenetic factors. Identification of these regulators should provide new targets for enhancing immunotherapy.

microRNAs (miRNAs) are short endogenous non-coding RNAs that are approximately 20 nucleotides in length that negatively regulate protein expression by inhibiting translation and/or by targeting mRNAs for degradation. Dysregulation of miRNA expression is important to the development of many cancers and although numerous studies have described the molecular alterations that are involved in PDA development and progression, few studies have investigated the miRNA profile and associated inflammatory changes within the TME from the earliest pre-malignant pancreatic intraepithelial neoplasias (PanINs) to PDA.

The overall goal of this research is to construct a comprehensive profile of miRNA expression within the inflammatory and stromal cells that develop in the earliest PanIN lesions in the *Kras*$^{G12D/+}$*;Trp53*$^{R172H/+}$*;Pdx-1-Cre* (KPC) mouse model, an endogenous model that recapitulates human PDA tumorigenesis. Specifically, we aim to investigate the functional roles of key differentially

expressed miRNAs in establishing and propagating the earliest PanIN lesions within the TME via modulating the signaling between transformed ductal epithelial cells and the recruited cancer associated fibroblasts (CAFs) that comprise the majority of the cancer-supportive immunosuppressive desmoplastic stroma that characterizes PDA.

We conducted miRNA microarray analysis to determine the levels of 750 unique miRNAs in the pancreata of KPC mice ranging from 4 to 12 weeks of age (pre-PanIN1 to PDA). miRNA expression was quantified by Taqman miRNA OpenArrays and confirmed by qPCR analysis. Out of the 750 rodent miRNAs, 4 miRNAs (miR-21, miR-16, miR-19b, and miR-224) were significantly upregulated throughout PDA development. miR-21 and miR-224 are of particular interest for their regulation of targets in cancer promoting inflammatory pathways and epithelial-mesenchymal transition.

To investigate the roles that miR-21 and miR-224 play in the developing TME, primary KPC pancreatic ductal epithelial and fibroblast cell lines were established via fluorescence activated cell sorting (FACS) in order to perform *in vitro* miRNA knock-in and knock-out studies. qPCR of these primary cell lines show that miR-21 is significantly upregulated in KPC tumor cells and miR-224 is overexpressed in CAFs. miRNA fluorescence *in situ* hybridization (miR-FISH) was performed to examine the endogenous spatial expression of these two miRNAs throughout early TME progression. miR-FISH revealed that miR-21 is expressed at low levels in normal pancreata, but is highly expressed particularly in ductal epithelial cells of late stage KPC pancreata and PDA. Conversely, miR-

224 is expressed by the infiltrating stromal compartment surrounding advanced lesions. Stable lentiviral inhibition of miR-21 in KPC tumor cells reduced cell proliferation and migration, whereas overexpression of miR-224 in normal pancreatic fibroblasts increased their migratory capacity. Additional studies are underway to further determine the functional roles of these miRNAs in PDA development and progression. Such studies will elucidate potential miRNAs that can be targeted for novel PDA therapies or used as adjuvants for enhancing immunotherapy efficacy, while further revealing the molecular mechanisms of microenvironment regulation of PDA progression.

INTRODUCTION

PDA accounts for 90% of all pancreatic cancer types and is ranked fourth amongst all cancer-related deaths in the United States with an overall median survival of 4-6 months.[1] PanIN lesions grades 1-3 are the most common precursors to invasive PDA.[2] A hallmark of PDA is the presence of extensive desmoplastic reaction, or fibro-inflammatory stroma, that mediates its resistance to chemotherapies and results in poor prognosis.[3,4] This dense desmoplasia is a major component of a dynamic TME that is composed of not only tumor epithelial cells, but also recruited fibroblasts, pancreatic stellate cells, inflammatory/immune cells, and extracellular matrix (ECM) proteins, that all serve to drive disease progression from early stage PanINs to PDA.[5] The majority of the tumor volume is not composed of neoplastic cells, rather it predominantly consists of local dense desmoplastic reaction that involves proximal vital structures, which limits the complete excision of these tumors and precludes 85% of patients as candidates for surgical resection.[6]

The KRAS driver mutation initiates PanIN formation and early development of the cancer-supportive TME via recruitment of the fibro-inflammatory stroma. Not only is mutant *KRAS* required for the initiation of PDA[3,7], but it is necessary for the maintenance and continual propagation of the disease.[3] *KRAS* mutation is one of the earliest catalytic events and most highly expressed mutation in PDA development present in over 90% of human PanIN1 lesions and over 95% of PDA cases[2], hence mutant *KRAS* serves as an attractive target for early stage intervention.

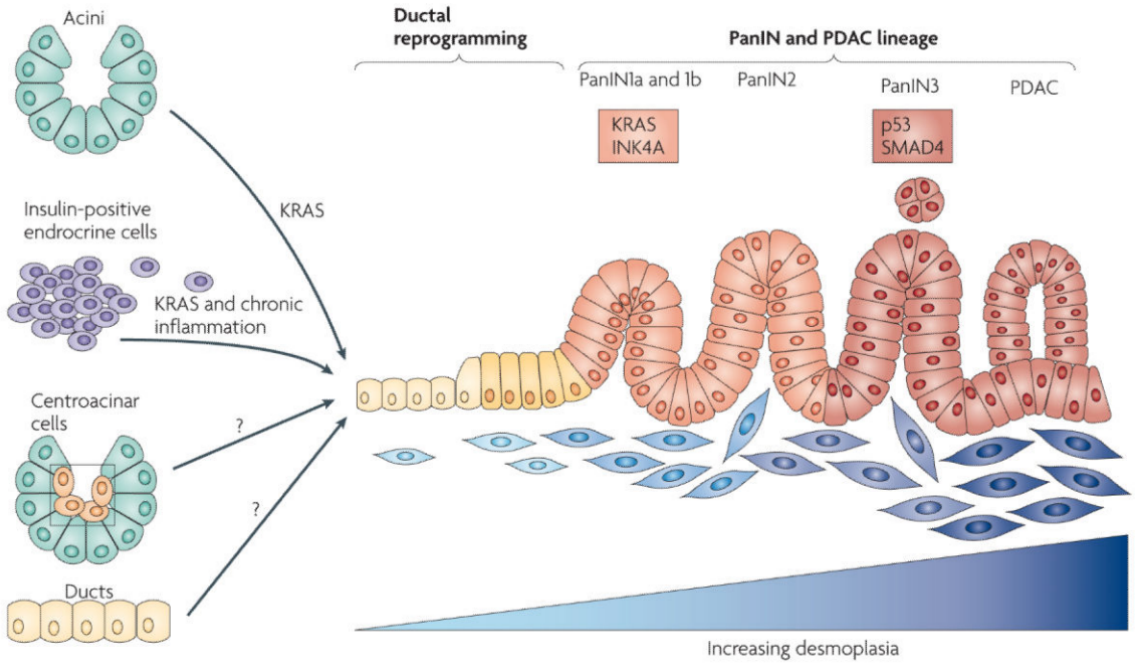

Figure 1.1 PDA Progression Model

Highlights the role of *KRAS* driver mutation in ductal reprogramming to initiate PanIN formation and concurrent establishment of a dynamic TME. Figure from Morris IV et al.[8]

Activating mutations in the *KRAS* proto-oncogene unleashes a cascade of events that initiate tumorigenesis due to its critical role in many intracellular signal transduction pathways. KRAS, a membrane-bound GTPase that is a member of the ras family of proto-oncogenes, once mutated is unable to hydrolyze GTP to GDP and therefore becomes constitutively active. In human cancers, activating KRAS mutations are single amino acid substitutions predominantly at residues 12, 13, and 61 that render the GTPase constantly active.[9] This gain-of-function mutation persistently activates all downstream

signaling pathways that trigger tumor initiation, progression, and malignant metastasis.[5,10] Primary pathways that are upregulated are Raf/MEK/ERK and PI3K/Akt/mTOR pathways that result in increased cell proliferation, survival, and metabolic reprogramming.[10,11] Hence many therapeutics have been developed to target KRAS directly, inhibit downstream KRAS effectors, or prevent the localization of KRAS to the plasma membrane.[12] However, the clinical benefit of these therapeutics have been limited by cellular compensatory mechanisms, drug toxicities, and narrow windows of efficacy.[12]

Tantamount to mutant *KRAS*'s ability to transform cells is its ability to establish a cancer-supportive TME that serves to maintain and propagate PDA progression. Once ductal reprogramming is initiated, the transformed pancreatic epithelial cells expressing mutant *KRAS* also secrete many inflammatory cytokines such as Sonic Hedgehog (SHH), interleukin-6 (IL-6), interleukin-8 (IL-8), prostaglandin E (PGE), and TGFβ that recruit the desmoplastic stroma.[8,11,13,14] PGE directly activates proximal pancreatic stellate cells (PSCs), which in turn increases proliferative, migratory, and invasive potential of tumor cells in a paracrine fashion.[5] Additionally, activated resident PSCs produce collagen and angiogenic factors in localized tissue.[5,11] TGFβ is a key cytokine that increases fibrosis and ECM deposition by recruiting CAFs and PSCs to the site of tumorigenesis.[6] These inflammatory signals generate a phenotypic response similar to that of wound healing in which fibrosis develops as a result of certain cell populations, mainly CAFs, that are recruited to the site of injury. [15,16] Unlike the normal wound healing response, recruited CAFs remain activated and

increase the fibrotic stromal compartment that supports and propagates the developing tumor.[16] In fact, studies utilizing a DNA vaccine expressing human fibroblast activation protein (FAPα) for the targeted immune-mediated eradication of CAFs successfully reduces tumor burden in a murine model of breast and colon cancer.[17,18] 80% of PDA tumor volume is comprised of stroma[19], therefore CAFs, which are major components of the stroma, should be targeted along with tumor cells. Our research aims to employ miRNA-mediated modulation of these two main cell types within the developing PDA TME.

For accurate preclinical modeling of PDA, the dynamic TME must be endogenously recapitulated to examine intervention strategies for multiple components. For our developmental studies, we utilized the *Kras*$^{G12D/+}$*;Trp53*$^{R172H/+}$*;Pdx-1-Cre* (KPC) mouse model that spontaneously develops invasive PDA and naturally mimics the histopathological and molecular features of human PDA development.[20] Our KPC mice are fully backcrossed to a C57BL/6 background. The KPC mice express dominant negative activating point mutation in the proto-oncogene *KRAS* and inactivating mutation in the tumor suppressor gene *Trp53*, the two hallmark genetic alterations in human PDA.[20] The KPC mice will develop tissue specific pancreatic cancer via the Cre-lox system, where mutant *KRAS* is expressed under the control of pancreatic specific promoter, Pdx1 (**Figure 1.2**).[20] The KPC mice will exhibit a stepwise progression to PDA via multiples states of premalignant lesions resembling human PDA by genetic instability and histology.[20]

Figure 1.2

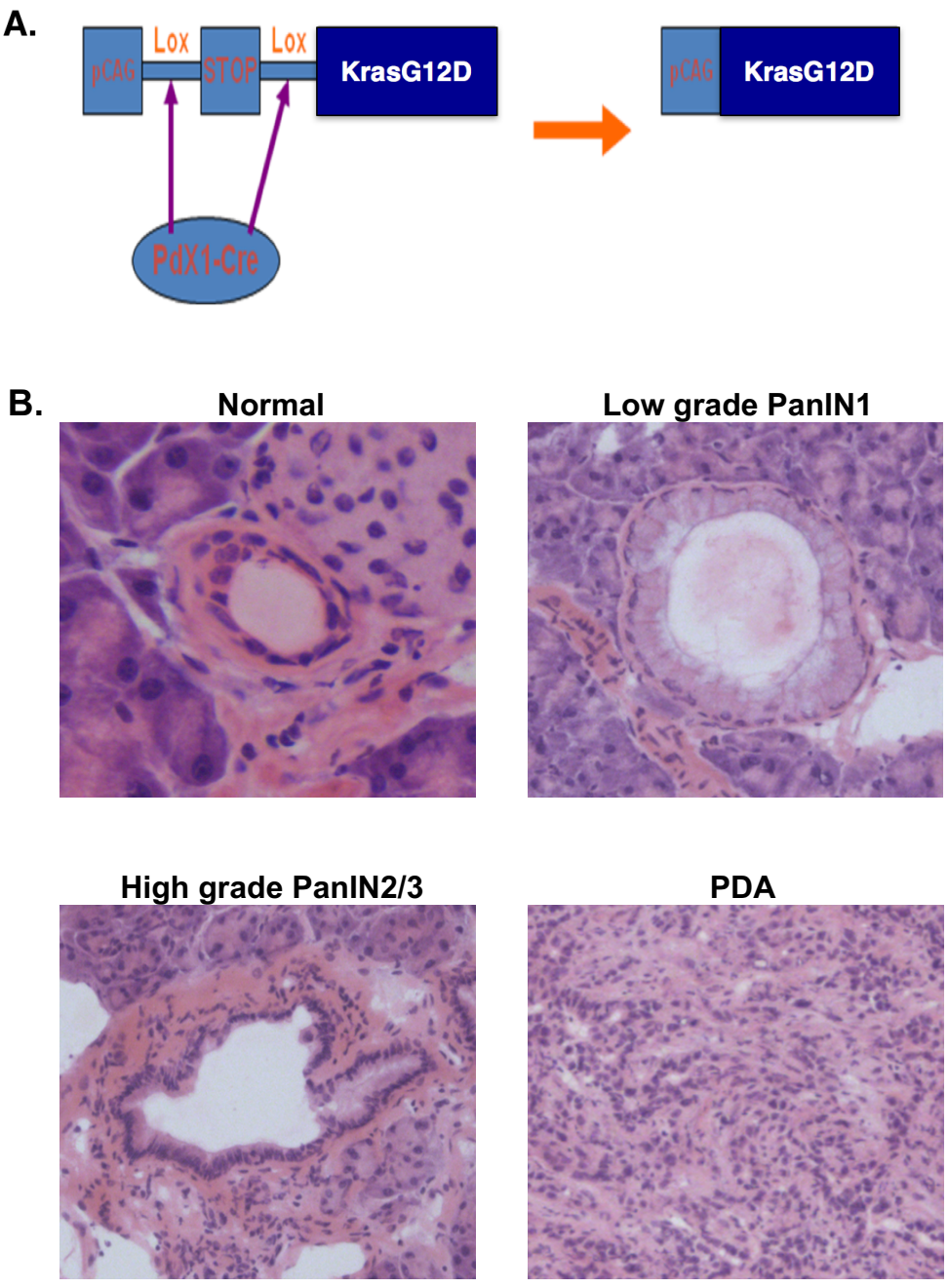

Figure 1.2 KPC transgenic mouse model mimics human pancreatic cancer

(A) Expression of *KRAS*^{G12D} allele after PDX-1 Cre-mediated excision-recombination of *LSL- KRAS*^{G12D}allele.

(B) Representative H&E images of premalignant PanIN progression to PDA.

miRNAs present a new and promising therapeutic platform for cancer and many other diseases. The first miRNA lin-4 was discovered in *C. elegans* in 1993 and the first mammalian miRNA let-7 was discovered 7 years later.[21] Since then thousands of miRNAs have been discovered in humans alone and are being investigated as potential cancer intervention and therapeutic strategies. miRNAs are short non-coding RNAs (ncRNAs) that are 19-25 nucleotides in length that post-transcriptionally regulate gene expression by binding to complementary target mRNAs resulting in their translational inhibition and/or degradation.[21,22] miRNA genes are located in intronic regions of the genome and once transcribed by RNA polymerase II, they are cleaved and processed in the nucleus by DROSHA to produce 60-70 nucleotide long precursor miRNAs (pre-miRNAs).[23] Pre-miRNAs are subsequently exported to the cytoplasm by exportin 5 where further processing occurs by DICER1 to produce a double-stranded mature miRNA.[23] The single guide strand of the mature miRNA is loaded into the RNA-induced silencing complex (RISC) containing DICER and Argonaute proteins.[23] The guide strand directs the RISC to achieve translational repression or mRNA decay via degree of complimentary sequence binding to the target mRNA.[22] Perfect complimentary binding to the 3'-UTR of target transcripts leads to mRNA cleavage and degradation, while imperfect binding (most cases in mammals) results in translational blockage.[22] The 3'-UTR of mRNAs contain regions complimentary to many miRNAs, therefore a single miRNA may target several transcripts while a single transcript may be targeted by many miRNAs.[24] Due to

this mechanism of inhibition, miRNAs are powerful regulators that have the ability to modulate multiple targets in multiple pathways.

miRNAs have been shown to play important regulatory roles in the biology of PDA. Both transformed tumor epithelial cells and stromal cell populations are regulated by miRNAs whose levels are dysregulated by tumorigenesis. In pancreatic cancer cells, mutant *KRAS* activation alters downstream miRNA expression such as those of miR-21, miR-31, miR-155, and miR-221.[22,25] Conversely, several miRNAs also directly regulate *KRAS* expression and can therefore act as tumor-suppressors.[26] miR-30b, miR-30c, miR-181a, miR-193b/365a, miR-613, and miR-134 all regulate *KRAS* in various models of cancer, while let-7 family, miR-126, miR-96, miR-143, and miR-217 modulate *KRAS* expression specifically in PDA.[5,26–28] miRNAs are also potent regulators of many cell populations in the stromal compartment, which is critical to PDA maintenance and propagation. miR-155 secreted by pancreatic cancer cells converts normal fibroblasts to CAFs[29], while miR-21 modulates the migration and invasion of PSCs.[30] miR-221 targets phosphatase and tensin homolog (*PTEN*) and tissue inhibitor of metalloproteinases-2 (*TIMP-2*) which increases the proliferative, migratory, and invasive capacity of CAFs.[22,30] Signaling pathways of TGFβ, a key inflammatory cytokine that activates quiescent PSCs and fibroblasts to increase desmoplasia, is modulated by miR-34b, miR-483-3p, and miR-21 which inhibits SMAD3, SMAD4, and SMAD7 respectively.[31–34] Additionally, TGFβ1 stimulation leads to decreased expression of miR-29 in activated PSCs and CAFs, which results in increased ECM deposition furthering

fibrosis, an effect that is reversed with ectopic expression of miR-29.[35] These data indicate how miRNAs are key regulators of multiple components of PDA. Such findings also suggest that miRNAs may be utilized to delay or halt early premalignant PanIN progression by targeting initiating driver mutation *KRAS* and the early TME. Although many studies have examined the roles of miRNAs in established PDA, few studies have investigated miRNA regulation in early PDA development that may be targeted for PDA prevention and early interception.

Name (company)	Therapeutic agent	Delivery system	Target diseases	Trial details	ClinicalTrials.gov identifier
miRNA-based therapeutics					
Mirvirasen (Santaris Pharma A/S and Hoffmann-La Roche)	AntimiR-122	LNA-modified antisense inhibitor	Hepatitis C (chronic infections included)	Single-centre phase I, completed	NCT01646489
				Multicentre phase II, completed	NCT01200420
				Multicentre phase II, ongoing	NCT01872936
				Single-centre phase II, ongoing	NCT02031133
				Single-centre phase II, ongoing	NCT02508090
RG-101 (Regulus Therapeutics)	AntimiR-122	GalNAc-conjugated antimiR	Chronic hepatitis C	Phase I, completed	–
				Multiple phase II, ongoing	–
RG-125/ AZD4076 (Regulus Therapeutics)	AntimiR-103/107	GalNAc-conjugated antimiR	Patients with type 2 diabetes and non-alcoholic fatty liver diseases	Single-centre phase I, ongoing	NCT02612662
				Single-centre phase I/IIa, ongoing	NCT02826525
MRG-106 (miRagen Therapeutics)	AntimiR-155	LNA-modified antisense inhibitor	Cutaneous T cell lymphoma and mycosis fungoides	Multicentre phase I, ongoing	NCT02580552
MRG-201 (miRagen Therapeutics)	miR-29 mimic	Cholesterol-conjugated miRNA duplex	Scleroderma	Single-centre phase I, ongoing	NCT02603224
MesomiR-1 (EnGenelC)	miR-16 mimic	EnGenelC delivery vehicle	Mesothelioma, non-small cell lung cancer	Multi-centre Phase I, ongoing	NCT02369198
MRX34 (Mirna Therapeutics)	miR-34 mimic	LNPs (Smarticles)	Multiple solid tumours	Multicentre phase I, terminated	NCT01829971

Table 1.1 miRNA therapeutics in clinical trials for various diseases

miR-16 mimic is currently being tested for non-small cell lung cancer and miR-34 mimic is being tested for multiple solid tumors. miRNAs for the treatment of PDA have yet to advance to clinical trials, an area that warrants further research. Table from Rupaimoole et al.[21]

The poor prognosis and high lethality of PDA is due to late detection of the disease. More than 80% of patients present with late stage metastatic cancer at the time of diagnosis[1], hence there is a great need for early detection methods. Recent studies have shown that profiles of circulating cell-free miRNAs in the peripheral blood of cancer patients have provided specific sets of miRNAs that are indicative of certain cancers.[36–38] Not only are circulating miRNAs diagnostic biomarkers of disease, but they are also predictors of patient response to chemotherapies and likelihood of cancer recurrence, hence the levels of circulating miRNAs are sensitive to specific physiological stresses and phenomenon.[39–42] Additionally, the non-invasive isolation of circulating miRNAs from a simple blood draw along with its stability in harsh conditions (freeze-thawing, RNase digestion, wide pH range) confers feasibility to utilizing circulating miRNAs for cancer screening in the clinic.[40,43] The stability of circulating miRNAs is achieved by its secretion in exosomes and microvesicles, which are currently also being profiled to assess their potential in enhancing circulating miRNA biomarker specificity.[44] Utilizing the developmental KPC mouse model, we aim to build a developmental profile of circulating serum miRNAs in which alterations in circulating miRNA levels as compared to the levels of WT C57BL/6 mice may be indicative of the presence of low grade PanINs and initiation of early PDA disease progression. Such studies will generate circulating miRNA signatures that can be feasibly utilized in the clinic for early PDA screening.

MATERIALS & METHODS

KPC Mice

Lox-STOP-Lox-*Trp53*$^{R172H/þ}$; Lox-STOP-Lox-*Kras*$^{G12D/þ}$; and Pdx-1-Cre strains on a mixed C57BL/6 background, were gifted from Dr. David Tuveson (Cold Spring Harbor Laboratory, Cold Spring, NY). These mice were backcrossed to the C57BL/6 genetic background for 12 generations and interbred to obtain KC and KPC mice. All animals were kept in pathogen-free conditions and treated in accordance with Institutional Animal Care and Use Committee of the Johns Hopkins University and American Association of Laboratory Animal Care approved guidelines.

Laser Capture Microdissection (LCM)

Pancreata were isolated from aged KPC (4-20 weeks) or WT C57BL/6 mice and frozen in Tissue-Tek OCT (Sakura Finetek USA). Guide slides were sectioned and stained with H&E by the Johns Hopkins University Oncology Tissue Services. Guide slides containing various grades of PanINs were identified by a pathologist (R.A. Anders). 10, 10um frozen sections adjacent to guide sections were mounted on membrane slides (Zeiss) and stained with Cresyl Violet (Ambion). Normal, low grade PanIN1, high grade PanIN2/3, and PDA tissue were microdissected using LCM (Leica LMD7000).

miRNA Profiling Using miRNA Microarray

RNA was extracted from LCM samples using RNAqueous™-Micro Total RNA Isolation Kit (Thermo Fisher Scientific), quantified with NanoDrop 1000 Spectrophotometer (Thermo Fisher Scientific), and converted to cDNA using

TaqMan™ MicroRNA Reverse Transcription Kit (Thermo Fisher Scientific) and Megaplex™ RT Primers Rodent Pool A and B (Thermo Fisher Scientific). cDNA was preamplified 18 cycles using TaqMan™ PreAmp Master Mix (Thermo Fisher Scientific) and Megaplex™ PreAmp Primers Rodent Pool A and B (Thermo Fisher Scientific). miRNA microarray was performed by the Johns Hopkins School of Medicine Genetic Resources Core Facility using TaqMan® OpenArray® Rodent MicroRNA Panel (Thermo Fisher Scientific) and TaqMan® OpenArray® Real-Time PCR Master Mix (Thermo Fisher Scientific). All Ct values were normalized to endogenous levels of U6 snRNA. Fold changes were quantified utilizing the $\Delta\Delta$Ct method in which all PanIN groups were normalized to the normal group (normal ducts isolated from WT C57BL/6 mice).

Quantitative RT-PCR (qPCR) of Top miRNA Candidates

RNA was extracted from LCM samples or primary cell lines using RNAqueous™-Micro Total RNA Isolation Kit (Thermo Fisher Scientific), quantified with NanoDrop 1000 Spectrophotometer (Thermo Fisher Scientific), and converted to cDNA using TaqMan™ MicroRNA Reverse Transcription Kit (Thermo Fisher Scientific) with Taqman miRNA RT Assays (Thermo Fisher Scientific). cDNA was preamplified 12 cycles using TaqMan™ PreAmp Master Mix (Thermo Fisher Scientific) and Taqman miRNA TM Assays (Thermo Fisher Scientific). qPCR was performed using Taqman Universal Master Mix II (Thermo Fisher Scientific) on the StepOnePlus Real-Time PCR System (Life Technologies) and analyzed by ExpressionSuite Software (Thermo Fisher Scientific). All Ct values were normalized to endogenous levels of U6 snRNA. Fold changes were quantified

utilizing the ΔΔCt method in which all PanIN groups, KPC tumor cells, and KPC CAFs were normalized to normal ducts isolated from WT C57BL/6 mice, WT pancreatic epithelial cells, or PNAFs respectively.

Primary Cell Lines and Cell Culture

Primary KPC tumor epithelial cell line, KPC CAF, and C57BL/6 pancreatic normal associated fibroblasts (PNAF) were gifted from Dr. Lei Zheng. We performed fluorescent activated cell sorting (FACS) to further purify and enrich for each cell line. KPC tumor cells were surface stained and sorted using anti-CD326 (EpCAM)-FITC (eBioscience). KPC CAFs were stained with primary antibody anti-FAP (Abcam) and secondary antibody Brilliant Violet 421 Donkey anti-rabbit IgG (BioLegend). PNAFs were stained with anti-PDGFRα-APC (Biolegend). All cell lines were dissociated with Cell Dissociation Buffer, enzyme free (Thermo Fisher Scientific), washed twice with sterile sorting buffer (PBS with 2% FBS), stained with primary antibody for 1 hour at 4 degrees in the dark, washed twice with sorting buffer, stained with secondary antibody for 30 minutes at 4 degrees in the dark, washed twice with sorting buffer, and then sorted using FACSAria Fusion SORP cell sorter (Becton Dickinson) by the Sidney Kimmel Comprehensive Cancer Center Flow Cytometry Core. KPC tumor cells were sequenced to ensure that they have the appropriate *KRAS* and *Trp53* mutations. KPC Tumor cells, KPC CAFs, and PNAFs were maintained in RPMI 1640 (Life Technologies) supplemented with 10% FBS (Gemini Bio-products), 1 mM sodium pyruvate (Sigma), 2 mM L-glutamine (Life Technologies), 1% nonessential amino acids (Life Technologies), penicillin (50 U/ml)/streptomycin (50 μg/ml) (Life

Technologies), and 0.2 U/ml human insulin (NovoLog) in a humidified incubator (37 degrees, 5% CO_2). C57BL/6 Mouse Primary Pancreatic Epithelial Cells (WT epithelial cells) were purchased from CellBiologics. WT epithelial cells were maintained in Complete Epithelial Cell Medium with Kit (CellBiologics).

Western Analysis of Phenotypic Markers

Cells were trypsinized then lysed with RIPA buffer (Thermo Fisher Scientific) supplemented with Halt Protease and Phosphatase Inhibitor Cocktail (Thermo Fisher Scientific). Protein was quantified using Pierce BCA Protein Assay Kit (Thermo Fisher Scientific) according to the manufacturer's instructions. For Western Blotting, SDS PAGE was performed using the BioRad gel electrophoresis system. Protein lysate samples were mixed with XT Reducing Agent (BioRad) and XT Sample Buffer (BioRad), run on 4-12% bis-tris Criterion XT gels (BioRad) at 150V, and transferred to nitrocellulose membrane (GE Healthcare). Membranes were blocked using Odyssey Blocking Buffer, TBS (LI-COR) for 1 hour at room temperature or overnight at 4 degrees with gentle shaking. Primary antibodies anti-Vimentin (Abcam), anti-E-cadherin (Abcam), anti-α-smooth muscle actin (α-SMA) (Abcam), and anti-FAP (Abcam) were stained with secondary antibody IRDye® 800CW Donkey anti-Rabbit IgG (H + L) (LI-COR). Endogenous control primary antibody anti-β-Actin (Abcam) was stained with secondary antibody IRDye® 680RD Donkey anti-Chicken IgG (H + L) (LI-COR). Membranes were stained with primary antibodies diluted in Odyssey Blocking Buffer+0.2% Tween20 for 2 hours at room temperature with gentle shaking, washed 3 times with TBST (TBS with 0.1% Tween20), stained

with secondary antibodies diluted in Odyssey Blocking Buffer+0.2% Tween20 for 1 hour at room temperature with gentle shaking in the dark, washed 3 times with TBST, then visualized with an Odyssey Infrared Imaging System scanner (LI-COR). Signal intensities were measured using FIJI software (ImageJ).[45]

Proliferation, Invasion, and Migration Assays

Cell Counting Kit-8 (CCK8) (Dojindo Molecular Technologies) was used for proliferation assays for all cell lines. Cells were seeded on 96 well plates and after a 90 minute incubation with CCK8 solution in a humidified incubator (37 degrees, 5% CO_2) the absorbance was measured at 450nm. This procedure was repeated every 24 hours starting on day 0 to day 4. Invasion and migration assays were performed using Cultrex 96 Well BME Cell Invasion Assay kit (Trevigen) according to the manufacturer's instructions. The transwells were coated overnight with 1X basal membrane extract (BME) for invasion assays, while no BME coating was performed for migration assays. For both assays, cells were serum-starved for 24 hours before plating. Invasion and/or migration was measured 48 hours after plating cells using CCK8. Scratch assay or wound healing assay to quantify migratory capacities was performed by seeding 24 well plates at high density to produce immediate confluency. Once confluent, wells were scratched with a p200 pipet tip to produce a clear vertical partition and images were taken at 20X magnification using an Eos Rebel T2i camera (Canon) attached to a phase-contrast microscope. After a 24-48 hour incubation (depending on cell line used) in a humidified incubator, another image was taken and migration was measured by quantifying the percent partition closure relative

to the 0 hour time point. Area of partition at each time point was quantified using FIJI software (ImageJ).

miRNA Fluorescence In Situ Hybridization (miR-FISH)

In situ detection of miR-21, miR-224 and U6 snRNA was performed using miRCURY LNA microRNA ISH Optimization Kit (Exiqon) as per the manufacturer's instruction with modifications for frozen tissue sections. H&E slides of aged KPC pancreata prepared by the Johns Hopkins University Oncology Tissue Services were examined by a pathologist (R.A. Anders) and PanINs of various grades were identified. Subsequent 10 um frozen sections from histologically analyzed pancreata were fixed in 10% neutral buffered formalin overnight at room temperature. All washes were done with DEPC-PBS. Proteinase K (20ug/ml) digestion was carried out in an ACD HybEZ hybridization oven at 38 degrees for 15 min. Two 3 min washes with 3% hydrogen peroxide solution in DEPC-PBS was used to block endogenous peroxidases. All locked-nucleic acid (LNA) miRNA probes are double digoxigenin (DIG) labeled on the 5' and 3' ends, except for LNA-U6 which is DIG labeled only on the 5' end. Hybridization with each LNA miRNA probe was performed at specific optimal temperatures. LNA-miR-21 (TCAACATCAGTCTGATAAGCTA, 40nM) was hybridized at 54 degrees, LNA-miR-224 (AACGGAACCACTAGTGACTT, 40nM) was hybridized at 52.5 degrees, LNA-miR-Scramble (GTGTAACACGTCTATACGCCCA, 40nM) was hybridized at 54 degrees, and LNA-U6 (CACGAATTTGCGTGTCATCCTT, 1 nM) was hybridized at 54 degrees. All LNA probes were hybridized for 1 hour in a humidified hybridization oven.

After decreasing concentrations of 5 min SSC washes at probe hybridization temperatures, tissue sections were blocked for 15 min at room temperature in a humidified chamber using 5X *In Situ* Hybridization (ISH) Blocking Solution (Vector Laboratories), diluted with sterile water to 1X working concentration. Sections were stained with primary antibody HRP-labeled anti-DIG (Gallus Immunotech) diluted in blocking solution for 60 min at room temperature in a humidified chamber. TSA Plus Fluorescein (Perkin Elmer) detection substrate was applied to sections two times 5 min each in the dark in order to produce an amplified fluorescent signal. Sections were then stained with nuclear dye Hoechst (Thermo Fisher Scientific) for 15 min in the dark. Slides were mounted with Prolong Diamond Antifade Mountant (Thermo Fisher Scientific) and cured overnight in the dark with proper ventilation. Slides were imaged the next day on Eclipse E800 fluorescence microscope (Nikon) at 20X magnification using the DAPI filter to capture nuclear staining and the FITC filter to capture miRNA staining. *In situ* miRNA expression was quantified by FITC intensity/nuclei using FIJI software (ImageJ).

Lentiviral Stable Transduction of Primary Cell Lines with miRNA Mimics and Inhibitors

All miRNA lentiviral particles were purchased from GeneCopoeia. The GeneCopoeia third generation self-inactivating HIV-based lentiviral vector system meet Biosafety Level 2 (BSL-2) requirements based on the criteria outlined by the Centers for Disease Control. Transduction of primary cell lines were performed according to the manufacturer's protocol. Viral suspension contained

8μg/ml of Polybrene (Sigma) and 10μl of lentivirus diluted in complete media appropriate for each cell line to be transduced. Plates containing cells and viral suspension were placed in 4 degrees for 1.5 hours prior to overnight incubation in a humidified incubator (37 degrees, 5% CO_2) to increase transduction efficiency. Successfully transduced cells were selected via antibiotic selection using either 4μg/ml puromycin (Sigma) or 400μg/ml hygromycin B (Thermo Fisher Scientific). Transduced cells after selection were viewed at 20X magnification under Eclipse TE200 inverted fluorescence microscope (Nikon) to assess transduction efficiency. Cells were FACS sorted by eGFP or mCherry expression using FACSAria Fusion SORP cell sorter (Becton Dickinson) by the Sidney Kimmel Comprehensive Cancer Center Flow Cytometry Core to further enrich for successfully transduced cells.

Isolation and Preparation of Serum miRNA for Circulating miRNA Profile

Whole blood was isolated via cardiac puncture of the right atrium using a 26 gauge subcutaneous needle (Becton Dickinson) immediately after aged KPC mice were euthanized. After whole blood extraction, the pancreas was isolated and formalin fixed. Whole blood was allowed to coagulate at room temperature for a minimum of 30 minutes and a maximum of 2 hours before spinning at 2,000 g's for 25 min at 4 degrees. Serum was isolated and kept at -80 degrees until further processing. H&E slides of pancreata (prepared by the Johns Hopkins University Oncology Tissue Services) of aged KPC mice in which serum was isolated from, were graded by a pathologist (R.A. Anders) based on the highest PanIN stage (or PDA) present. Samples were grouped based on graded

biological groups normal. Serum samples were thawed and spun at 16,000 g's for 10 min at 4 degrees to remove cryoprecipitates. *C. elegans* miR-39 mimic (Ambion) was spiked into 200ul of serum before total RNA extraction using miRNeasy Serum/Plasma Kit (Qiagen). RNA concentrations were quantified with NanoDrop 1000 Spectrophotometer (Thermo Fisher Scientific). Subsequent cDNA generation, preamplification, and serum miRNA microarray profiling was performed as described above for in-tissue miRNA microarray profiling.

Statistical Analysis

Statistical analysis was performed using GraphPad Prism v7.0b (GraphPad Software). The data are presented as the means ±SEM. Comparisons between groups were made using two-tailed unpaired Student *t* tests and one-way or two-way ANOVA. For all analyses, P-values ≤ 0.05 were considered statistically significant.

RESULTS

Comprehensive profile of miRNA expression in early PDA development in KPC mice

While miRNA profiling has been performed for established PDA and models of late stage metastases, very few studies have constructed a comprehensive profile of key dysregulated miRNAs in early PDA development and progression. Our profiling is performed using KPC mice, an endogenous model of PDA in which disease progression recapitulates human PDA initiation and development via expression of driver mutation $KRAS^{G12D}$ and loss-of-function tumor suppressor *Trp53* in pancreatic epithelial cells. These mice develop increasing grades of premalignant PanINs before invasive PDA. To construct our developmental miRNA profile, we isolated varying grades of PanINs from sections of aged KPC pancreata and performed miRNA microarray analysis quantifying the levels of 750 know murine miRNAs.

To narrow down this extensive list to a few key miRNA candidates for further investigation, we employed specific selection criteria that all key candidates must meet. First, we chose miRNAs that have low Ct values, indicating that they are strongly expressed. Secondly, candidate miRNAs must have high ΔRq values, indicating that there are large fold changes either increasing or decreasing over PanIN development. Thirdly, we chose miRNAs who's fold changes are significantly changing (P-value ≤ 0.05) between developmental PanIN groups, and lastly, our key miRNAs have either putative or proven roles in cancer promoting pathways. Our top 14 miRNA candidates

selected from our initial screen are miR-21, miR-16, miR-224, miR-19b, miR-106b, miR-29a, miR-20a, miR-28, miR-142-3p, miR-15b, miR-301b, miR-222, miR-221, and miR-216b. The expression levels of all candidate miRNAs were validated by in-house qPCR (**Figure 1.3**) and exhibited the same trends and fold changes produced by the initial microarray screen. **Table 1.2** summarizes the fold changes over PanIN development and PDA of our top 14 miRNA candidates. Dysregulation of key miRNAs occur as early as low-grade PanIN1 and persist consistently to PDA. Expression levels of well-characterized onco-miR-21 are increased by 55-fold in PanIN1 lesions and 333-fold in PDA as compared to the expression levels in normal ducts of WT C56BL/6 mice.

Figure 1.3

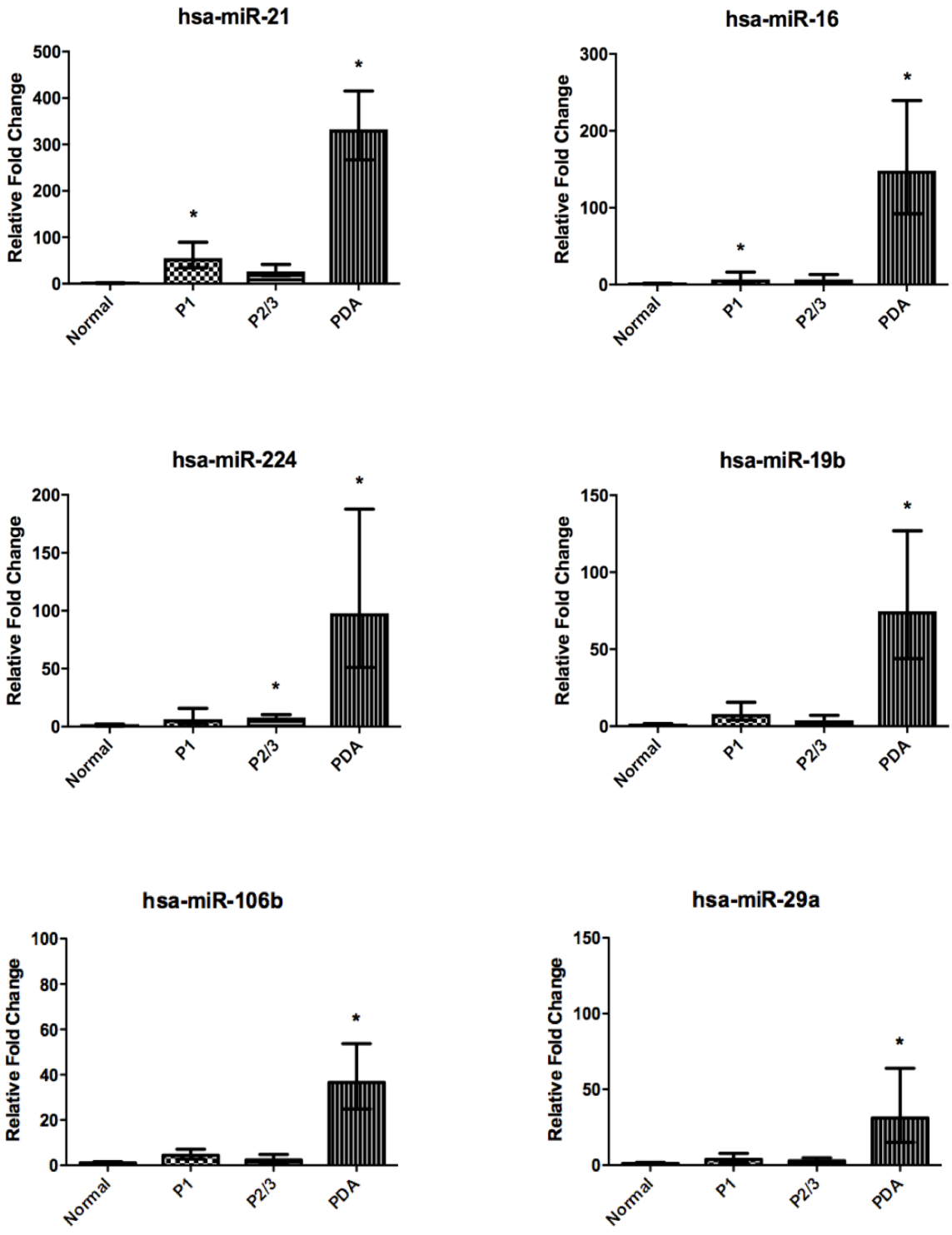
hsa-miR-21
Relative Fold Change
500
400
300
200
100
0
Normal
P1
P2/3
PDA
hsa-miR-16
Relative Fold Change
300
200
100
0
Normal
P1
P2/3
PDA
hsa-miR-224
Relative Fold Change
200
150
100
50
0
Normal
P1
P2/3
PDA
hsa-miR-19b
Relative Fold Change
150
100
50
0
Normal
P1
P2/3
PDA
hsa-miR-106b
Relative Fold Change
100
80
60
40
20
0
Normal
P1
P2/3
PDA
hsa-miR-29a
Relative Fold Change
150
100
50
0
Normal
P1
P2/3
PDA

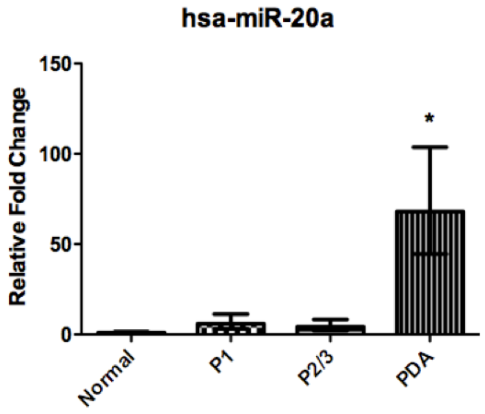
hsa-miR-20a
Relative Fold Change
150
100
50
0
*
Normal
P1
P2/3
PDA

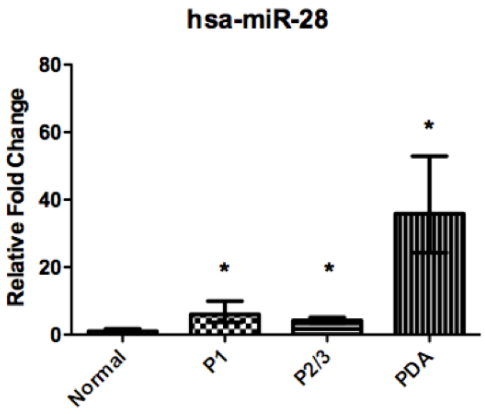
hsa-miR-28
Relative Fold Change
80
60
40
20
0
*
*
*
Normal
P1
P2/3
PDA

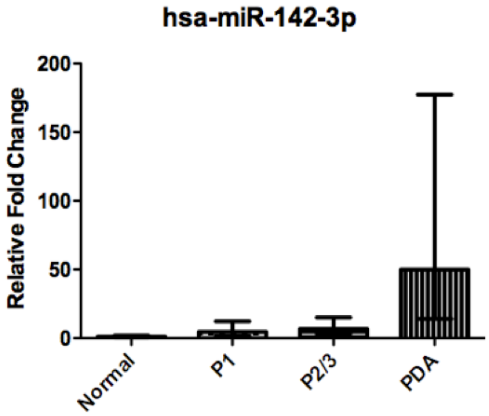
hsa-miR-142-3p
Relative Fold Change
200
150
100
50
0
Normal
P1
P2/3
PDA

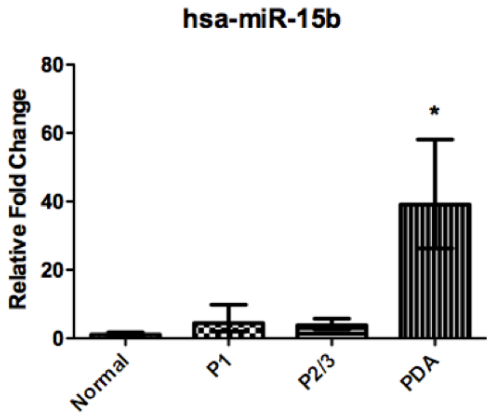
hsa-miR-15b
Relative Fold Change
80
60
40
20
0
*
Normal
P1
P2/3
PDA

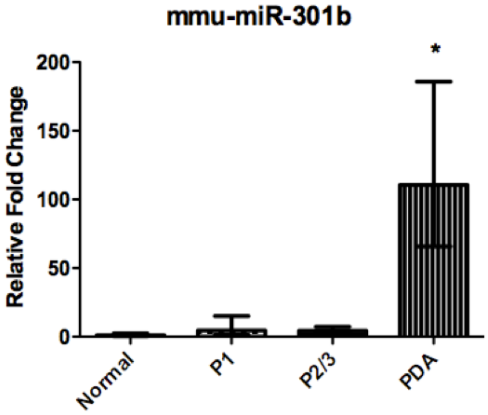
mmu-miR-301b
Relative Fold Change
200
150
100
50
0
*
Normal
P1
P2/3
PDA

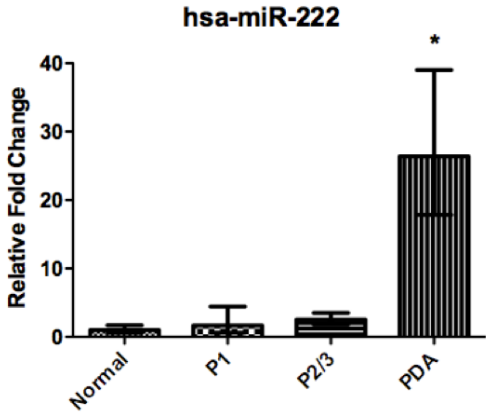
hsa-miR-222
Relative Fold Change
40
30
20
10
0
*
Normal
P1
P2/3
PDA

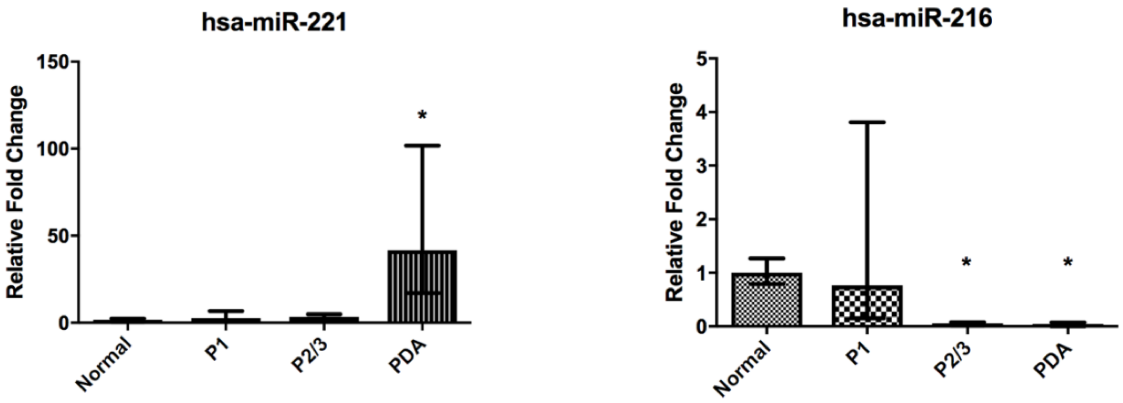

Figure 1.3 Expression of top 14 miRNA candidates in early PDA development. Expression levels were quantified utilizing the ΔΔCt method in which all Ct values were first normalized to endogenous control U6 snRNA and low-grade PanIN1 (P1), high-grade PanIN2/3 (P2/3), and PDA groups were normalized to the normal group (normal ducts isolated from WT C57BL/6 mice) to generate all fold changes. Error bars represent average ± SE. The *hsa* prefix denotes miRNAs that are found in both mice and humans due to sequence conservation.

Table 1.2

Increased				
miRNA	**Normal**	**P1**	**P2/3**	**PDA**
hsa-miR-21	1	55	27	333
hsa-miR-16	1	7	7	148
hsa-miR-224	1	6	8	98
hsa-miR-19b	1	8	4	75
hsa-miR-106b	1	4	2	37
hsa-miR-29a	1	4	3	31
hsa-miR-20a	1	6	4	68
hsa-miR-28	1	6	4.2	36
hsa-miR-142-3p	1	5	7	50
hsa-miR-15b	1	4	4	39
mmu-miR-301b	1	5	4	111
hsa-miR-222	1	2	3	26
hsa-miR-221	1	3	3	42
Decreased				
miRNA	**Normal**	**P1**	**P2/3**	**PDA**
hsa-miR-216b	1	1	29	100

Fold changes of the top 14 dysregulated miRNAs over early PDA development. Quantified fold changes of miRNA expression, either increasing or decreasing, over developmental groups normalized to the expression levels in normal ducts of WT C56BL/6 mice.

Establishment of primary cell lines of the TME for in vitro functional studies

The PDA TME is very dynamic, composed of many cellular populations and sub-cellular constituents that all serve to propel early progression of the disease. PDA predominantly consists of tumor epithelial cells and recruited activated fibroblasts that comprise the dense stromal compartment of the tumor. To study the mechanistic regulation of the key miRNAs derived from our screen in early PanIN lesions and TME development, we established primary cell lines derived from primary KPC tumors and WT C57BL/6 pancreata for *in vitro*

functional studies. We established primary KPC CAFs, which are major components of the desmoplastic stroma characteristic of PDA. Additionally, primary KPC tumor epithelial cells were isolated in order to study the miRNA-mediated signaling mechanisms between tumor cells and CAFs in the TME. The WT counterparts for these two cell lines were derived as well for comparison of transformed and activated phenotypes. Normal pancreatic associated fibroblasts (PNAFs), the resident fibroblasts of the pancreas, were isolated from WT C57BL/6 mice. Lastly, normal pancreatic epithelial cells were purchased from Cell Biologics.

Following tissue dissociation and serial trypsin digestions, we employed FACs to further enrich for each cell line. To isolate a pure population of PNAFs, we utilized platelet-derived growth factor receptor, alpha (PDGFRα) as a marker for cell sorting since PDGFRα is a surface marker for stromal cells, especially fibroblasts, of mesenchymal origin.[46] For the enrichment of CAFs, we sorted using fibroblast activation protein (FAP), which is selectively expressed on activated stromal fibroblasts of epithelial cancers.[17] To increase the purity of KPC tumor epithelial cells, we stained and sorted using epithelial cell adhesion molecule (EpCAM), which is a surface glycoprotein exclusively expressed on epithelia and epithelial-derived tumors.[47] **Figure 1.4** displays the flow cytometric analysis of the markers used for the sorting of each primary cell line along with the morphology of each cell line after sorting. The proper morphology characteristic of each cell type post-FACs indicated that the sort was successful.

Figure 1.4

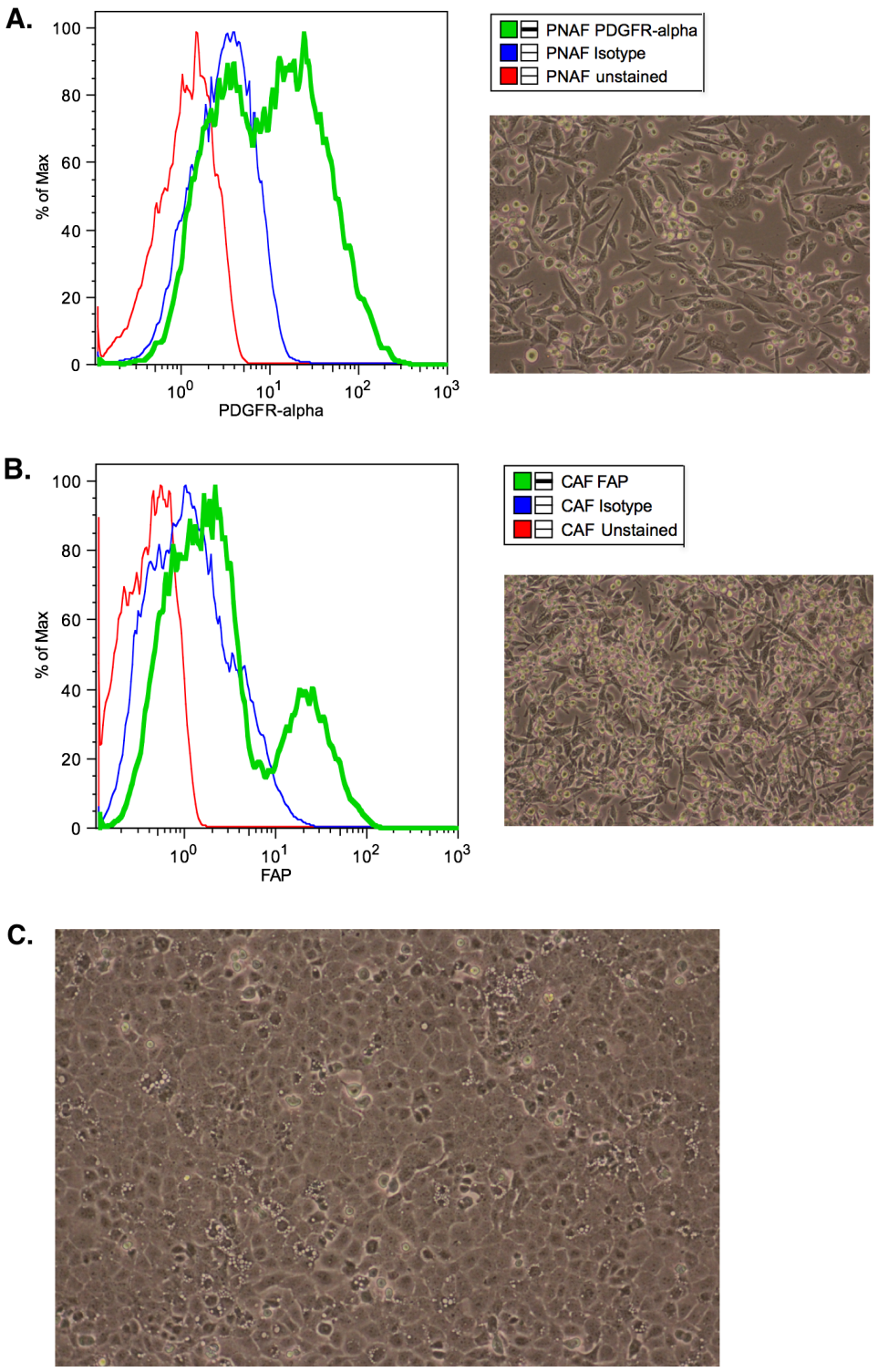
A.
100
80
60
40
20
0
% of Max
10^0
10^1
10^2
10^3
PDGFR-alpha
PNAF PDGFR-alpha
PNAF Isotype
PNAF unstained
B.
100
80
60
40
20
0
% of Max
10^0
10^1
10^2
10^3
FAP
CAF FAP
CAF Isotype
CAF Unstained
C.

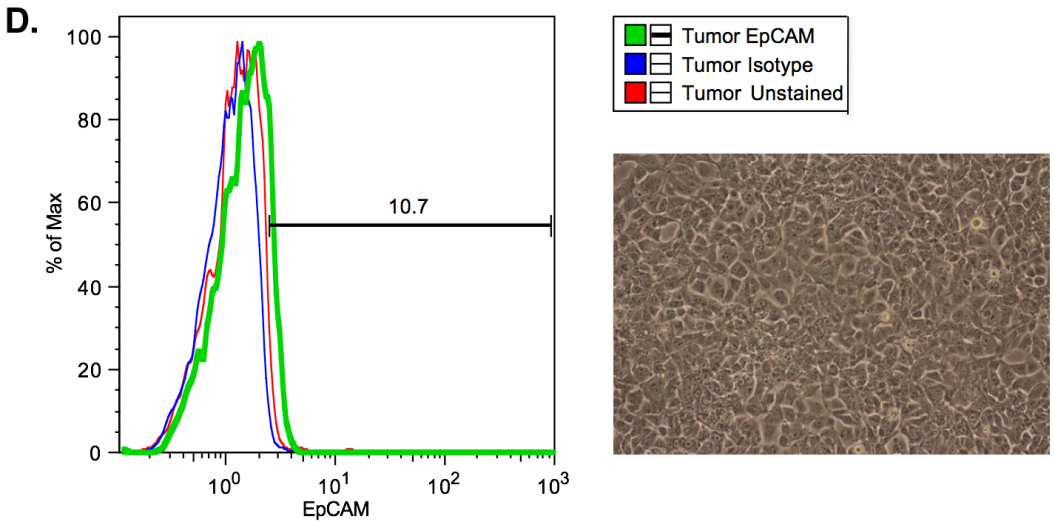

Figure 1.4 FACs sorting and morphology of primary cell lines of the TME.

(A) Sorting of PNAFs isolated from WT C57BL/6 pancreas using PDGFRα. Classic spindle-shaped morphology of fibroblasts is observed post-sort.

(B) Sorting of CAFs isolated from a KPC tumor using FAP. Classic spindle-shaped morphology of fibroblasts is observed post-sort.

(C) WT C57BL/6 pancreatic epithelial cells from Cell Biologics exhibited classic cuboidal-shaped morphology.

(D) Sorting of KPC tumor epithelial cells isolated from a KPC tumor using EpCAM. Classic cuboidal-shaped morphology of epithelial cells is observed post-sort.

Phenotypic validation of primary cell lines by Western analysis, proliferation, and migration assays

While the expression of PDGFRα for CAFs and FAP for PNAFs were robust, the expression of EpCAM for KPC tumor cells was weakly detected (10.7%) while sorting, hence further phenotypic confirmation is required for the validation of established primary cell lines. We quantified protein expression of phenotypic markers of each cell type via Western Blot analysis (**Figure 1.5**). To distinguish between WT C57BL/6 pancreatic epithelial cells and KPC tumor epithelial cells, we compared the expression of epithelial markers vimentin and E-cadherin. The significant upregulation of vimentin and downregulation of E-cadherin in KPC tumor cells as compared to WT epithelial cells confirms the transformed and untransformed phenotype of the two primary cell lines. To validate PNAFs and CAFs, we quantified the expression of α-smooth muscle actin (α-SMA) and FAP. The increased expression of FAP and slight upregulation of α-SMA in CAFs confirms its activated state compared to PNAFs.

A defining phenotype of fully transformed and activated cells is increased proliferative capacity. Thus, we utilized proliferation as another measure of distinct phenotypes of our established primary cell lines. The CCK8 proliferation assay takes advantage of the WST-8 compound, which produces a water-soluble formazan dye upon reduction in the presence of electron mediators, such as dehydrogenases, in viable cells. The colorimetric detection of the formazan dye at 450nm directly correlates with cell viability. **Figure 1.6** shows that KPC CAFs and tumor cells have the highest absorbance at 450nm, and therefore, proliferate

more than their WT counterparts (PNAFs and WT epithelial cells respectively) over 3 days, in which proliferation was measured every 24 hours.

Like proliferation, increased cell migration is another acquired characteristic of a transformed and activated phenotype. Utilizing the scratch assay or wound-healing assay, we quantified how quickly our primary cell lines migrated to close a partition generated by a scratch made on a confluent cell surface. **Figure 1.7** shows that after 24 hours in culture, KPC tumor cells achieved 94% wound closure whereas WT pancreatic epithelial cells only achieved 24% wound closure, demonstrating the significantly increased migratory capacities of transformed KPC tumor cells. Similarly, KPC CAFs achieved 100% wound closure after 24 hours as compared to PNAFs that only migrated to cover 74% of the partition, indicating that CAFs migrate more than PNAFs. Cumulatively, the quantified differences in marker expression, cell proliferation, and migration confirm the phenotypes of our primary cell lines on a protein and functional level.

Figure 1.5

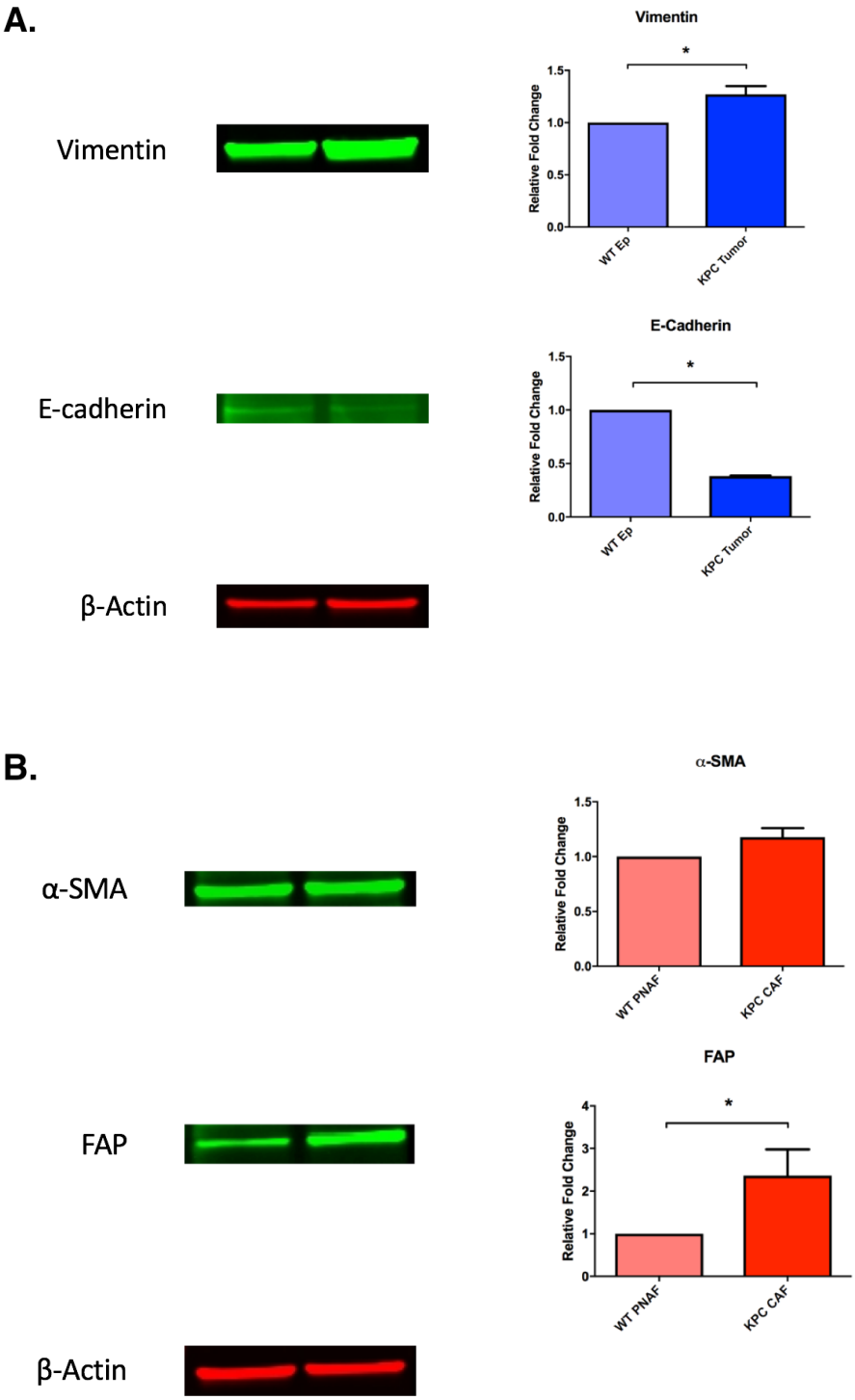
A.
Vimentin
E-cadherin
β-Actin
Vimentin
Relative Fold Change
1.5
1.0
0.5
0.0
*
WT Ep
KPC Tumor
E-Cadherin
Relative Fold Change
1.5
1.0
0.5
0.0
*
WT Ep
KPC Tumor
B.
α-SMA
FAP
β-Actin
α-SMA
Relative Fold Change
1.5
1.0
0.5
0.0
WT PNAF
KPC CAF
FAP
Relative Fold Change
4
3
2
1
0
*
WT PNAF
KPC CAF

Figure 1.5 Protein expression of specific markers validate primary cell line phenotypes.

(A) Representative blots and quantified protein expression of tumor epithelial markers vimentin and E-cadherin in WT pancreatic epithelial cells and KPC tumor cells.

(B) Representative blots and quantified protein expression for activated fibroblast markers α-SMA and FAP in PNAFs and KPC CAFs.

Figure 1.6

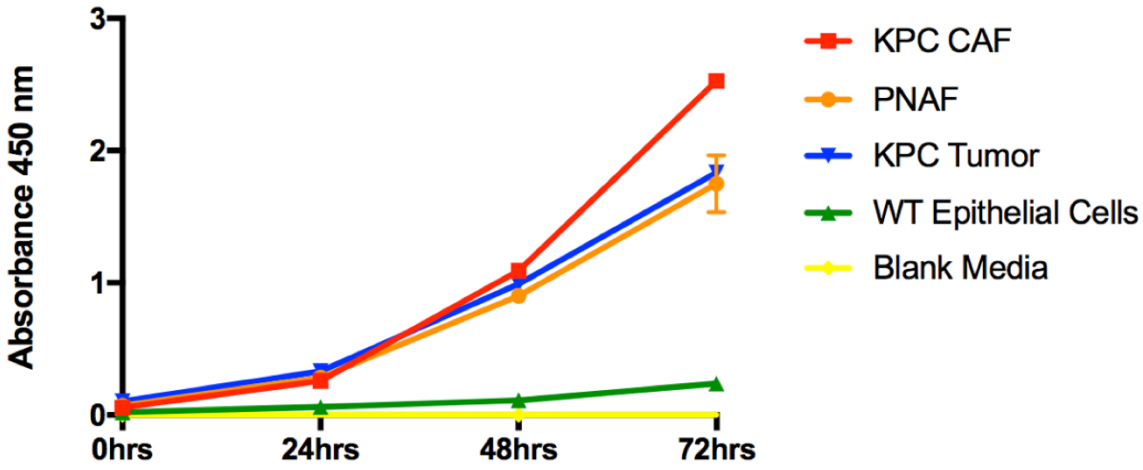

Figure 1.6 KPC tumor cells and CAFs proliferate more than WT epithelial cells and PNAFs respectively.

Cells were plated at time 0 and proliferation was measured using CCK8 every 24 hours up to 72 hours.

Figure 1.7

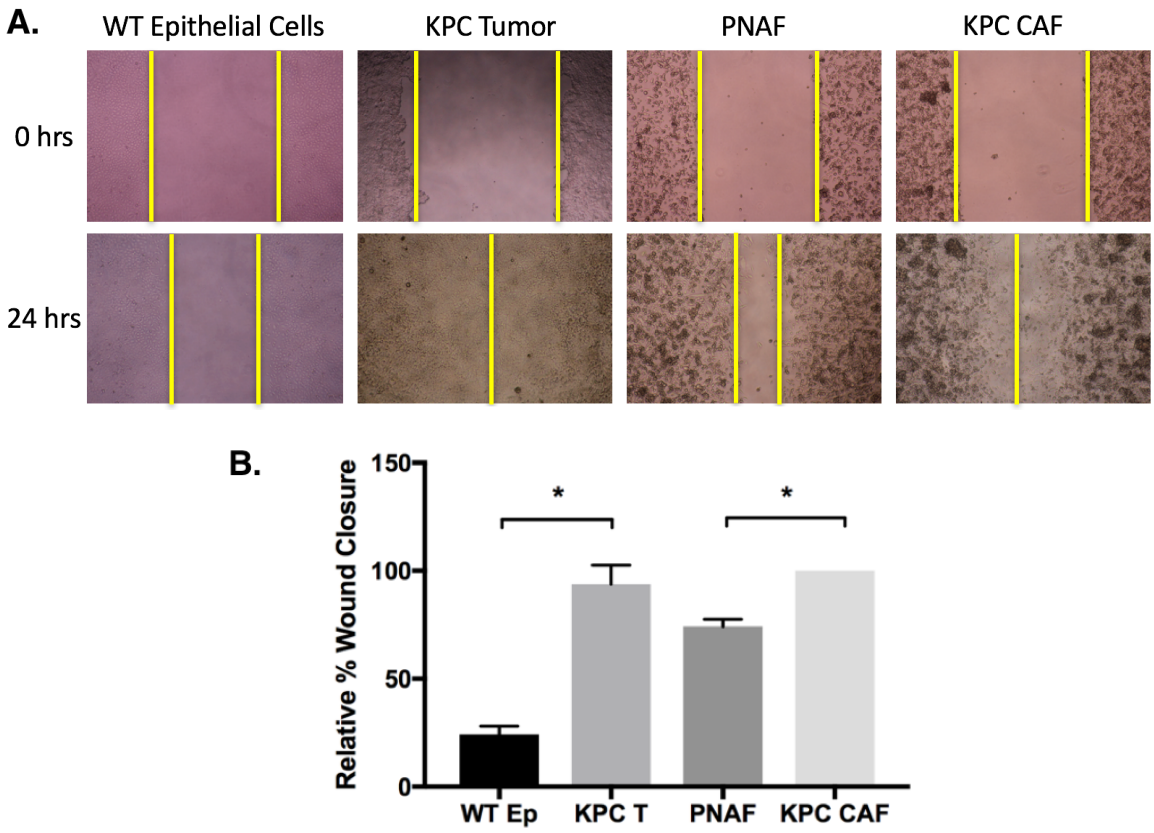

Figure 1.7 Migratory capacities are increased in transformed KPC tumor epithelial cells and activated CAFs.

(A) Representative images of partitions for each cell line at 0 hours and 24 hours. Cells were seeded at high density to produce immediate confluency. Wells were scratched to produce a clear partition at 0 hours. The degree of wound closure was measured 24 hours later normalized to the 0 hour gap.

(B) Quantified relative % wound closure by measuring surface area of partitions at 0 and 24 hours.

miR-21 expression is increased in KPC tumor cells while miR-224 expression is increased in CAFs

Once the primary cell lines of the TME have been isolated and phenotypically validated, we investigated the expression levels of the top 4 dysregulated miRNA candidates over early PDA development in our primary cell lines. The top 4 dysregulated miRNA candidates (miR-21, miR-16, miR-19b, and miR-224) were selected out of those that were validated in-house based on their largest increases in expression over early disease progression. The top 4 miRNAs were also selected due to their sequence homology to human miRNAs; all 4 miRNAs sequences are conserved between mice and humans, allowing for more optimal translational investigation in human models. **Figure 1.8** shows the relative fold changes in expression of miR-21, miR-16, miR-19b, and miR-224 in KPC tumor cells and KPC CAFs as compared to WT pancreatic epithelial cells and PNAFs respectively. miR-21 expression is significantly increased by 7-fold specifically in KPC tumor cells as compared to WT epithelial cells, and miR-224 expression is significantly increased by 10-fold specifically in KPC CAFs as compared to PNAFs. This data demonstrates that the expression of each miRNA varies between specific cell populations in the TME. Furthermore, the activation state of each cell type may regulate or be regulated by changes in miRNA expression. Due to the cell-type specific increases of miR-21 and miR-224 and their regulation of targets in cancer-promoting inflammatory pathways[48] and epithelial-mesenchymal transition[49], we decided to further investigate the mechanistic role of these two miRNAs in regulating the functionalities of our

primary cell lines in the developing PDA TME.

Figure 1.8

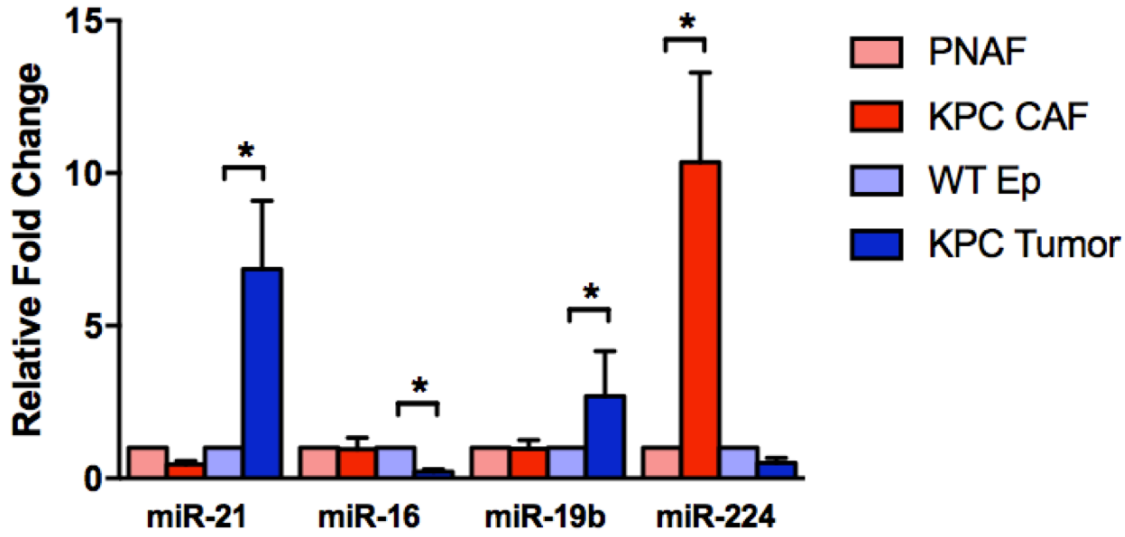

Figure 1.8 Expression of top 4 miRNAs in primary cell lines of PDA TME. Relative fold changes of all 4 miRNAs were quantified using the ΔΔCt method in which all Ct values were first normalized to endogenous control U6 snRNA and KPC tumor and CAF groups were normalized to WT pancreatic epithelial cells (WT Ep) and PNAFs respectively. Error bars represent average ± SE.

miR-FISH analysis to quantify endogenous spatial-temporal expression of miR-21 and miR-224 throughout early PDA development

We employed miRNA fluorescence *in situ* hybridization (miR-FISH) to examine the endogenous expression of miR-21 and miR-224 in specific structures and/or cell populations in early TME progression to PDA. miR-FISH allows the fluorescent visualization of miRNAs in sections of whole tissue. The intensity of the fluorescent signal directly correlates to the amount of endogenous miRNA expression. For the detection of miRNAs in cryosections of whole tissue, we used locked nucleic acid (LNA) probes that are complimentary in sequence and therefore hybridize to miRNAs of interest at specific hybridization temperatures. LNA probes are modified bicyclic RNA nucleotides that exhibit increased thermal stability in a duplex state post-hybridization.[50,51] Additionally, the chemical modification of LNA probes improves mismatch discrimination to increase target accuracy.[51] Increased thermal stability of duplexes in combination with improved accuracy of high-affinity hybridizations, make LNA probes ideal for detecting short miRNA targets.[50,51]

Figure 1.9 shows a general schematic of how miR-FISH detects endogenous miRNA in sections of whole tissue along with representative images of positive and negative controls used to define our experiments. **Figure 1.10** shows the increased spatial-temporal expression of miR-21 specifically concentrated in the ductal epithelial cells of PanIN lesions over PDA development. The quantified fluorescent signal of miR-21 demonstrates that there is a 6-fold increase of miR-21 expression in PDA tissue as compared to the

expression in normal WT C57BL/6 ducts, a fold increase that correlates closely to the fold increase obtained from qPCR analysis of miR-21 expression in KPC tumor cells as compared to WT pancreatic epithelial cells. Interestingly, miR-FISH analysis of miR-224 shows that miR-224 expression is concentrated in the invading stromal compartment surrounding high grade PanIN2/3 lesions and persists to PDA (**Figure 1.11**). The varying compartmental-specific expression of miR-224 in the early stroma mirrors the qPCR findings in primary cell lines in which miR-224 expression is specifically upregulated in KPC CAFs, which are recruited to the site of tumorigenesis, as compared to PNAFs. Moreover, similar to miR-21, the quantified fluorescent signal of miR-224 produced by miR-FISH demonstrates that the 10-fold increase of miR-224 in the stroma surrounding high-grade lesions, correlates closely to the fold increase obtained from qPCR analysis of miR-224 expression in KPC CAFs as compared to PNAFs. Our miR-FISH data not only confirms our qPCR results obtained from analysis of TME cell lines, but also further informs us of the compartmental-specific expression of miR-21 and miR-224 throughout early PDA development.

Figure 1.9

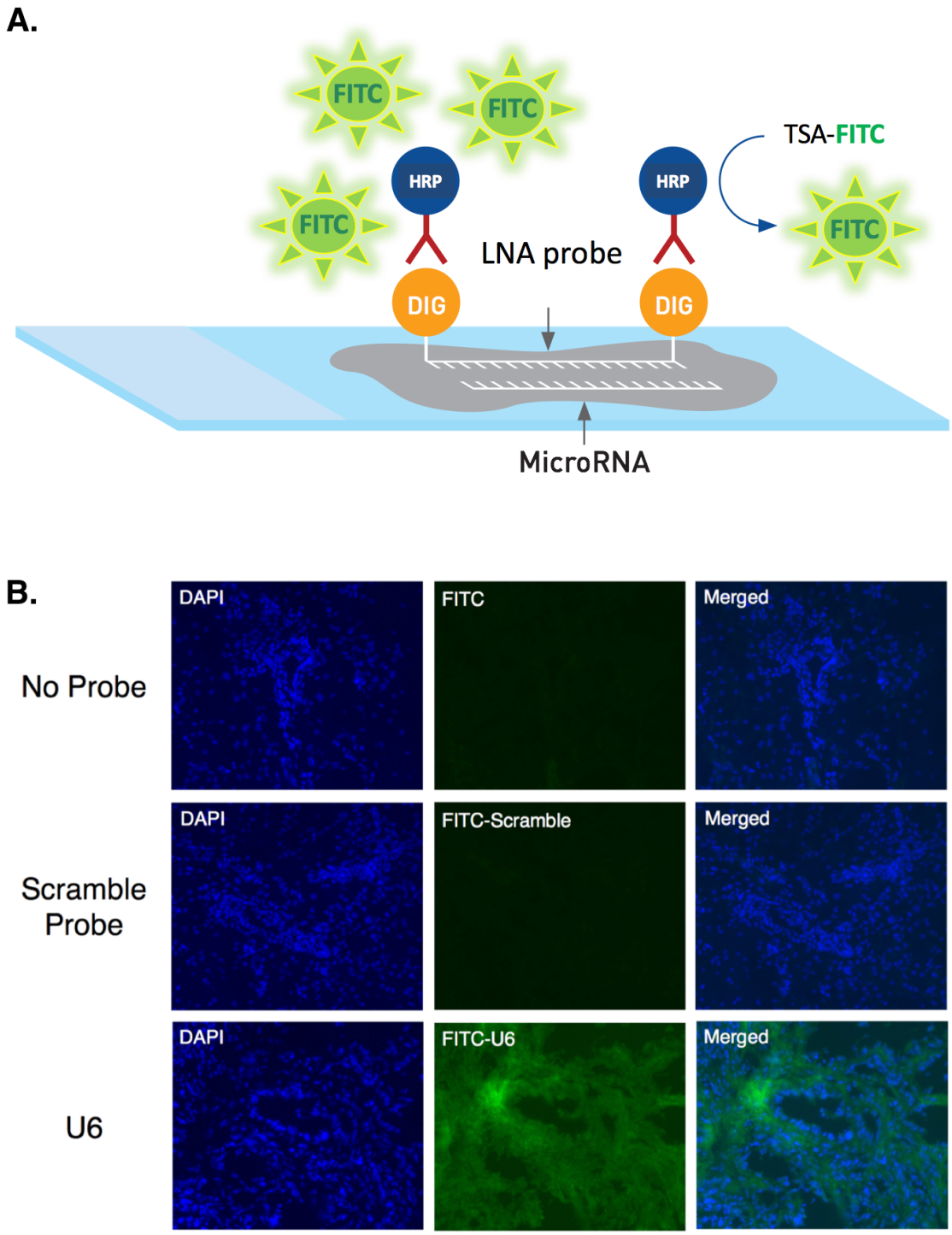
A.
FITC
FITC
FITC
HRP
HRP
TSA-FITC
FITC
LNA probe
DIG
DIG
MicroRNA
B.
No Probe
Scramble Probe
U6
DAPI
FITC
Merged
DAPI
FITC-Scramble
Merged
DAPI
FITC-U6
Merged

Figure 1.9 miR-FISH detects endogenous miRNA in sections of whole tissue.

(A) LNA probes labeled with plant hapten digoxigenin (DIG) will hybridize to complimentary target miRNA sequences in sections of whole mouse pancreas. Sections are then stained with an HRP-conjugated, anti-DIG antibody. Upon application of the detection substrate (TSA-FITC), HRP will catalyze the deposition of FITC where the target miRNA is expressed. The detection substrate amplifies the expression signal by the deposition of many FITC fluorophores proximal to the miRNA of interest. Endogenous miRNA expression is visualized with high resolution by fluorescent microscopy.

(B) Representative fluorescent images of sections of pancreas stained with either no probe, scramble-miRNA probe that doesn't target any miRNA, or U6 positive control probe. No fluorescent signal was observed with no probe or scramble-miRNA probe staining, however strong and ubiquitous fluorescent signal was observed upon staining with U6 positive control probe.

Figure 1.10

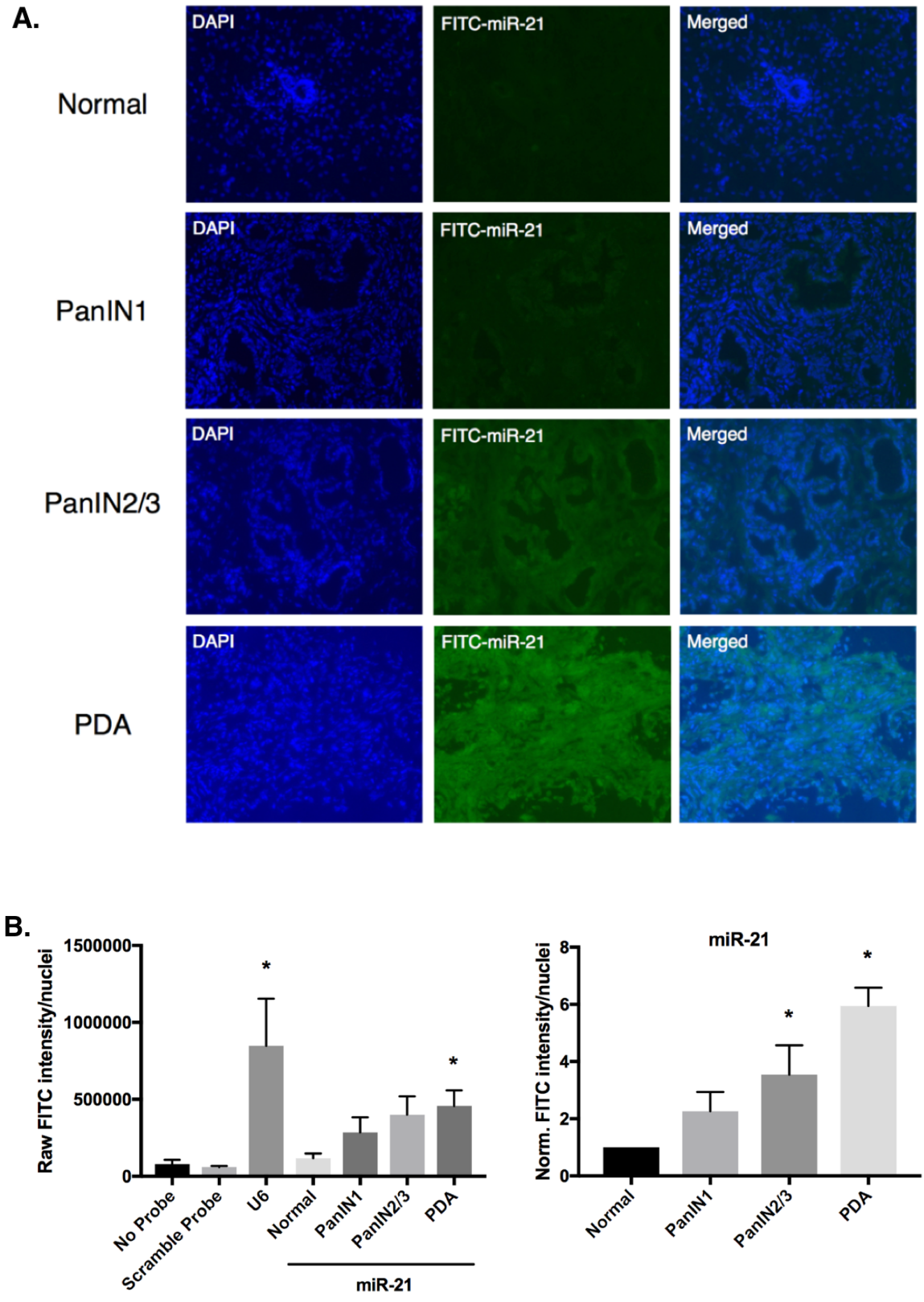
A.
Normal
PanIN1
PanIN2/3
PDA
DAPI
FITC-miR-21
Merged
B.
Raw FITC intensity/nuclei
1500000
1000000
500000
0
No Probe
Scramble Probe
U6
Normal
PanIN1
PanIN2/3
PDA
miR-21
Norm. FITC intensity/nuclei
8
6
4
2
0
miR-21

Figure 1.10 Increased spatial-temporal expression of miR-21 in the developing TME over PDA progression.

(A) Representative fluorescent images of normal ducts, increasing grades of PanIN lesions, and PDA tissue stained with miR-21. Expression of miR-21 is concentrated in ductal epithelial cells.

(B) Quantified image analysis of miR-21 fluorescent signal. Raw fluorescent signals were quantified by FITC intensity/nuclei. PanIN1, PanIN2/3, and PDA raw signals were normalized to that of normal pancreatic ducts of WT C57BL/6 mice to generate relative signal intensities.

Figure 1.11

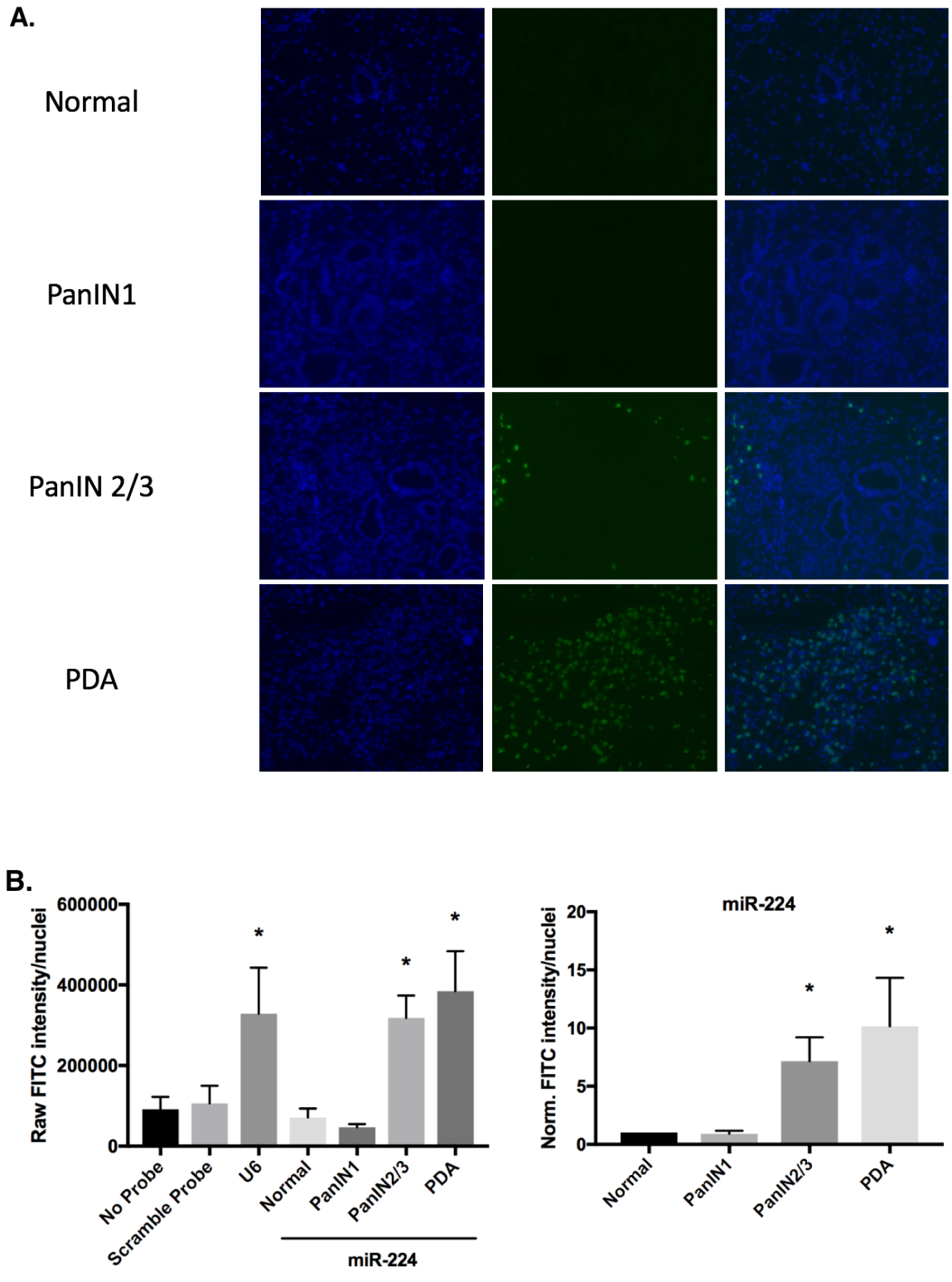
A.
Normal
PanIN1
PanIN 2/3
PDA
B.
Raw FITC intensity/nuclei
600000
400000
200000
0
No Probe
Scramble Probe
U6
Normal
PanIN1
PanIN2/3
PDA
miR-224
miR-224
Norm. FITC intensity/nuclei
20
15
10
5
0
Normal
PanIN1
PanIN2/3
PDA

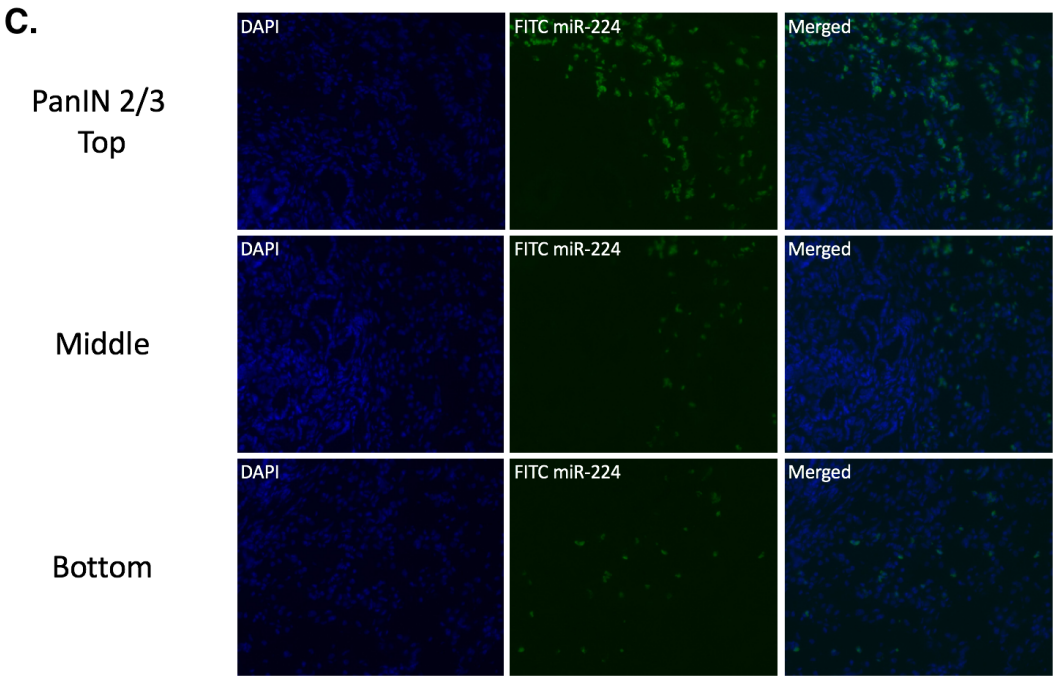

Figure 1.11 Increased spatial-temporal expression of miR-224 in the developing TME over PDA progression.

(A) Representative fluorescent images of normal ducts, increasing grades of PanIN lesions, and PDA tissue stained with miR-224. Expression of miR-224 is concentrated in stromal compartment surround high-grade PanIN2/3 and PDA.

(B) Quantified image analysis of miR-224 fluorescent signal. Raw fluorescent signals were quantified by FITC intensity/nuclei. PanIN1, PanIN2/3, and PDA raw signals were normalized to that of normal pancreatic ducts of WT C57BL/6 mice to generate relative signal intensities.

(C) Tiled fluorescent images of the top, middle, and bottom of the invasive stroma surrounding PanIN2/3 lesions highlighting the stromal compartmentalization of miR-224 expression.

Lentiviral stable transduction of primary cell lines with miR-21 and miR-224 inhibitors and mimics

To investigate how miR-21 and miR-224 functionally regulate early PDA development, we stably transduced the primary cell lines of the TME with miRNA inhibitors and mimics to investigate miR-21's and miR-224's mechanistic roles in mediating early disease progression. Since KPC tumor cells express more miR-21 than WT pancreatic epithelial cells and KPC CAFs express more miR-224 than PNAFs, we used lentiviral vectors to stably inhibit endogenous levels of miR-21 in KPC tumor cells and miR-224 in KPC CAFs. The inhibition occurs through expression of miRNA inhibitors that bind to target miRNAs via sequence complementation to prevent the loading of target miRNAs onto the RISC complex. Conversely, we transduced WT pancreatic epithelial cells and PNAFs to endogenously overexpress miR-21 and miR-224 respectively. **Figure 1.12** shows the miRNA inhibitor construct used, hygromycin selection post-transduction, and transduction efficiency achieved in KPC tumor cells and CAFs. **Figure 1.13** shows the miRNA mimic construct used, puromycin selection post-transduction, and transduction efficiency achieved in WT pancreatic epithelial cells and PNAFs. We sorted by each transduced cell line's fluorescent marker (mCherry or eGFP) to further enrich for stably transduced cells after antibiotic selection. **Table 1.3** summarizes the lentiviral vectors, target cell lines, fluorescent markers, and antibiotic selection used to generate specific stable functionalities for downstream *in vitro* assays. Stable modulation of these miRNAs will allow us to assess whether altering endogenous miRNA levels can

produce specific gain or loss-of-function phenotypes.

Figure 1.12

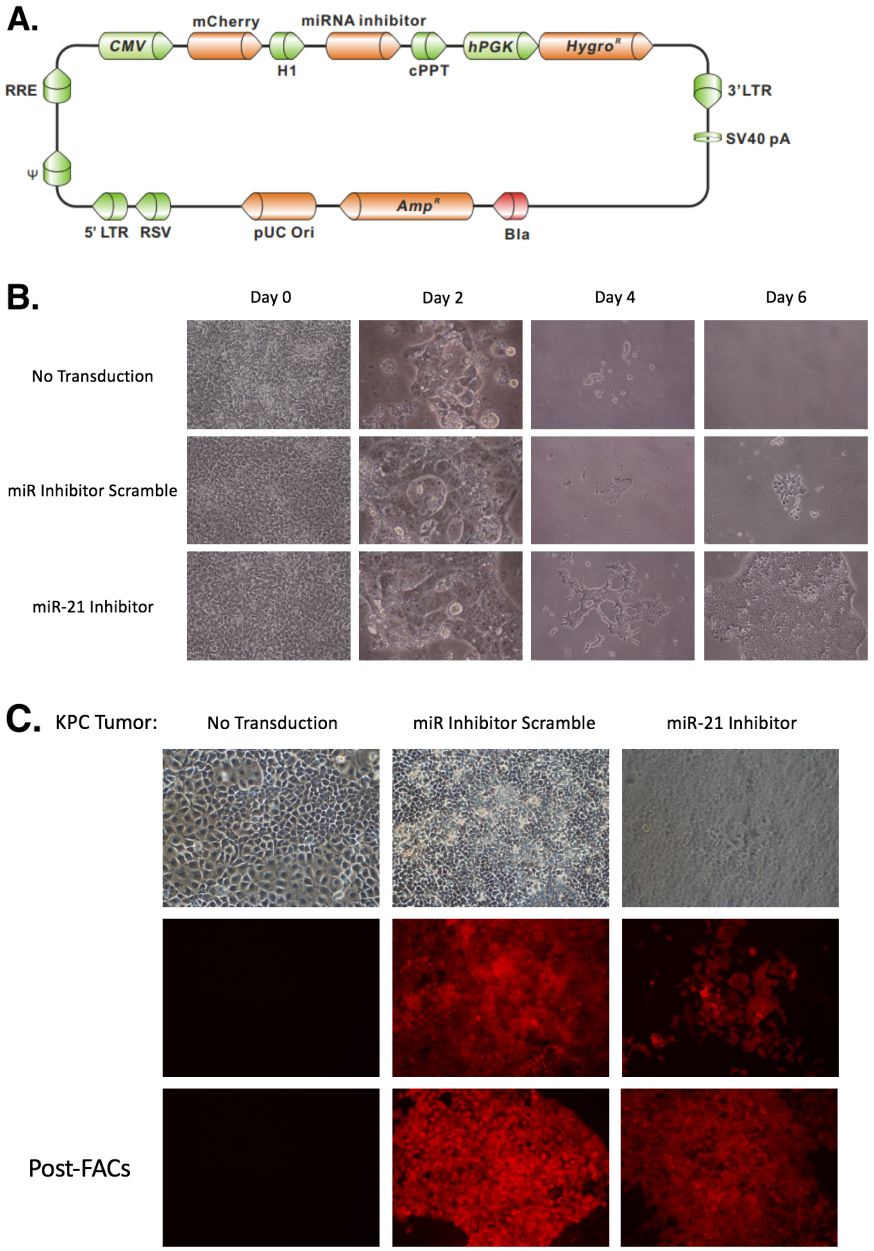

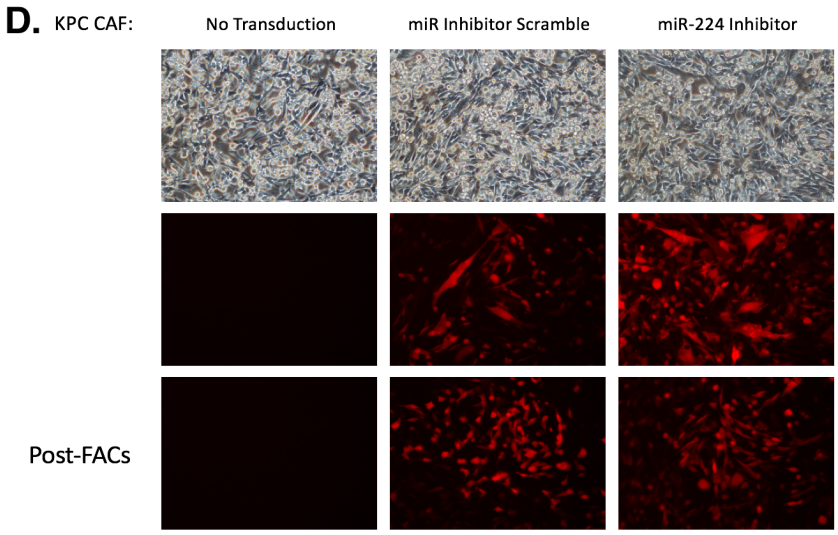

Figure 1.12 Stable inhibition of miR-21 in KPC tumor cells and miR-224 in CAFs.

(A) miRNA inhibitor construct for miR-21 and miR-224

(B) Hygromycin selection of stably transduced cells achieved at day 6 and onward. Non-transduced KPC tumor cells and CAFs did not survive past day 6. However, cells transduced with scramble and miRNA inhibitor constructs possess hygromycin resistance and remain viable beyond day 6 under selection pressure.

(C) Transduction efficiency of KPC tumor cells post-hygromycin selection visualized by mCherry fluorescence. Sorting further enriched for stably transduced KPC tumor cells evidenced by increased mCherry fluorescence.

(D) Transduction efficiency of KPC CAFs post-hygromycin selection visualized by mCherry fluorescence. Sorting maintained high population of stably transduced KPC CAFs.

Figure 1.13

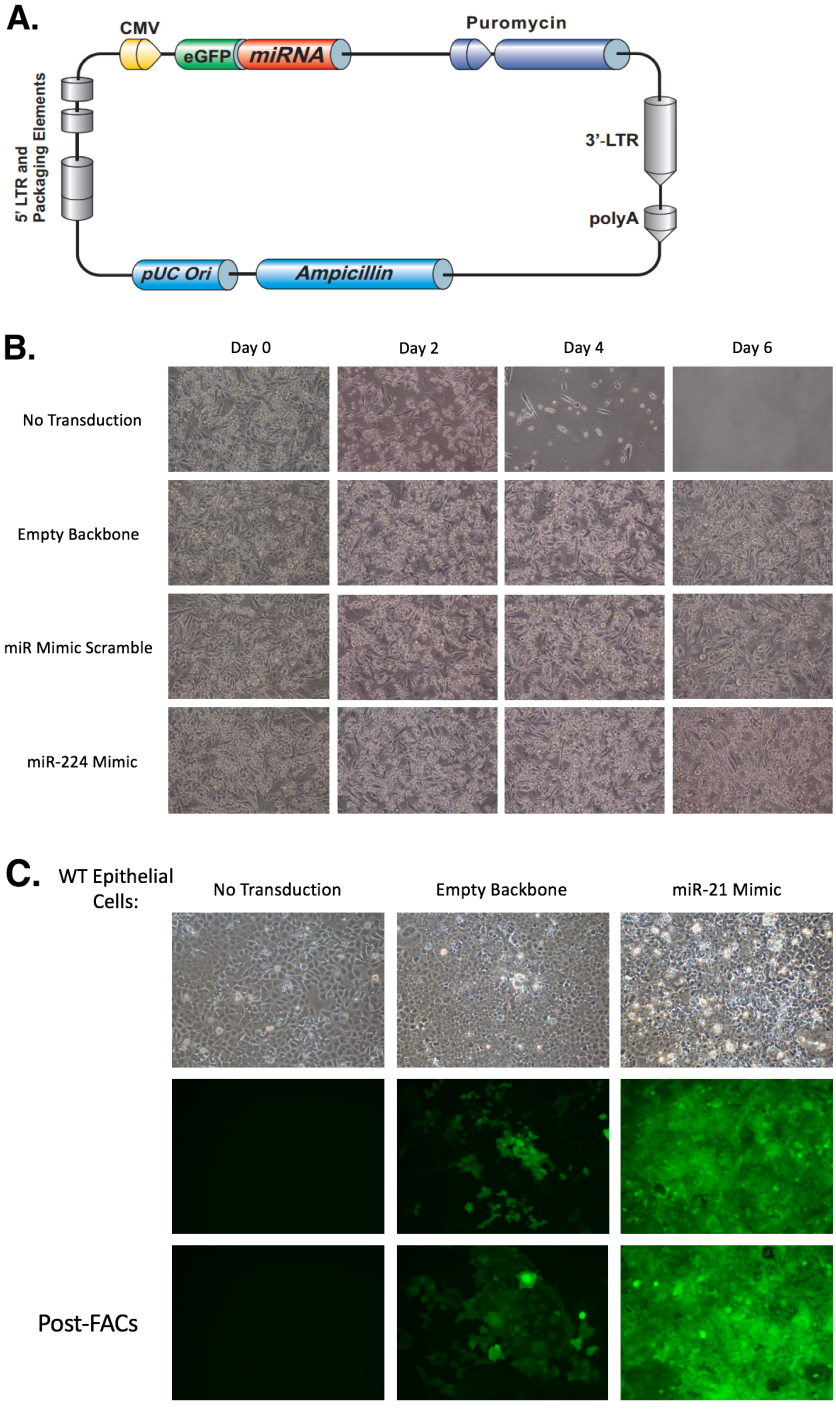
A.
CMV
eGFP
miRNA
Puromycin
3'-LTR
polyA
5' LTR and Packaging Elements
pUC Ori
Ampicillin
B.
Day 0
Day 2
Day 4
Day 6
No Transduction
Empty Backbone
miR Mimic Scramble
miR-224 Mimic
C.
WT Epithelial Cells:
No Transduction
Empty Backbone
miR-21 Mimic
Post-FACs

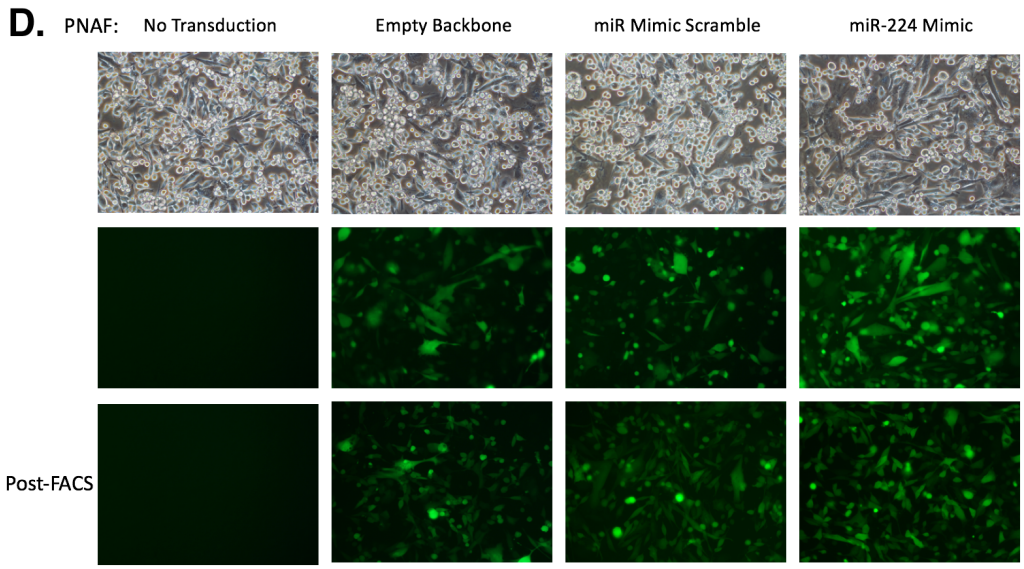

Table 1.13 Stable overexpression of miR-21 in WT pancreatic epithelial cells and miR-224 in PNAFs.

(A) miRNA mimic construct for miR-21 and miR-224

(B) Puromycin selection of stably transduced cells achieved at day 6 and onward. Non-transduced WT epithelial cells and PNAFs did not survive past day 6. However, cells transduced with scramble and miRNA mimic constructs possess puromycin resistance and remain viable beyond day 6 under selection pressure.

(C) Transduction efficiency of WT epithelial cells post-puromycin selection visualized by eGFP fluorescence. Sorting further enriched for stably transduced WT epithelial cells evidenced by increased eGFP fluorescence.

(D) Transduction efficiency of PNAFs post-puromycin selection visualized by eGFP fluorescence. Sorting maintained high population of stably transduced PNAFs.

Table 1.3

Lentiviral Vector	Cell Line Transduced	Function	Fluorescent Marker	Antibiotic Selection
hsa-miR-21 Inhibitor	KPC Tumor	Inhibit miR-21	mCherry	Hygromycin
hsa-miR-224 Inhibitor	KPC CAF	Inhibit miR-224	mCherry	Hygromycin
miR-Scramble Inhibitor	KPT Tumor and KPC CAF	Inhibitor specificity control (does not bind to any miRNA)	mCherry	Hygromycin
hsa-miR-21 Mimic	WT Epithelial cells (WT Ep)	Overexpress miR-21	eGFP	Puromycin
hsa-miR-224 Mimic	PNAF	Overexpress miR-224	eGFP	Puromycin
miR-Scramble Mimic	WT Ep and PNAF	Mimic specificity control (does not bind to any gene target)	eGFP	Puromycin
Empty Vector	WT Ep and PNAF	Transduction control	eGFP	Puromycin

Table 1.3 Summary of lentiviral stable transduction of primary cell lines.

Expression of miR-21 in KPC tumor cells and miR-224 in KPC CAFs are reduced post-stable inhibition

Degree of miRNA inhibition was measured by qPCR to assess whether endogenous expression of miR-21 in KPC tumor cells and miR-224 in CAFs was successfully reduced by stable transduction of miRNA inhibitor constructs. **Figure 1.14** shows the expression of miR-21 and miR-224 post-transduction. Successful transduction of miRNA inhibitor constructs significantly reduced the expression of miR-21 in KPC tumor cells and miR-224 in CAFs by slightly more than 2-fold.

Figure 1.14

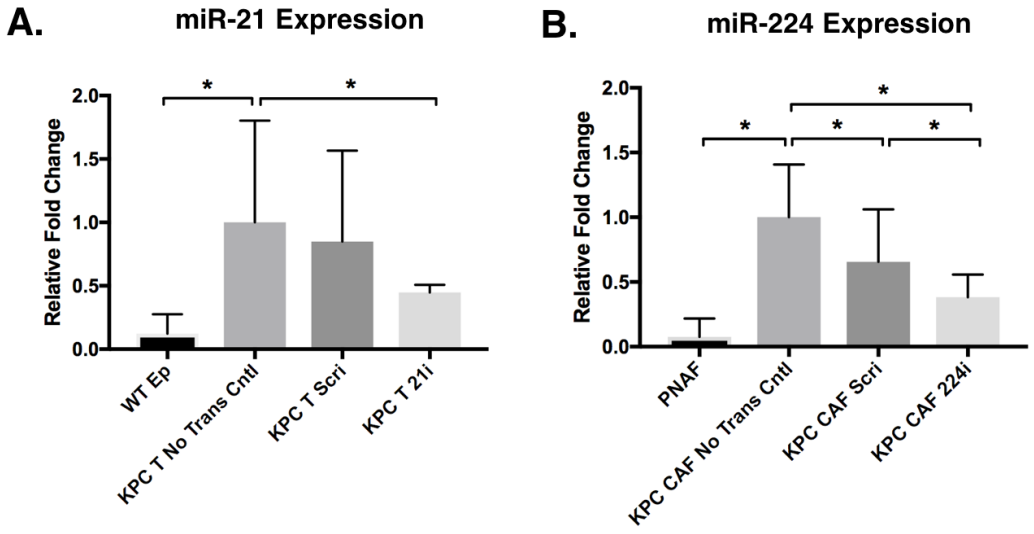

Figure 1.14 Stable transduction of miRNA inhibitor constructs reduced expression of miR-21 and miR-224.

Relative fold changes of miR-21 and miR-224 were quantified using the ΔΔCt method in which all Ct values were first normalized to endogenous control U6 snRNA and all experimental groups were normalized to non-transduced KPC tumor cells and CAFs respectively. Error bars represent average ± SE.

(A) Relative miR-21 expression in WT pancreatic epithelial cells (WT Ep) and KPC tumor cells transduced with either miR-scramble inhibitor (KPC T Scri) or miR-21 inhibitor (KPC T 21i) compared to expression in non-transduced KPC tumor cells.

(B) Relative miR-224 expression in PNAFs and CAFs transduced with either miR-scramble inhibitor (KPC CAF Scri) or miR-224 inhibitor (KPC CAF 224i) compared to expression in non-transduced CAFs.

Inhibition of miR-21 in KPC tumor cells decreased cell proliferation, migration, and invasion

Because endogenous miR-21 expression was successfully reduced in KPC tumor cells post-stable transduction, we next investigated the subsequent functional changes as a result of miR-21 modulation. We therefore measured the proliferative, migratory, and invasive capacities of transduced KPC tumor cells to assess whether these functional phenotypes characteristic of transformed and activated cells were altered (**Figure 1.15**). Our data demonstrates that miR-21 inhibition in KPC tumor cells reduced proliferation by 2-fold as compared to non-transduced KPC tumor cells. Additionally, downregulation of miR-21 expression in KPC tumor cells significantly reduced both migration and invasion to levels comparable to that of WT pancreatic epithelial cells. These findings indicate miR-21 is a powerful mediator of cell proliferation, migration, and invasion and furthermore, that reduction of miR-21 levels in KPC tumor cells can revert the cell's migratory and invasive capacities to normal un-transformed levels.

Figure 1.15

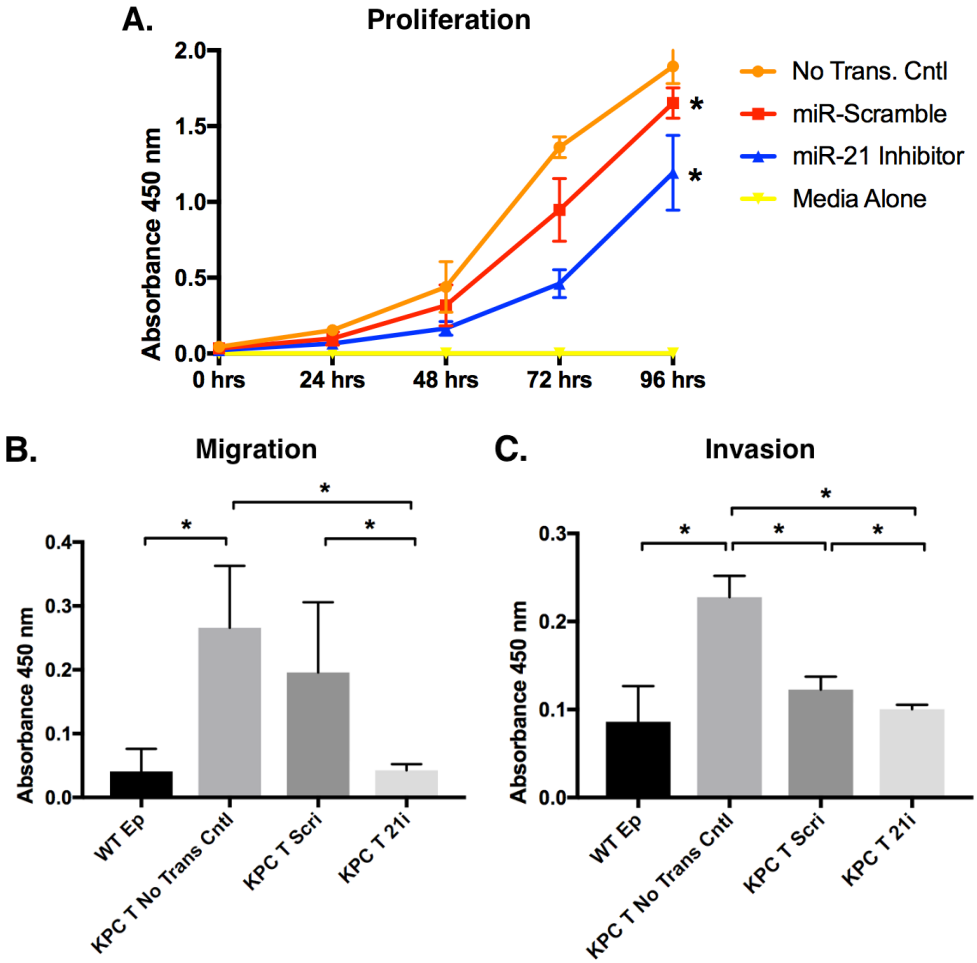

Figure 1.15 Inhibition of miR-21 in KPC tumor cells decreased cell proliferation, migration, and invasion.

(A) Proliferation assay of non-transduced KPC tumor cells, KPC tumor cells transduced with either miR-scramble inhibitor or miR-21 inhibitor, and media alone. Cells were plated at time 0 and proliferation was measured using CCK8 every 24 hours up to 96 hours.

(B) Migration assay of WT pancreatic epithelial cells (WT Ep), non-transduced KPC tumor cells, and KPC tumor cells transduced with either miR-scramble inhibitor (KPC T Scri) or miR-21 inhibitor (KPC T 21i). Cells were seeded in a

transwell without BME coating and migration was measured using CCK8 48 hours later.

(C) Invasion assay of WT Ep, non-transduced KPC tumor cells, KPC T Scri, and KPC T 21i. Cells were seeded in a transwell with 1X BME coating and invasion was measured using CCK8 48 hours later.

Overexpression of miR-224 in PNAFs increased their migratory capacity

Parallel to our investigation of the functional regulation of miR-21 inhibition in KPC tumor cells, we examined the functional effects of endogenous miR-224 overexpression in PNAFs. While additional experiments are currently underway to measure the effects of miR-224 overexpression on PNAF proliferation and invasion, we have shown that PNAF migration is significantly increased as a result of increased miR-224 levels (**Figure 1.16**). The wound-healing assay, also known as scratch assay, demonstrated that, upon upregulation of miR-224 expression, PNAFs increased their migratory capacity by 2-fold compared to non-transduced PNAFs to achieve 100% wound closure after 24 hours of migration. This migratory ability is equal to that of KPC CAFs, indicating that miR-224 overexpression can confer activated functional phenotypes, such as migration, to normal pancreatic fibroblasts.

Figure 1.16

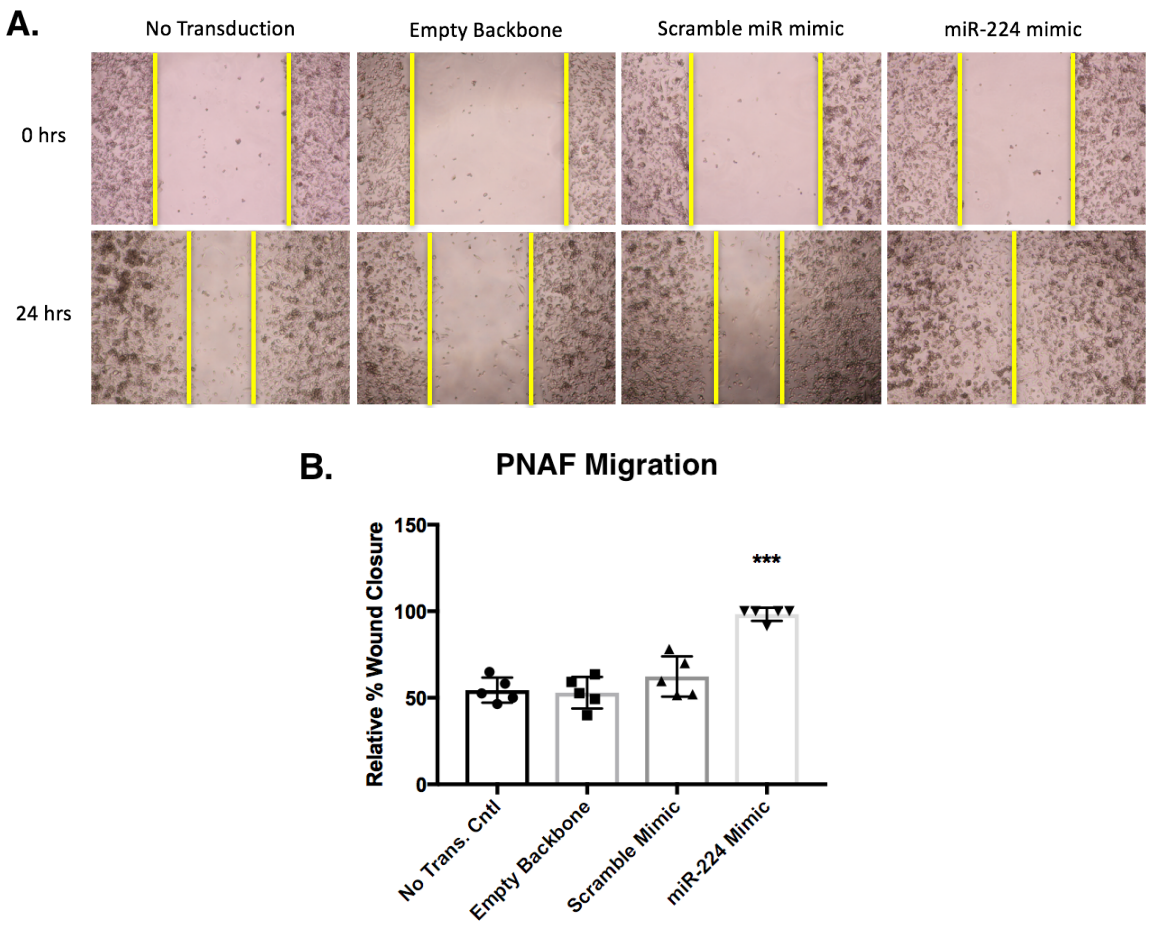

Figure 1.16 Increased PNAF migration due to miR-224 overexpression.

(A) Representative images of partitions for non-transduced PNAFs and PNAFs transduced with either empty backbone, miR-scramble mimic, or miR-224 mimic at 0 hours and 24 hours. Confluent surfaces were scratched to produce a clear partition at 0 hours. The degree of wound closure was measured 24 hours later normalized to the 0 hour gap.

(B) Quantified relative % wound closure by measuring surface area of partitions at 0 and 24 hours.

Comprehensive profile of circulating miRNAs in the serum of KPC mice over early PDA development

The poor prognosis of PDA is due to the late detection of the disease. There is a great need for early biomarkers that can be feasibly used in the clinic to identify individuals with premalignant PanIN lesions before the onset of invasive PDA so that these high-risk individuals may be eligible for curative procedures and therapies. Specific cell-free circulating miRNA profiles have been shown to be indicators of cancer occurrence and are predictors of patient responses to radiation and chemotherapies. Hence, we aim to develop a comprehensive profile of serum miRNAs that may serve as an early signature for the presence of PanIN lesions. Additionally, with the establishment of our in-tissue miRNA profile over early PDA progression, we investigated whether the key miRNAs that are dysregulated in the early TME are reflected in circulation. We assessed whether the levels of dysregulated serum miRNAs mirror those that are dysregulated in tissue, and can therefore be utilized as an accurate and accessible indicator of early disease.

Utilizing our KPC mouse model, we isolated serum from aged KPC mice that possessed specific grades of PanIN lesions and PDA confirmed by histologic analysis. Post-miRNA isolation, expression levels of 750 know murine miRNAs were quantified by the same miRNA microarray platform used to generate our comprehensive in-tissue profile. **Table 1.4** summarizes the top 18 dysregulated serum miRNAs over early PDA development derived from our screen. All fold-changes were quantified using the $\Delta\Delta$Ct method in which all Ct values were first

normalized to endogenous control miR-16, a validated and commonly used internal control for circulating miRNA normalization.[52–55] miR-16's mature sequence is also perfectly conserved between mice and humans.[52] Serum miRNA levels of PanIN1, PanIN2/3, and PDA groups were then normalized to levels obtained from the serum of normal WT C57BL/6 mice. Comparing the top dysregulated miRNAs found in-tissue (**Table 1.2**) to the ones found in serum (**Table 1.4**), only miR-222 is the common miRNA produced from both screens to exhibit the largest increase in expression over early PDA progression. miR-222 increases up to 26-fold in-tissue and up to 2-fold in serum throughout early disease development. Additionally, miR-222, miR-338-3p, miR-190, miR-155, and let-7f have increased expression in human PanINs leading to PDA as shown by Goggins' group.[56] Additional in-house validation of key dysregulated serum miRNAs are necessary and are currently being performed.

Table 1.4

miRNA	Normal	PanIN1	PanIN2/3	PDA	
mmu-miR-467e	1	21.504	44.55	149.354	
hsa-miR-367	1	0.312	0.648	40.286	
hsa-miR-338-3p	1	8.01	3.373	5.112	*
rno-miR-190b	1	13.462	46.877	4.707	
mmu-miR-503	1	5.732	1.62	3.831	
rno-miR-207	1	11.203	2.476	3.273	
hsa-miR-190	1	2.778	22.681	3.266	*
mmu-miR-7b	1	5.32	7.23	3.162	
hsa-miR-125a-5p	1	1.061	1.446	3.161	
mmu-miR-155	1	1.733	188.821	2.941	*
mmu-miR-380-5p	1	3.453	7.576	2.45	
mmu-miR-383	1	4.641	2.502	2.444	
hsa-let-7f	1	21.992	27.353	2.403	*
mmu-miR-467a	1	1.721	5.803	2.209	
hsa-miR-147b	1	0.45	2.026	2.138	
hsa-miR-222	*1*	*1.497*	*1.434*	*2.022*	*
mmu-miR-298	1	0.234	2.902	2.002	
mmu-miR-467c	1	2.472	2.411	1.928	

Table 1.4 Fold changes of top 18 dysregulated serum miRNAs over early PDA development.

Asterisk denotes miRNAs that are also increased in expression in human PanIN lesions.

DISCUSSION

miRNAs are vast and potent regulatory networks that control many signaling pathways and therefore many cell populations within the dynamic PDA TME. Further mechanistic understanding of these regulatory networks will uncover new targets for therapeutic intervention and potential for improving current PDA therapies. In this study, we constructed a comprehensive profile of miRNA expression throughout early PDA development and assessed whether key dysregulated miRNAs can functionally modulate specific cell populations within the PDA TME. Utilizing the KPC mouse model that endogenously develops tissue specific PDA that recapitulates human disease progression, we've elucidated key dysregulated miRNAs whose levels of expression are altered in early PanIN lesions before the onset of invasive carcinoma. Expression levels of miR-21, miR-16, miR-224, and miR-19b are upregulated in early low-grade PanIN1 lesions and consistently increase to established PDA. This data demonstrates that dysregulation of specific miRNAs occurs even in the earliest premalignant lesions following activation of driver mutation *KRAS* which may contribute to early propagation of the disease.

To investigate how these key miRNAs mechanistically regulate PDA progression, we established primary cell lines of the PDA TME for *in vitro* functional studies. A hallmark of PDA is the dense stromal compartment that supports and propagates the tumor, therefore we aim to understand how components of this desmoplastic stroma can be modulated via miRNA mechanisms. CAFs are major constituents of the fibrotic stroma, hence we

established a primary CAF cell line in addition to a tumor epithelial cell line derived from resected primary KPC tumors for our studies. Normal pancreatic fibroblasts and normal pancreatic ductal epithelial cells from WT C57BL/6 mice were obtained for comparison of transformed and activated phenotypes. After all primary cell lines were sorted to enrich for purity, we phenotypically validated each cell line by assessing cell morphology, quantifying expression of specific epithelial (vimentin and E-cadherin) and fibroblast (α-SMA and FAP) markers, and measuring their proliferative and migratory capacities. Each cell lines' transformed and activated states were successfully confirmed. With these 4 phenotypically validated primary cell lines of the PDA TME, we have established an effective *in vitro* model to examine microenvironment dynamics, specifically inter-cell signaling and regulation. These cell lines can also be utilized for future *in vivo* experimentation in immunocompetent C57BL/6 mice of identical background.

To examine how our key miRNAs are regulating cell types within the PDA TME, we first quantified the expression of miR-21, miR-16, miR-224, and miR-19b in our established primary cell lines. We discovered that miR-21 expression was specifically upregulated in KPC tumor cells and miR-224 expression was specifically upregulated in KPC CAFs compared to WT pancreatic epithelial cells and PNAFs respectively. This demonstrates that specific cell populations of the PDA TME have differential abundance of unique miRNAs, suggesting that distinct cell types in the TME are subject to miRNA species-specific regulation. We decided to further investigate miR-21 and miR-224 in early PDA development

due to their KPC tumor cell- and CAF-specific dysregulation. Upon stable lentiviral inhibition and overexpression of miR-21 and miR-224 in our primary cell lines, we found that endogenous inhibition of miR-21 reduced KPC tumor cell proliferation, migration, and invasion. Moreover, the levels of migration and invasion achieved post-miR-21 inhibition in KPC tumor cells were comparable to that of WT pancreatic epithelial cells, demonstrating that miR-21 is a powerful mediator of EMT and its inhibition can revert transformed phenotypes to that of normal untransformed cells. The endogenous overexpression of miR-224 in PNAFs significantly increased their migratory capacity similar to that of CAFs. This may be due to miR-224's targeting and subsequent downregulation of Rho-GTPase activating proteins ARHGAP9 and ARHGAP21 thereby increasing cell motility and migration via activation of the RhoA/ROCK pathway.[57] Additional studies are underway to further investigate the functional consequences of miR-21 and miR-224 modulation in these cell lines. Concurrently, we are utilizing Nanostring to profile the transcriptome and proteome of the stably transduced cell lines to assess the gene targets and major signaling pathways that are regulated by miR-21 and miR-224.

To examine the endogenous spatial-temporal expression of miR-21 and miR-224 in whole tissue over early PDA development, we performed miR-FISH on sections of aged KPC pancreata to observe miRNA specific distributions throughout early disease progression. miR-FISH revealed that miR-21 is expressed at low levels in normal pancreata, but is highly expressed particularly in ductal epithelial cells of high grade PanINs and PDA in KPC pancreata.

Conversely, miR-224 is specifically expressed by the infiltrating stromal compartment surrounding advanced lesions. Quantified fluorescent intensity data strongly correlates with relative expression data from qPCR of miR-21 and miR-224 in KPC tumor cells and CAFs respectively. Collectively, the miR-FISH data demonstrates the compartmental-specific expression of miR-21 and miR-224 in the early PDA TME.

Our study also aimed to explore the potential of utilizing serum miRNA profiles as surrogate diagnostic molecular signatures for the presence of early stage PanINs. Such diagnostic profiles will identify high-risk individuals prone to develop invasive PDA so that they may receive therapies early in disease development to improve prognosis. Our serum miRNA profiling produced 18 key miRNAs in circulation that was increasing in expression over PDA development in KPC mice. Five of which, miR-338-3p, miR-190, miR-155, let-7f, and miR-222, are also found to be increased in human PanIN lesions.[56] Further validation needs to be performed for the top serum miRNA candidates. Once validated, the serum miRNA profile needs to be assessed for its ability to accurately and sensitively detect specific grades of premalignancies in KPC mice. Our data indicates that serum miRNAs can be promising diagnostic tools for early stage PDA screening in the clinic.

miR-21 has been well-studied in many cancers and its oncogenic roles in tumorigenesis and the inflammatory TME have been well-characterized.[48] However, the role of miR-224 in CAFs has not been reported. Our studies show for the first time that miR-224 expression is not only increased in CAFs, but also

specific to the stromal compartment of the early PDA TME *in vivo* and has the ability to increase motility of normal fibroblasts to that of activated CAFs. Taken altogether these data show that CAFs recruited to the PDA TME have high expression of miR-224 which may contribute to the activation of proximal normal resting fibroblasts to exhibit activated phenotypes. This mechanism of action may be mediated by the inflamed PDA TME and subsequent elevated activation of the NFkB pathway in CAFs,[19,58] leading to increased NFkB transcription factor binding directly to the promoter region of miR-224 causing its overexpression.[57] Higher levels of miR-224, encapsulated in exosomes, may also be secreted into the PDA TME to increase migration of proximal normal fibroblasts in a paracrine fashion.

In this study, we have shown miR-21 to be upregulated in transformed KPC tumor cells leading to their increased proliferation and EMT. However, it has been reported that miR-21 is also overexpressed in CAFs, which increases TGFβ-mediated fibrosis via directly targeting SMAD7, an inhibitor of the TGFβ pathway.[31,32] In fact, in vivo inhibition of miR-21 attenuated fibrosis in a mouse model of fibrotic lung disease[31], a finding that is very promising for our efforts to employ miRNA-mediated interception of PDA development because the dense fibrotic stroma is an integral component of the TME that propels PDA. Additionally, miR-21 has been shown to skew tumoricidal pro-inflammatory M1 macrophages to tumor-supportive anti-inflammatory M2 macrophages, or tumor-associated macrophages (TAMs), once recruited to the TME.[48] Therefore miR-21 exerts its oncogenic effects on multiple cell populations in the developing

TME, providing strong rationale for inhibiting this miRNA in early disease progression.

Utilizing our developmental KPC mouse model, we will administer miR-21 and miR-224 inhibitors, either alone or in combination, to KPC mice 4-5 weeks of age in which pancreata will predominantly contain normal ducts and low-grade PanIN1 lesions. After drug regimen, we will histologically analyze the degree of PanIN progression in KPC pancreata and assess whether early intervention with inhibitors that target these oncogenic miRNAs will slow disease progression. We hope that by targeting miR-21 and miR-224 concurrently, we will mount a potent and multi-level attack on the early PDA TME to impede disease progression and establishment.

CHAPTER TWO: Combination immunotherapy intercepts murine pancreatic cancer progression

SUMMARY

Immunotherapy agents that activate T cells are changing clinical treatments for solid metastatic malignancies. Vaccines targeting viral oncogenes successfully prevent the development of hepatocellular and cervical cancers, carcinomas that result from tissue-specific viral infections. We therefore tested the hypothesis that a vaccine targeting the oncogene that initiates pancreatic cancer (PDA) given in combination with immunotherapy agents that reprogram the earliest procarcinogenic inflammatory changes will slow or intercept PDA development. The *KRAS* oncogene is a driver mutation expressed in >90% of pancreatic intraepithelial neoplasms (PanINs) and an ideal candidate target for early vaccination against PDA. However, even early PanINs have immunosuppressive microenvironments that highly express inhibitory immune checkpoint molecules like CTLA-4, and are well-infiltrated with immunosuppressive cell populations such as T regulatory cells (Tregs) that significantly dampen the efficacy of current immunotherapies.

The overall goal of our study is to reprogram the immunosuppressive TME while specifically activating immunity against early premalignancies to prevent PDA development. We previously reported that early dosing of *Kras*$^{G12D/+}$*;Trp53*$^{R172H/+}$*;Pdx-1-Cre* (KPC) mice, a spontaneous model of human PDA tumorigenesis, with the Treg depleting and inactivating agents cyclophosphamide (Cy) and PC61 antibody in combination with an attenuated

Listeria monocytogenes vaccine expressing mutant $KRAS^{G12D}$ (LM-Kras) can slow tumorigenesis in 40% of mice. In this study, we aimed to improve the efficacy of this vaccine approach by specifically inhibiting the immunosuppressive effects of the CTLA-4 immune checkpoint on Tregs with a CTLA-4 blocking antibody to enhance activation of the immune system against early lesions.

KPC mice at 4-5 weeks of age with low-grade PanIN1 lesions received 2 doses of LM-Kras and Cy/PC61 and 8 doses of anti-CTLA-4 antibody. Control mice received isotype antibody with LM-Kras and Cy/PC61 or no treatment. At the end of the drug regimen in which KPC mice were 10-11 weeks of age, pancreata were histologically evaluated for various grades of PanINs or PDA tissue to assess degree of disease progression. Mice that received triple treatment (LM-Kras, Cy/PC61, and anti-CTLA-4) had a significantly lower incidence of PanINs and PDA compared to controls. Furthermore, they did not develop lesions beyond PanIN1, indicating that the combination therapy may halt PDA development at early stages.

To investigate the immune profiles of mice receiving treatment, flow cytometry was performed on tumor-infiltrating lymphocytes (TILs) isolated from pancreata to assess abundance of Tregs, infiltration of effector and memory T cell populations, and expression of inhibitory immune checkpoint molecules. Mice that received triple combination therapy had decreased numbers of Tregs, decreased expression of specific immune checkpoints, increased activation of cytotoxic CD8+ T cells that produced more effector cytokines, increased memory T cells, and higher CD8+ T cell to Treg ratio in the microenvironment compared

to controls. Additional mechanistic studies are underway to further characterize the immune changes in the microenvironment following treatment. Collectively, our data demonstrates that our combination treatment successfully reprograms the early TME through several immune mechanisms to intercept PDA development.

INTRODUCTION

The field of cancer immunoprevention has achieved significant progress in the last two decades with the implementation of prophylactic vaccines that target viral oncogenes to prevent the development of primary cancers that result from chronic viral infections.[59] These "infectious tumors" account for 10-20% of all human tumors.[60] The most successful examples of cancer-preventing prophylactic vaccines are ones that target hepatitis B virus (HBV) and human papillomavirus (HPV).[60–62] Initially developed to prevent acute chronic hepatitis, the HBV vaccine produced the unexpected beneficial effect of dramatically reducing the incidence of post-hepatitis hepatocellular carcinoma.[60,61] However, the original intent of developing the HPV vaccine was to prevent cervical cancer caused by persistent HPV infection, hence the HPV vaccine was the first "pure" implementation of human cancer immunoprevention.[60] Although the efficacy of HPV vaccines in preventing cervical cancer has yet to be fully determined due to its recent worldwide distribution, the very promising results from ongoing clinical trials predict a near complete prevention of cancer occurrence.[60] Since the majority of human cancers are not caused by viral infection, the next step and current goal in the field is to translate the successes of prophylactic vaccine development against infectious tumors to the development of immune-based strategies to prevent non-infectious tumors.[63]

The successful immunoprevention of the remaining >80% of human cancers not induced by viral infection relies on strategic vaccine design. Selection of target antigen determines tumor-specific vaccine efficacy, degree of

immunologic response, and potential of associated toxicities. An optimal antigen target should be an early alteration of a normal gene that is likely an initiator (driver) of tumorigenesis so that the immune response is directed toward a "causative" signal without which the developing tumor cannot survive.[3,63] Vaccination against such a target is likely to produce an immunologic response that is both efficacious and the least toxic, mounting a focused and concerted immune response to early neoplasms.[63,64] There are major classifications of tumor antigens that are currently being utilized as targets for prophylactic vaccine efficacy studies. Tumor specific antigens (TSAs) are exclusively expressed on tumor cells and not on any other cell, therefore these targets are unique to the tumor and are optimal candidates for vaccine-based immunotherapies due to their specificity. TSAs are often mutated proteins such as KRAS, HER-2/neu, and EGFR.[2,65–67] Tumor associated antigens (TAAs), however, are endogenous antigens present on both tumor and normal cells but are overexpressed specifically in transformed cells. MUC1, Cancer-testis (CT) antigens, and ENO1 are examples of TAAs currently under investigation.[62,68–71] Specifically in PDA, mutant KRAS is an ideal TSA for early immune-mediated disease interception due to its mutated state conferring target specificity, role as a driver mutation of PDA tumorigenesis, high expression throughout premalignant progression (90% in PanIN1 lesions and 95% in PDA)[2], and accessible location on the plasma membrane for immune recognition. Hence for our vaccine studies, we have utilized a $KRAS^{G12D}$ for targeted PDA intervention.

Mutant KRAS not only transforms ductal epithelial cells, but it also

simultaneously establishes and propagates the early desmoplastic stroma to create an immunosuppressive, non-immunogenic TME. The PDA TME contains many immunosuppressive immune populations that are either directly recruited to the site of tumorigenesis or become reprogrammed to exhibit immunosuppressive phenotypes once exposed to the abundant pro-tumorigenic signaling in the local TME (**Figure 2.1**). The transformed tumor cells expressing mutant *KRAS* secrete IL-6, IL-8, and granulocyte macrophage colony stimulating factor (GM-CSF) that recruit Tregs and myeloid-derived suppressor cells (MDSCs) to the early TME.[72–74] Tregs are a major immune inhibiting population that produces immunosuppressive cytokines TGFβ and IL-10.[73] Additionally, Tregs express the immune checkpoint molecule cytotoxic T lymphocyte associated protein 4 (CTLA-4) that tethers co-stimulatory signals, thereby inhibiting CD4 and CD8 activation and expansion.[72,73] MDSCs, upon TME infiltration, produce reactive oxygen species that result in T cell apoptosis.[75] They also deplete L-arginine, an essential amino acid necessary for T cell function.[75] CCL2, CSF-1, and VEGF are also secreted by tumor cells to recruit circulating monocytes to the TME where they are locally induced by TGFβ and IL-10 to become tumor-associated macrophages (TAMs) that closely resemble anti-inflammatory M2 macrophages.[76,77] In addition to the inhibitory immune checkpoint CTLA-4, the PDA TME is also rich in other checkpoint molecules such as PD-L1 and LAG-3.[73] Collectively, the cellular pathways and signaling mechanisms that normally prevent auto-immunity are exploited by the tumor and TME to promote immune inactivation and tolerance, ultimately allowing the

developing tumor to evade immune recognition and eradication. Therefore, combination immunotherapy must be employed to both activate the immune system against driver mutations and reprogram multiple immunosuppressive mechanisms in the early PDA TME to prevent disease progression.

Figure 2.1

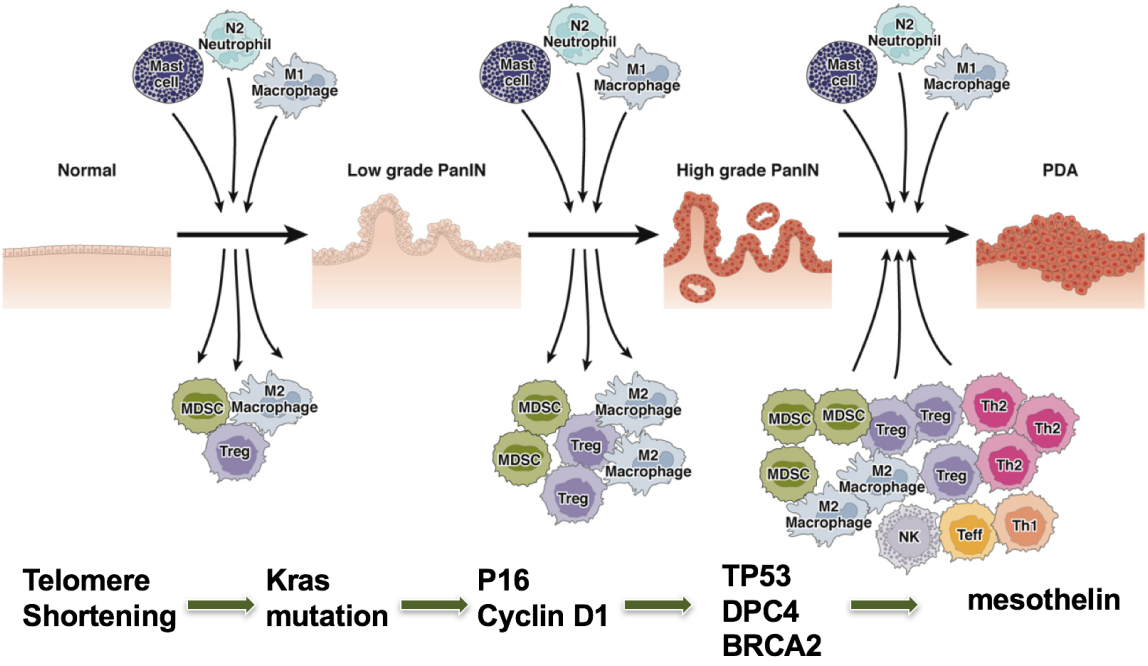

Figure 2.1 Genetic changes recruit and reprogram immune populations in the early PDA TME.

Figure from Zheng et al.[72]

The timing of immunotherapeutic administration determines disease prevention efficacy. It has been shown that inactivation of mutant *KRAS* only at the early PanIN stage in an inducible mouse model of endogenous PDA led to complete tissue recovery: lesion regression, metaplasia reversal, and stromal

remodeling.[3] While inactivation of mutant *KRAS* at later stages (during high-grade PanINs) during did not achieve full tissue regression, but led to massive local cell death. This finding not only further emphasizes the requisite role of mutant *KRAS* activation in forming and maintaining the TME, but it demonstrates that mutant KRAS intervention needs to occur at early stages of PanIN development in order for complete reversal of premalignant lesion and stromal formation, before cells are in a state of oncogene addiction.[3] This finding is also supported by our group in which only the early administration of LM-Kras vaccine in combination with Treg depleting and inactivating agents conferred survival benefit to KPC mice. However, mice that received LM-Kras vaccine alone did not have increased overall survival or delayed PanIN progression despite early administration and significant peripheral mutant KRAS-specific CD8 T cell responses.[78] These data demonstrate that the early vaccine-mediated targeting of mutant KRAS needs to be coupled with early adjuvant modulation of the immunosuppressive TME so that the primed and activated antigen-specific T cells can traffic to and infiltrate the TME, while remaining activated to recognize its antigenic target to achieve tumor cell killing.[78,79] Our study aims to build upon the findings of Keenan et al. by adding immune checkpoint blockade to our combination immunotherapy to further reduce inhibitory TME signaling and enhance immunity against early PDA development.

For our studies, we utilized recombinant live-attenuated intracellular bacterium *Listeria monocytogenes* expressing $KRAS^{G12D}$ (LM-Kras) as a vaccine to induce potent innate and adaptive immune responses against mutant

$KRAS^{G12D}$ tumor antigen. Upon vaccination, LM-Kras is actively phagocytosed by antigen-presenting cells (APCs) where $KRAS^{G12D}$ is secreted into the cytosol and subsequently processed and presented through both class I and II antigen-processing pathways, inducing specific CD4 and CD8 T cell immunity.[80] The strain of *Listeria* used has a deletion of two virulence factors ActA (Δ*actA*) and Internalin B (Δ*inlB*) that significantly reduces its toxicity (>1000 fold reduction as compared to WT *Listeria*) while maintaining it immunopotency *in vivo*.[81] Δ*actA* blocks cell-to-cell infection from adjacent phagocytic cells, while Δ*inlB* prevents infection of nonphagocytic cells.[81] Vaccinated mice produced durable effector and memory T cell responses without liver toxicity.[81] In clinical trials, an LM vaccine expressing mesothelin safely induced mesothelin-specific T cell responses in patients with lung, ovarian, and pancreatic cancers.[82] *Listeria*-based vaccines are effective in delivering TSAs and TAAs to elicit potent antitumor immune responses.

Inhibitory Tregs in the early TME are inactivated and depleted using a low dose of Cyclophosphamide (Cy), a chemotherapeutic DNA-alkylating agent[83], in combination with PC61 monoclonal antibody. Naturally occurring Tregs are a subset of CD4 T cells that play a critical role in the maintenance of self-tolerance.[84] However, in the context of cancer, their immunosuppressive functions facilitate tumor progression by preventing the activation of effector T cells in the TME. Tregs specifically express Foxp3, a transcription factor that is essential for the development of their regulatory phenotype.[85] Foxp3 produces TGFβ, an immunosuppressive cytokine that further expands Tregs, polarizes

TAMs/M2 macrophages, and increases stromal fibrosis to support the developing tumor.[73,85] Additionally, Tregs induce *in vitro* and *in vivo* effector T cell apoptosis by sequestering IL-2 through the constitutive expression of high-affinity IL-2 receptors, depriving the local environment of this key pro-inflammatory cytokine.[86] The number of Tregs in the TME increases as premalignancies advance to PDA[78] (**Figure 2.2**), and high frequency of tumor-infiltrated Tregs correlate with poor patient survival in many solid malignancies.[85] Therefore, to reduce Tregs in the TME, we utilized a low dose of Cy, which selectively suppresses Tregs at low concentrations[83,87], and PC61 antibody that binds to CD25 specifically on Tregs leading to depletion via macrophage phagocytosis.[88]

Figure 2.2

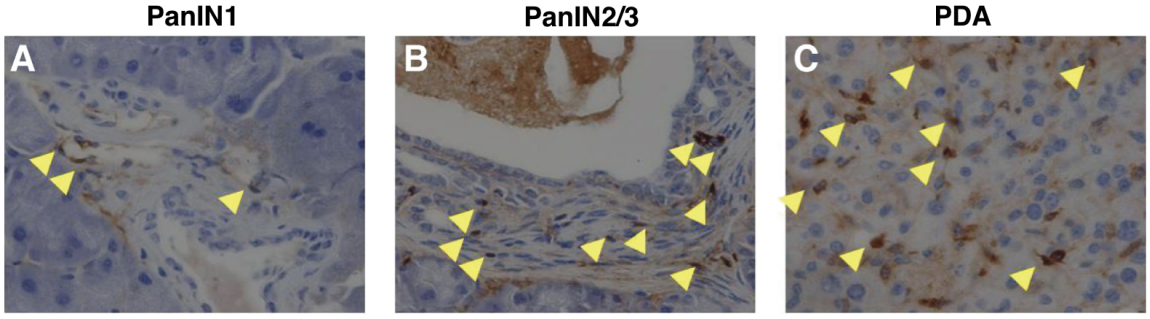

Figure 2.2 Increasing numbers of Foxp3$^+$ Tregs in KPC premalignant lesions to PDA.

Figure from Keenan et al.[78]

The third component in our combination immunotherapy is anti-CTLA-4 immune checkpoint inhibitor. CTLA-4 is a key negative regulator of T cell activation. It is an inhibitory checkpoint molecule expressed on the surface of T

cells post-activation to attenuate excessive immune stimulation in order to preserve self-tolerance; therefore, CTLA-4 is critical for maintaining immune homeostasis.[89] CTLA-4 has shared ligands with costimulatory receptor CD28.[89,90] However, when expressed, CTLA-4 binds with higher affinity, and therefore outcompetes CD28 for the binding of their shared ligands B7.1 (CD80) and B7.2 (CD86) on APCs.[89,90] CTLA-4's tethering of the shared ligands prevents transmission of CD28's costimulatory signal so the T cell remains inactivated in a state of anergy.[89,90] Although conventional T cells will express CTLA-4 upon activation, Tregs highly express CTLA-4 constitutively which greatly contributes to their suppressive role in the TME.[89,90] Due to this mechanism of inhibition, CTLA-4 compromises T cell survival, expansion, and recognition of target antigen, providing strong rationale for inhibiting this molecule to activate the immune system against early neoplasms.[89] Administration of CTLA-4 inhibitor depletes Tregs to enhance antitumor efficacy in mouse models of melanoma.[91,92] CLTA-4 blocking antibody mediates Treg depletion by binding to the receptor and triggering antibody-dependent cell-mediated cytotoxic (ADCC) lysis by nonclassical monocytes.[93] The fully humanized monoclonal CTLA-4 blocking antibody, Ipilimumab, was approved by the FDA in 2011 for the treatment of metastatic melanoma, and while single agent therapy was effective in immuno-permissive cancers such as melanoma, it failed in patients with refractory, immunologically "cold" cancers such as PDA in which the immunosuppressive TME is a formidable barrier to immune infiltration.[79,94,95]

Therefore, multi-component combination therapy must be utilized to produce a well-infiltrated, immunogenic early PDA TME for disease interception.

MATERIALS & METHODS

KPC Mice

Lox-STOP-Lox-*Trp53*$^{R172H/þ}$; Lox-STOP-Lox-*Kras*$^{G12D/þ}$; and Pdx-1-Cre strains on a mixed C57BL/6 background, were gifted from Dr. David Tuveson (Cold Spring Harbor Laboratory, Cold Spring, NY). These mice were backcrossed to the C57BL/6 genetic background for 12 generations and interbred to obtain KC and KPC mice. All animals were kept in pathogen-free conditions and treated in accordance with Institutional Animal Care and Use Committee of the Johns Hopkins University and American Association of Laboratory Animal Care approved guidelines.

Vaccine and Drug Treatments

Vaccine and immunotherapeutic agents were administered to KPC mice according to the dosing scheme outlined in **Figure 2.3**. LM-Kras (Aduro Biotech) 5 x 10^5 colony-forming units in 0.2 mL phosphate-buffered saline was administered intravenously (IV). Stock titers were determined for each batch of vaccine by dose titrations on brain heart infusion (BHI) agar plates. PC61 (50 μg/mouse)[96] and cyclophosphamide (Cy) (100 mg/kg; Bristol- Myers Squibb) were administered by intraperitoneal injection (IP). Anti-CTLA-4 (clone 9H10) or isotype antibody (both 100 μg/mouse; BioXcell) was also administered by IP.

Histologic Analysis of PanIN Lesions

At the end of the drug regimen, pancreata of KPC mice were formalin-fixed and paraffin-embedded, sectioned, and stained using routine H&E protocols by the Johns Hopkins University Oncology Tissue Services. For the assessment of drug treatment effects, 2 slides from each pancreas spaced 400 μm apart were graded based on the highest PanIN stage (or PDA) present by a pathologist (R.A. Anders) blinded to the treatment group.

Isolation of Tumor-Infiltrating Lymphocytes (TILs)

Pancreata were excised immediately after KPC mice were euthanized and placed in IMDM media (Life Technologies) supplemented with 5% FBS (Gemini Bio-products), 1% L-glutamine (Life Technologies), penicillin (50 U/ml)/streptomycin (50 μg/ml) (Life Technologies), and 0.09% 2-mercaptoethanol (Gibco). Pancreata were weighed, diced into small 2-3 mm pieces, and dissociated using the Tumor Dissociation Kit mouse (Miltenyi) and gentleMACS Octo Dissociator (Miltenyi) according to the manufacturer's protocols for soft and medium or tough tumors in the pancreata. The heating functionality was always applied. After tissue dissociation, cell suspensions were quenched with IMDM media, spun down for 10 minutes at 1700 rpm at 4 degrees, resuspended in IMDM, and mashed through a 70 μm strainer to produce a single cell suspension. We performed a 40%:80% percoll (GE Healthcare) gradient to isolate lymphocytes from whole cell suspension. Gradients were spun at 3500 rpm at room temperature for 25 minutes. Once the lymphocyte layer at the gradient interface was extracted, cells were quenched with IMDM, spun down, and counted. Lymphocytes were stimulated overnight (17 hours) in a 37 degrees

humidified incubator (37 degrees, 5% CO_2) using Dynabeads Mouse T-Activator CD3/CD28 magnetic beads (Gibco) per the manufacturer's instructions. Protein transport inhibitor GolgiPlug (BD Biosciences) was applied to lymphocytes during the last 5 hours of stimulation for the accumulation of intracellular cytokines. Post-stimulation, CD3/CD28 magnetic beads were removed using DynaMag-15 magnet (Thermo Fisher Scientific).

Cytokine Staining and Flow-Cytometry

Lymphocytes were washed with PBS, stained with LIVE/DEAD Fixable Aqua (Life Technologies) for 30 minutes on ice in the dark, washed 2 times with PBS, Fc blocked with anti-mouse CD16/CD32 (BD Biosciences) for 15 minutes on ice, and stained for surface markers diluted in FACS buffer (PBS with 1% FBS and 0.1% NaN_3) for 30 minutes on ice in the dark. Cells were washed 3 times with FACS buffer, fixed and permeabilized using the Foxp3 Transcription Factor Staining Buffer Set (eBioscience) for 30 minutes at 4 degrees in the dark, washed twice with permeabilization buffer (eBioscience), Fc blocked for 15 minutes on ice, and stained for intracellular markers for 1 hour at 4 degrees. After 3 washes with permeabilization buffer, cells were resuspended in FACS buffer and run on a Gallios flow cytometer (Beckman Coulter) after overnight storage at 4 degrees in the dark. Analysis was performed using FlowJo (Tree Star). All antibodies used for cytokine and marker staining are listed in **Table 2.1**.

Table 2.1

Antibody	Fluorochrome	Clone	Vendor
CD4	PerCP-Cyanine5.5	RM4-5	eBioscience
CD8	APC-Fire 750	53-6.7	BioLegend
CTLA-4	PE	UC10-4F10-11	BD Biosciences
PD-1	PE-Cyanine7	J43	eBioscience
Lag3	Brilliant Blue 515	C9B7W	BD Biosciences
Galectin-3	AF647	M3/38	BioLegend
Foxp3	AF700	FJK-16s	eBioscience
IFNγ	PerCP-Cyanine5.5	XMG1.2	eBioscience
TNF-α	AF700	MP6-XT22	BD Biosciences
Granzyme B	FITC	NGZB	eBioscience
CD44	Pacific Blue	IM7	BioLegend
CD62L	APC	MEL-14	BD Biosciences

Table 2.1 Flow Cytometry Antibodies

Statistical Analysis

Statistical analysis was performed using GraphPad Prism v7.0b (GraphPad Software). The data are presented as the means ±SEM. For the analysis of PanIN lesions, the Mann-Whitney test was used to compare ranks between treatment groups. Comparisons between multiple groups were made using one-way or two-way ANOVA. For all analyses, P-values ≤ 0.05 were considered statistically significant.

RESULTS

LM-Kras vaccine, Treg depleting agents, and CTLA-4 inhibition in combination intercepts PanIN progression

Utilizing our developmental KPC mouse model, we strove to improve upon what our group has previously shown that by early administration of driver mutation $KRAS^{G12D}$-targeting vaccine LM-Kras in combination with Treg depleting and inactivating agents Cy and PC61, we can successfully delay PDA progression at early premalignant stages by inducing $KRAS^{G12D}$-specific immunity and reprogramming the immunosuppressive TME. We have supplemented this immunotherapy with anti-CTLA-4 checkpoint blockade to reduce the inhibitory effects exerted on the immune system by this molecule, while simultaneously further depleting Tregs in the developing TME. We dosed KPC mice according to the timeline in **Figure 2.3a**. After 6 weeks of drug treatment, when KPC mice were 10-11 weeks old, we performed gross pathological analysis of the PanINs present in the pancreata of various treatment groups to assess the physiological effects our combination immunotherapy has on PDA progression. Our histology data (**Figure 2.3b**) revealed that KPC mice that had received triple treatment (LM-Kras, Cy/PC61, and anti-CTLA-4 antibody) developed significantly lower grades of PanIN lesions than all other groups. Furthermore, triple treatment mice did not develop lesions beyond low-grade PanIN1 indicating that triple combination immunotherapy was more effective at impeding PDA developing than what our group has previously achieved. Observing this promising physiological effect, we proceeded to investigate the

immune mechanisms that were being modulated by triple combination immunotherapy to halt PanIN progression.

Figure 2.3

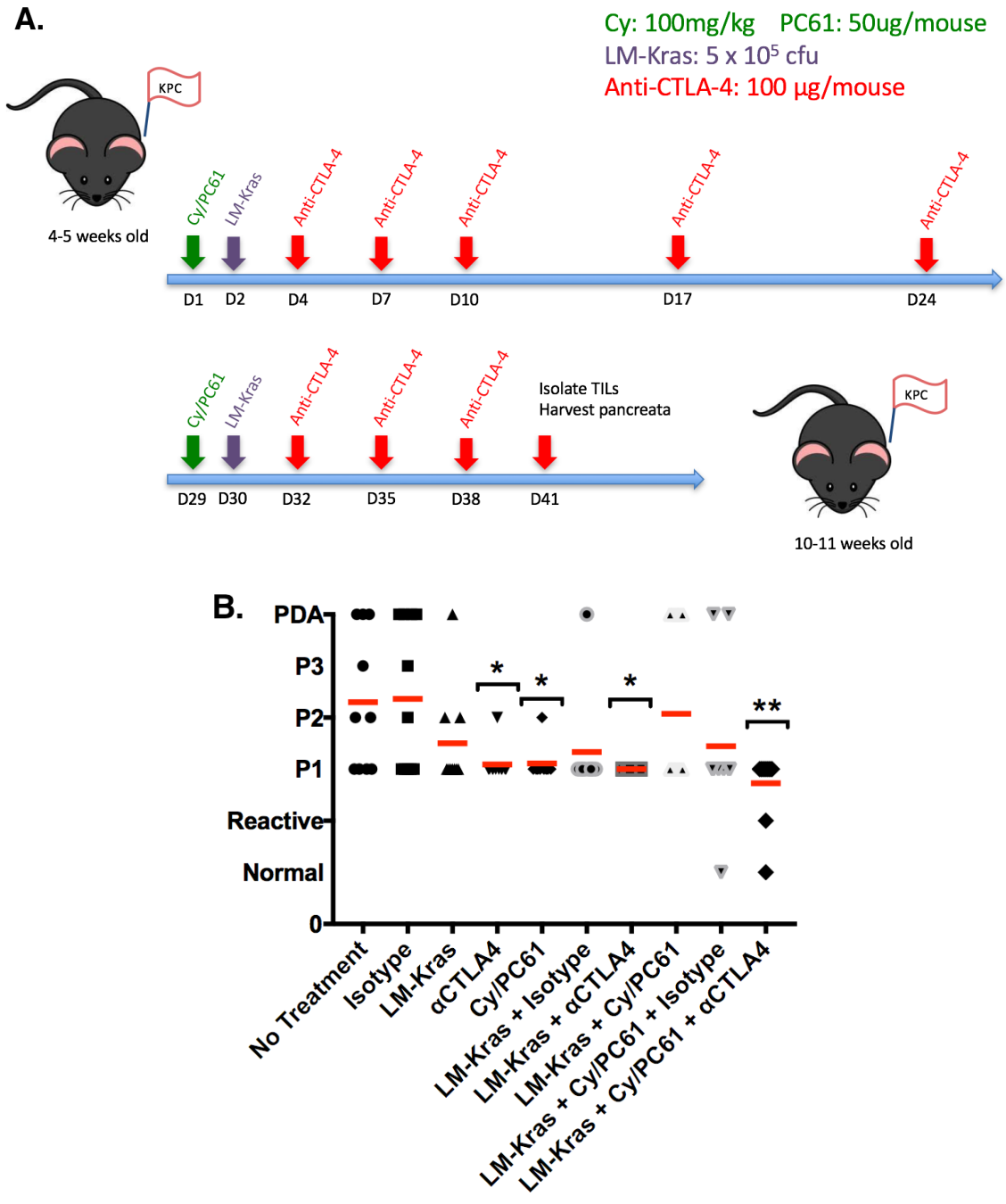

Figure 2.3 Triple combination immunotherapy delays PanIN development in KPC mice.

(A) Dosing scheme of KPC mice. 4-5 week-old KPC mice, when normal or low-grade PanIN1 lesions are predominantly present, are given Cy (100mg/kg) and PC61 antibody (50μg/mouse) IP one day before IV vaccination with LM-Kras (5 x 10^5 cfu). Two days after LM-Kras vaccination, three doses of anti-CTLA-4 antibody (αCTLA4) were given three days apart, followed by two more doses of αCTLA4 given one week apart. Four weeks after initial dosing with Cy/PC61, booster vaccinations were administered in the same fashion before pancreata were harvested for PanIN grading or TIL quantification.

(B) Quantification of PanIN lesions in KPC pancreata post-drug treatments (9-14 mice per treatment group)

Triple combination therapy depletes Tregs and reduces the remaining Treg-specific CTLA-4 expression in the early TME

Flow cytometric analysis of pancreatic TILs revealed that the total proportion of CD4 and CD8 T cells are unchanged in early KPC pancreata as a result of combination immunotherapy (**Figure 2.4A-B**); however, the proportion of Tregs in the early TME is reduced the most by triple treatment (8.7%) compared to all other treatment groups (**Figure 2.4C**). In the pancreata of KPC mice that received triple treatment, the proportion of Tregs was reduced by 3-fold as compared to mice that received no treatment (30.2%) and 2-fold as compared to mice that received LM-Kras in combination with Cy/PC61 and isotype antibody

(15.7%). Moreover, this data indicates that triple treatment also produced the largest pool of CD4 T effector cells ($CD4^{+}Foxp3^{-}$ non-Tregs) as a result of Treg depletion. Interestingly, the fewer Tregs that remain as result of triple treatment also express lower levels of CTLA-4 than the other remaining Treg pools of all other treatment groups (**Figure 2.4D**). Therefore, combination triple treatment produced the lowest proportion of total Tregs with the least CTLA-4 expression on those remaining Tregs. Triple combination therapy exerts negative synergistic effects on Tregs in the early PDA TME, enhancing localized immune activation, which may be a mechanism contributing to the delayed progression of PanIN lesions achieved by KPC mice in this treatment group.

Figure 2.4

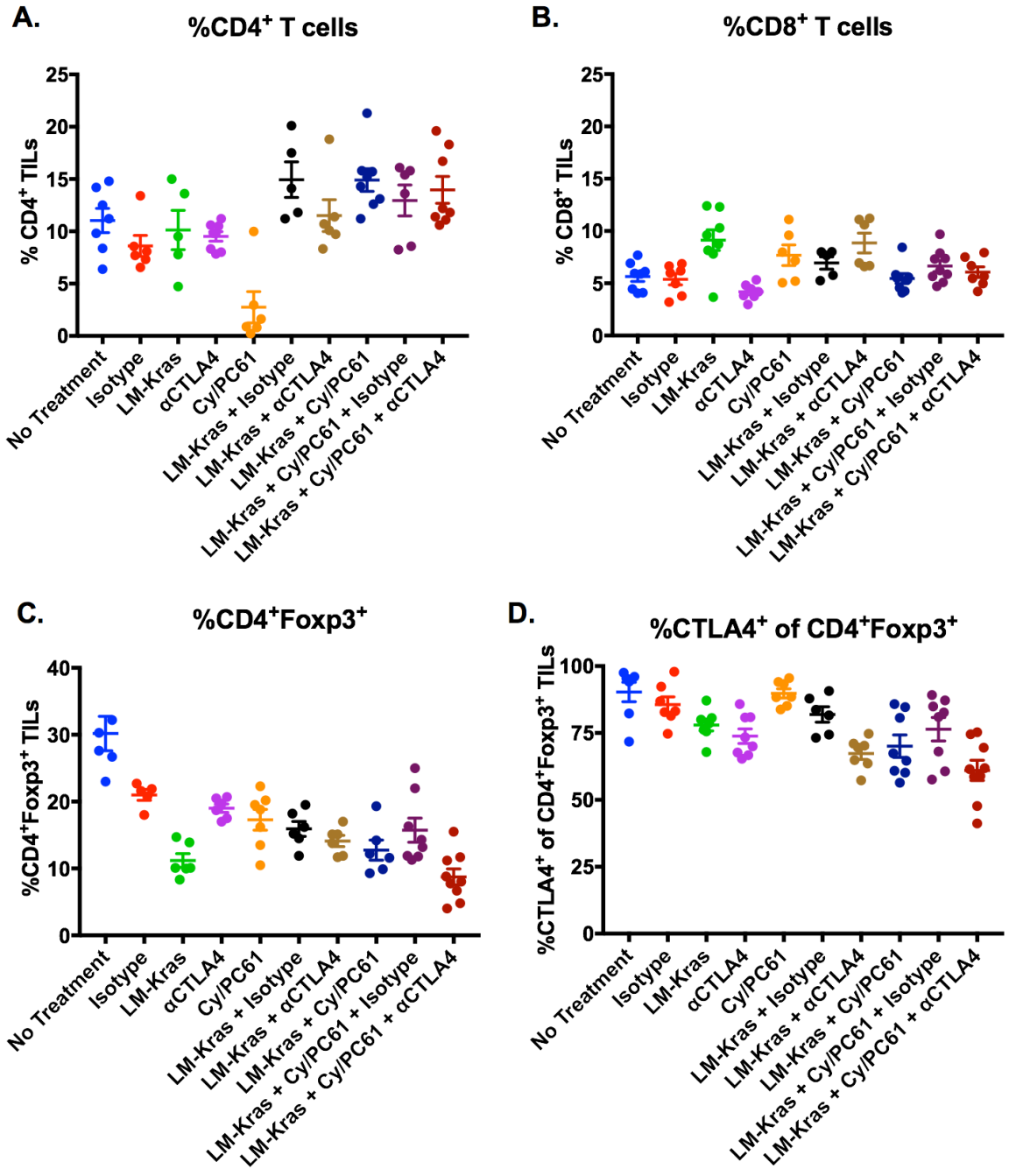

Figure 2.4 Total proportions of CD4, CD8, and Tregs present in premalignant KPC pancreata as a result of treatment.

(A) Percentages of $CD4^+$ T cells in TILs

(B) Percentages of $CD8^+$ T cells in TILs

(C) Percentages of Tregs ($CD4^+Foxp3^+$) in TILs

(D) Percentages of Tregs that express CTLA-4

LM-Kras vaccine, Treg depletion, and CTLA-4 blockade reprograms CD4 and CD8 T cell expression of inhibitory immune signals in early PDA development

After demonstrating that our triple combination treatment reduced the total Treg populations and the expression of CTLA-4 by remaining Treg populations as compared to all other treatment groups, we assessed whether combination immunotherapy affected the expression of other well-characterized immune checkpoint molecules programmed cell death protein 1 (PD-1) and lymphocyte activation gene-3 (LAG-3), as well as the immune modulating lectin galectin-3 on CD4 and CD8 T cells. We discovered that triple treatment produced the lowest proportion of $CTLA4^+PD1^+$ CD4 T cells compared to all other groups, and that all differences were statistically significant (**Figure 2.5A**). Additionally, the percentages of $CTLA4^+PD1^-$ CD4 T cells were significantly reduced by triple treatment (13.1%) as compared to no treatment (26.4%), anti-CTLA-4 alone (25.6%), and LM-Kras plus anti-CTLA-4 (26.4%). The proportion of PD-1 single positive ($CTLA4^-PD1^+$) CD4 T cells did not change due to treatment. However, our data demonstrated that the percentages of PD1 single positive CD8 T cells were much greater across all treatment groups as compared to CD4, showing that CD8 T cells have higher PD1 expression and are therefore more subject to PD1 negative regulation, providing rationale for utilizing PD1 blocking agents to

specifically enhance CD8 T cell activation in this model. Although there were no statistically significant differences due to treatment for double positive ($CTLA4^{+}PD1^{+}$) and single positive ($CTLA4^{+}PD1^{-}$ and CTLA4-$PD1^{+}$) CD8 T cell populations, there was a decreasing trend in $CTLA4^{+}PD1^{+}$ CD8 T cell percentages as result of treatment with triple combination therapy producing the lowest proportion (6.9%) of $CTLA4^{+}PD1^{+}$ CD8 T cells compared to all other treatment groups.

Although lower proportions of CD4 and CD8 T cells expressed LAG-3 and galectin-3 than CTLA-4 and PD-1, the reprogramming achieved by triple combination immunotherapy was still apparent in CD8 T cells. Triple treatment reduced both $LAG3^{+}GAL3^{-}$ CD4 and CD8 T cells percentages as compared to all other treatment groups (**Figure 2.5B**). The proportion of Galectin-3 single positive ($LAG3^{-}GAL3^{+}$) CD4 and CD8 T cells did not change due to treatment; however, only for double positive $LAG3^{+}GAL3^{+}$ CD8 T cells did triple treatment achieve the most percent population reduction compared to all other treatment groups. Additionally, there is a higher overall proportion of double positive $LAG3^{+}GAL3^{+}$ CD8 T cells than CD4 T cells indicating that galectin-3 binds to its LAG-3 partner preferentially on CD8 T cells in the early TME.

Figure 2.5

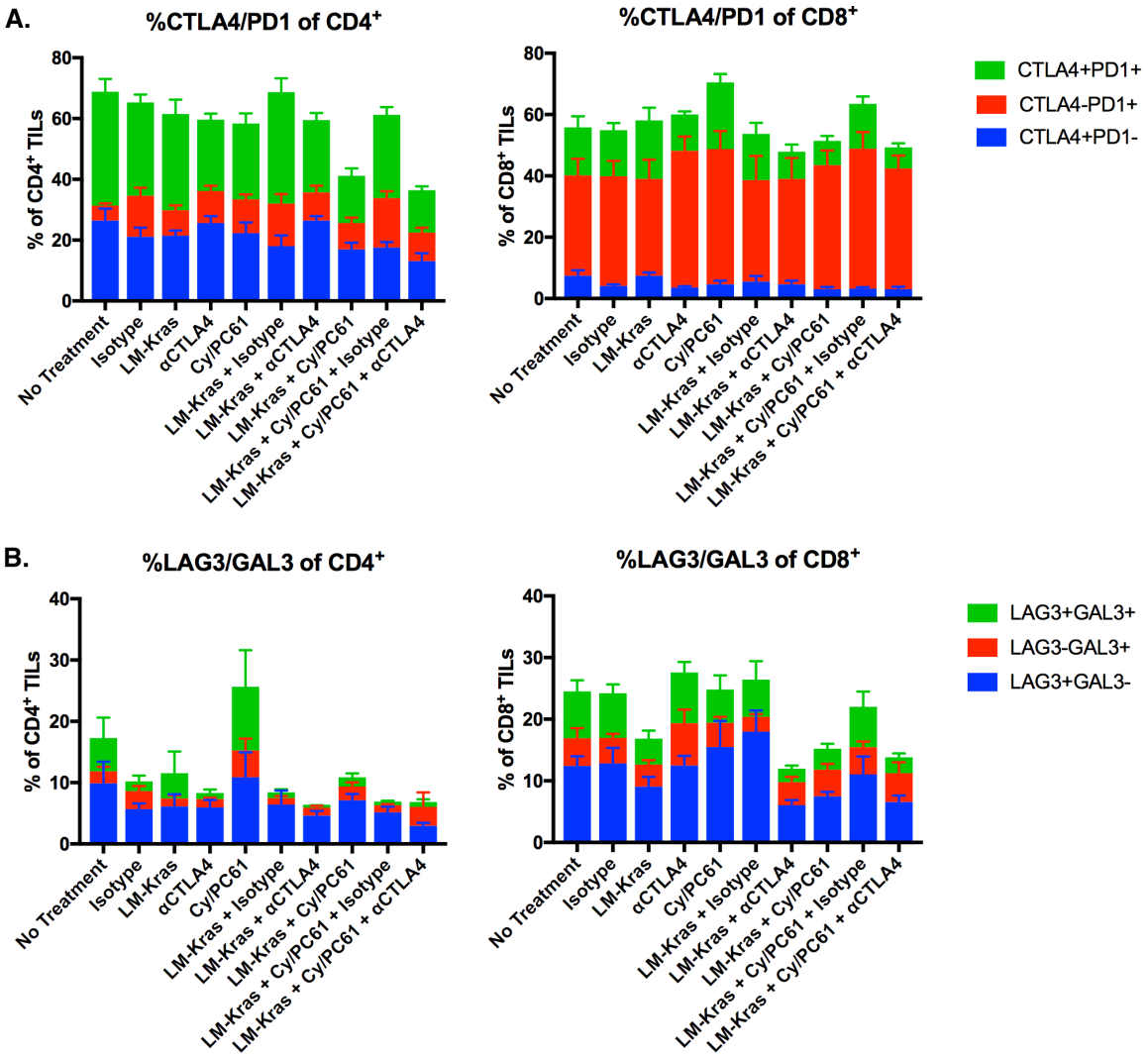

Figure 2.5 Triple combination immunotherapy differentially modulates expression of CTLA-4, PD-1, LAG-3, and galectin-3 in CD4 and CD8 T cells.

(A) Percentages of CD4 and CD8 T cells expressing CTLA-4 alone, PD-1 alone, or CTLA-4 and PD-1

(B) Percentages of CD4 and CD8 T cells expressing LAG-3 alone, galectin-3 (GAL3) alone, or LAG-3 and galectin-3

LM-Kras vaccine, Treg depletion, and CTLA-4 inhibition activates effector CD8 T cells enhancing their cytotoxic phenotype in the premalignant TME

As a result of Treg depletion, downregulation of inhibitory checkpoint molecules and factors, and vaccine-mediated antigen priming of T cells, our triple combination therapy significantly increased activation of CD8 T cells as compared to all other treatment groups (**Figure 2.6A)**. CD8 T cell activation was quantified by expression of CD44, a cell surface activation marker expressed by antigen-experienced lymphocytes. As a result of triple therapy, the proportion of activated $CD44^+$ CD8 T cells increased more than 3-fold (36.9%) as compared to no treatment (11.1%). Additionally, triple therapy produced more than 10% increase of activated $CD44^+$ CD8 T cells as compared to LM-Kras and Cy/PC61 (22.4%) and anti-CTLA-4 alone (23.4%).

Not only did CD8 T cells of the triple treatment group have the highest expression of activation markers, but they also produced the highest levels of cytotoxins and effector cytokines, indicative of increased effector function. The production of Granzyme B, a serine protease secreted by cytotoxic T lymphocytes (CTLs) to trigger caspase-mediated apoptosis in target cells[97], by CD8 T cells was significantly increased by triple treatment as compared to all other groups (**Figure 2.6B**). The proportion of CD8 T cells producing Granzyme B as a result of triple treatment increased 3-fold (16.1%) as compared to the no treatment group (5.9%) and 2-fold as compared to LM-Kras and Cy/PC61 (7.1%) and anti-CTLA-4 alone groups (8.4%). Triple combination therapy also resulted in the highest percentages of CD8 T cells expressing key proinflammatory

effector cytokine interferon gamma (IFNγ) as compared to all other treatment groups (**Figure 2.6C**). Despite relatively high percentages of IFNγ^+ CD8 T cells in all treatment groups, tumor necrosis factor (TNFα) was produced to a much lower degree and its expression on CD8 T cells did not change as a result of treatment. This observation can be explained in part due to TNFα's predominant production and secretion by macrophages, whereas IFNγ is one of the major effector cytokines produced specifically by activated antigen-experienced CD8 CTLs.

Figure 2.6

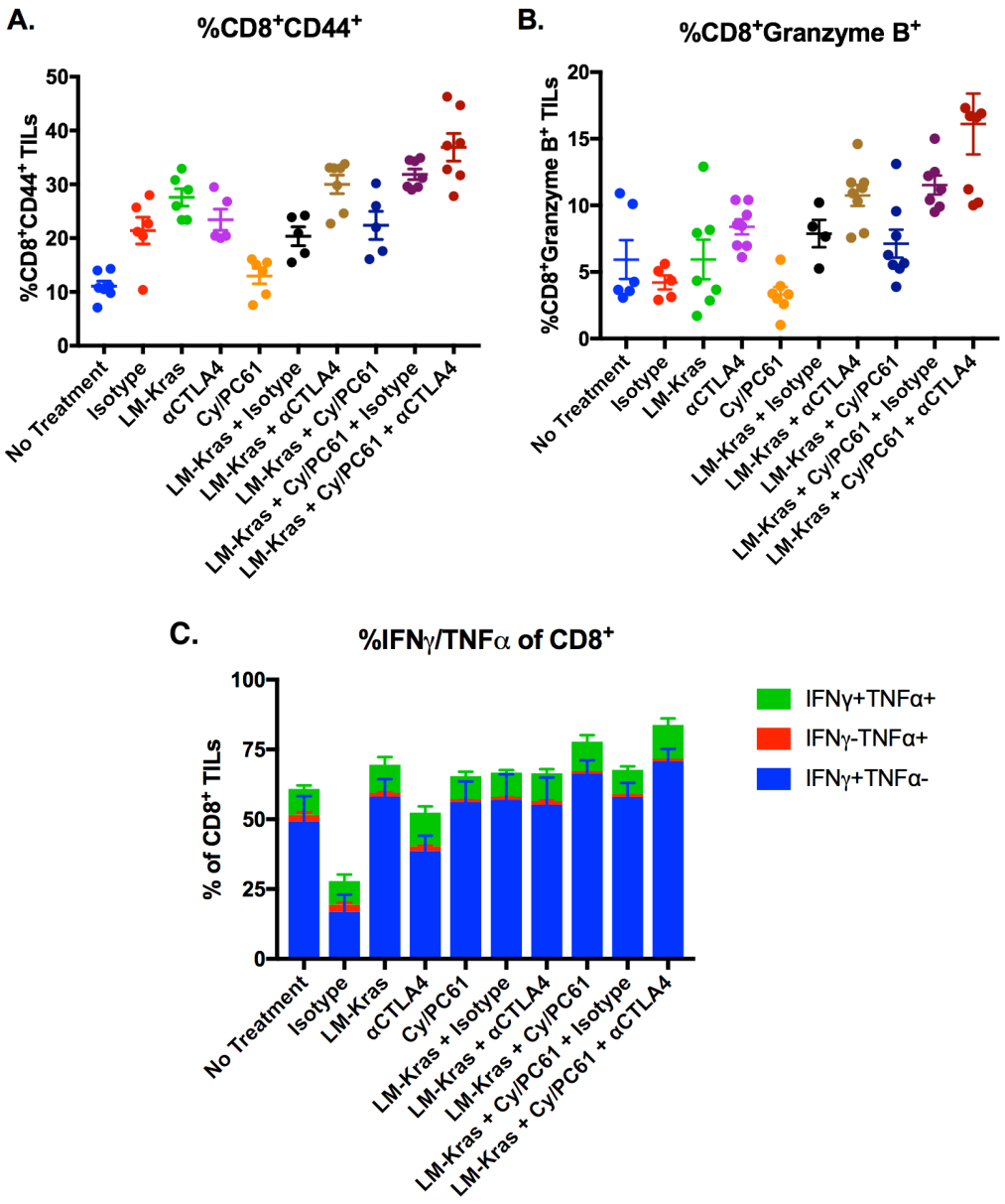

Figure 2.6 Triple combination immunotherapy increased CD8 T cell activation and production of Granzyme B and IFNγ

(A) Percentages of CD8 T cells expressing CD44

(B) Percentages of CD8 T expressing Granzyme B

(C) Percentages of CD8 T cells expressing IFNγ alone, TNFα alone, or IFNγ and TNFα

CTLA-4 blockade combined with Treg depletion during vaccine-mediated priming in early PDA progression enhances CD8 memory populations and T effector to Treg ratios conferring long term protection

Our research thus far has been investigating the altered early-stage immune-mediated mechanisms that result from combination immunotherapy in the context of early disease intervention. We next sought to explore how triple treatment would affect memory populations and other prognostic immune indicators of long term protection. We assessed how combination treatment affected CD8 T cell memory populations as defined by CD44, indicating antigen-experienced, and CD62L (L-selectin), an adhesion molecule commonly on T cells that traffics populations to secondary lymphoid tissues to reside until re-encountering with cognate antigens.[98] Memory CD8 T cells are therefore defined as being a $CD44^{+}CD62L^{+}$ population. We discovered that triple treatment produced the highest percentages of memory CD8 T cells as compared to all other groups (**Figure 2.7A**) indicating that our combination therapy was able to convert 35% of total CD8 T cells present in the early PDA TME to effector memory populations for continual long-term immunity against mutant $KRAS^{G12D}$.

CD8 T cell to Treg ratio (Teff:Treg ratio) in TILs has proven to be an effective prognostic indicator of overall survival in many cancer models, and a higher Teff:Treg ratio in patient TILs correlate with better prognosis, longer overall survival, and better patient response to immunotherapy in many human GI cancers including PDA.[99–102] In our study, KPC mice that received triple treatment had the highest Teff:Treg ratio as compared to all other treatment

groups (all differences were statistically significant) (**Figure 2.7B**). The ratio from triple treatment TILs (9) was more than 2-fold higher than that of LM-Kras and Cy/PC61 (4) and more than 4-fold higher than that of anti-CTLA-4 alone (2) or no treatment (2). The increased Teff:Treg ratio for our triple treatment group is not due to increased infiltration of CD8 T cells in our model, since our data demonstrated that the total proportion of CD8 T cells in the early TME was not changed due to treatment. Rather, it is the significant depletion of Tregs as a result of combination therapy that largely increases the ratio. These data suggest that our triple combination therapy successfully reprograms the early PDA TME to shift the balance of Teff:Treg ratio in favor of an early antitumor immune response. Additionally, for the first time, we report that high Teff:Treg ratio is also a good prognostic indicator of premalignant progression in early disease development, not just in established or metastatic tumors.

Figure 2.7

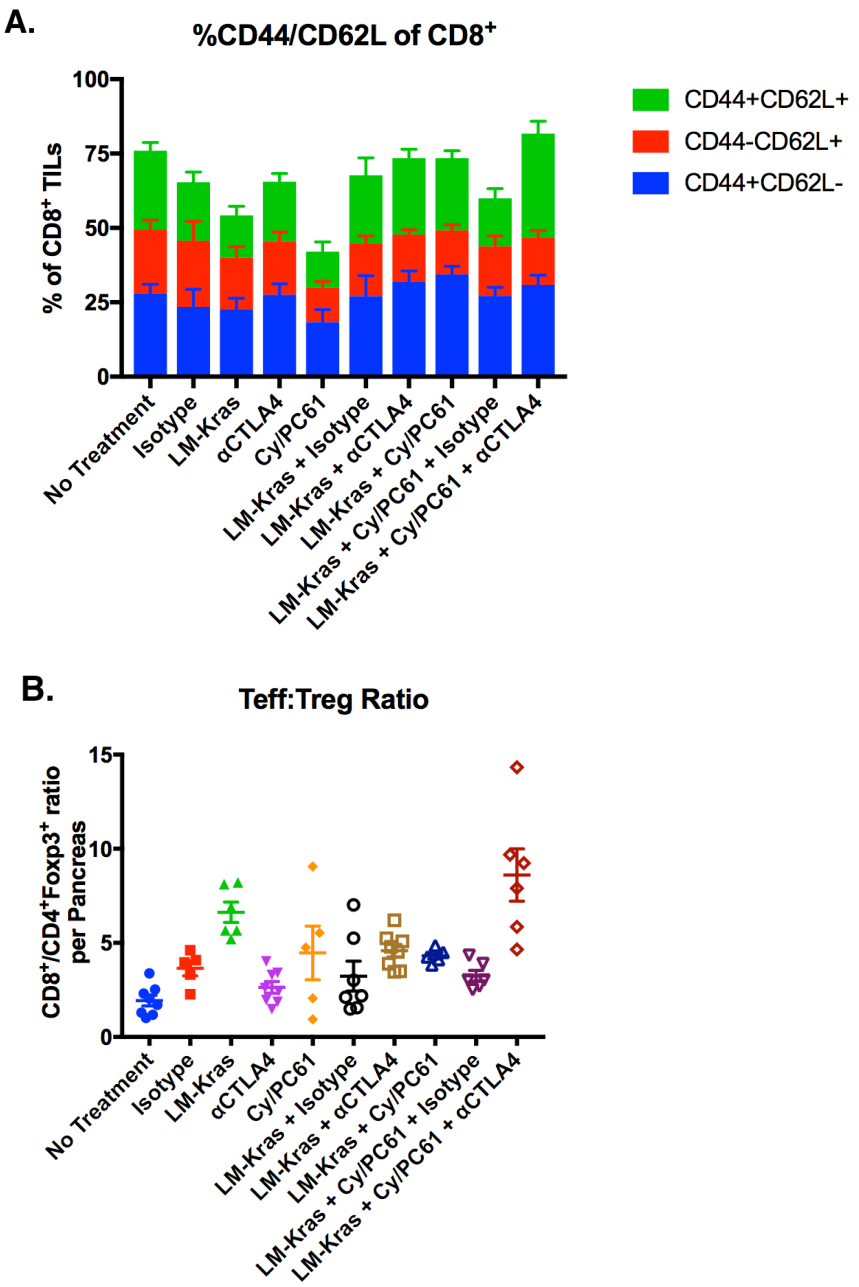

Figure 2.7 KPC mice that received triple combination therapy developed increased memory CD8 T cell population and higher Teff:Treg ratios.

(A) Percentages of CD8 T cells expressing CD44 alone, CD62L alone, or CD44 and CD62L

(B) $CD8^+$:$CD4^+Foxp3^+$ ratio determined from each KPC pancreas

DISCUSSION

PDA is considered an immunologically "cold" cancer due to its low mutational burden and extensive stromal reaction that creates a TME that propagates and protects the tumor from chemotherapeutic and immunotherapeutic penetration.[79] Due to the non-immunopermissive nature of the PDA TME, single agent immunotherapies have not been successful at eradicating the tumor. In addition to the dense fibrotic stroma that constitutes an immense physical barrier that immune cells must penetrate, there are multitudes of inhibitory immune populations and immunosuppressive checkpoint molecules within the TME that function to turn off the immune system. Pathways and signaling mechanisms that normally prevent auto-immunity and are essential for tissue homeostasis are hijacked by the tumor to evade recognition and eradication by the immune system. Therefore, multiple agent combination therapies that simultaneously target many cellular and acellular components must be employed to achieve a robust immunologic attack on the developing tumor and TME.

Our group previously reported that the use of a *Listeria monocytogenes* bacteria-based vaccine expressing driver mutation $KRAS^{G12D}$ (LM-Kras) in combination with Cy and PC61 to deplete the early PDA TME of immunosuppressive Tregs, significantly delayed PanIN progression and shifted the immune profiles in the early TME to that of a more proinflammatory antitumor phenotype. In this study, we aimed to improve the immunopreventative potential of the previously formulated combination therapy by supplementing with anti-

CTLA-4 checkpoint blockade to further deplete Tregs and inhibit this negative regulator of T cell activation. Histological analysis of PanIN lesions in KPC pancreata revealed that our combination immunotherapy supplemented with CTLA-4 blocking antibody, was successful in further intercepting PanIN progression as evidenced by the failure of lesions to advance beyond low-grade PanIN1. Encouraged by these improved results, we sought to understand the cellular mechanisms that are modulated by our triple combination therapy to achieve more effective disease prevention.

Flow cytometry of TILs isolated from treated KPC mice revealed that LM-Kras vaccine administered in combination with Treg depleting agents and CTLA-4 blockade reprograms CD4 and CD8 T cells in the early PDA TME into more activated effector phenotypes by significantly depleting the population of immunosuppressive Tregs and reducing the expression of several inhibitory checkpoint molecules in the premalignant TME. Adjuvant immune modulation of Tregs and checkpoints aids the priming of the T cells to mount a more robust adaptive immune response against the target antigen, mutant $KRAS^{G12D}$, one of the earliest gene products of the driver mutation that initiates PDA tumorigenesis and causes subsequent oncogene addiction that drives premalignant progression.[3] While our study achieved successful PanIN interception, the true prophylactic potential of our combination therapy may be more accurately assessed by using an inducible KPC mouse model in which vaccine regimen can be administered prior to the induction of mutant $KRAS^{G12D}$ expression, allowing antigen-engagement by the adaptive immune system before exposure to the

causative antigen. Such a model would be more accurate and a true translation of prophylactic vaccines for infectious tumors to non-infectious tumors. Jing Pan et al. demonstrated that administration of a multi-peptide KRAS vaccine before induction of mutant $KRAS^{G12D}$ expression in an inducible CCSP-TetO-$KRAS^{G12D}$ mouse model of lung cancer led to more than 80% reduction of primary lung tumor number and volume that coincided with peripheral immunologic responses to specific immunizing peptides.[103] The results from this study along with the results obtained from our study of targeting mutant $KRAS^{G12D}$ in early PDA development demonstrates that such a vaccination approach can be utilized for the primary prevention of other KRAS-driven cancers.

Quantification of CD4 and CD8 T cells from treated KPC TILs revealed that the total number of each T cell subset was not increased due to treatment. This may be due to the nature of T cell depletion of low dose Cy. Cy exerts its Treg depleting specificity due to Treg's high proliferation in both early and established PDA which causes Tregs to be the most sensitive to Cy toxicity.[83] However, when using immunomodulatory agents that activate the immune system, other effector T cell subsets will expand and proliferate, making them susceptible to Cy toxicity as well.[83] Another mechanism of action that can explain lack of increased CD4 and CD8 in the TME is Cy's ability to increase immunosuppressive MDSCs that can deactivated T cells thereby preventing their proliferation and expansion.[75,83] This dual effect of low dose Cy provides rationale for concurrent use of MDSC inhibiting agents to further enhance immune activation.

Our triple combination therapy depleted the most Tregs from the early PDA TME while reducing the most CTLA-4 expression on the remaining pool of Tregs out of all treatment groups. Our data demonstrates that the supplementation of anti-CTLA-4 antibody not only effectively diminished the raw numbers of Tregs, but that CLTA-4 blockade further decreased their specific CTLA-4-mediated inhibitory capabilities. Additionally, our data is consistent with previous studies that report the extremely high constitutive expression of CTLA-4 by Tregs. Out of the total Tregs isolated from KPC mice that received no treatment, nearly 100% of untreated isolated Tregs expressed CTLA-4, underscoring the potent immunosuppressive functionality of Tregs and the need for blocking CTLA-4 on this extremely inhibitory immune population.

Analysis of immune checkpoint expression on CD4 and CD8 T cells, revealed that triple treatment lowered the proportion of $CTLA4^{+}$ CD4 and CD8 T in the early PDA TME. Treatment with all three immunotherapeutic components in combination produced the highest level of CTLA-4 blockade as compared to all other treatment groups that will allow T cells in the early TME to be subject to less negative regulation and be less driven towards anergy. Currently, we are utilizing Nanostring to quantify the transcript abundance of these checkpoint molecules along with other regulators in immune signaling pathways to assess how combination treatment modulates mRNA expression. Our data shows that the protein levels of CTLA-4, both extracellular receptors and intracellular reserves, are reduced the most with treatment. We also want to assess whether levels of CTLA-4 mRNA expression is modulated in the same way.

The lower percentages of $LAG3^{+}GAL3^{+}$ CD8 T cells in the early PDA TME as a result of triple combination therapy may further contribute to the concurrent increased proportion of activated effector CD8 T cells with effector phenotypes, a finding that has been previously corroborated by other groups.[104–106] Galectin-3 binds to LAG-3 which leads to sequestering of the CD8 T cell receptor (TCR) and dissociation from its co-receptor producing non-functional CTLs.[106,107] Since galectin-3 directly binds to LAG-3, an association required for galectin-3 to mediate its immunosuppressive functions in the TME, it makes sense that decreased populations of $LAG3^{+}GAL3^{+}$ CD8 T cells would coincide with decreased populations of $LAG\text{-}3^{+}$ CD8 T cells, although the mechanism as to how our triple treatment is mediating the decreased expression of $LAG\text{-}3^{+}$ on CD8 T cells is unknown and warrants further investigation. The immunomodulation in this study predominantly targets CD4 T cells, but the high expression of PD-1 and substantial expression of LAG-3 checkpoints specifically on CD8 T cells indicates that future studies should supplement with blockade of these checkpoints to enhance immune activation and effector CD8 T cell function.

We report for the first time that early LM-Kras vaccine-mediated priming of T cells in combination with Treg depletion and CTLA-4 blockade effectively produced a substantial population of memory CD8 T cells in the early PDA TME that will confer continual and long-term protection against developing mutant $KRAS^{G12D}$ driven neoplasms in KPC mice. This mechanism of protection against early premalignancies may contribute to the delayed PanIN progression seen in

triple treated KPC mice. Our study also revealed that early administration of triple therapy significantly increased the Teff:Treg ratio which is a prognostic indicator of overall survival and robust immune response to combination therapy in human PDA. However, we have shown that this metric can also be applied to assess the efficacy of prophylactic immunotherapy in preventing early premalignant progression, not just in established PDA.

Beyond just quantifying the amount of specific immune populations and markers in the early TME, we are performing IHC to assess the spatial localization of these populations in association to specific structures in early PDA development. Such studies will reveal how combination treatment modulates the spatial recruitment of specific T cell subsets to varying grades of PanIN lesions. Additionally, we are performing TCR sequencing to see if TCR diversity and/or clonality is affected by treatment, which would provide deeper mechanistic insight as to how our triple combination therapy is enhancing immunity to premalignancies that are halted in early disease progression.

REFERENCES

1. Hidalgo M. Pancreatic Cancer. *N Engl J Med*. 2010;362(17):1605-1617.
2. Kanda M, Matthaei H, Wu J, et al. Presence of somatic mutations in most early-stage pancreatic intraepithelial neoplasia. *Gastroenterology*. 2012;142:730-733.
3. Collins MA, Bednar F, Zhang Y, et al. Oncogenic Kras is required for both the initiation and maintenance of pancreatic cancer in mice. *J Clin Invest*. 2012;122(2):639-653. doi:10.1172/JCI59227DS1
4. di Magliano MP, Logsdon CD. Roles for KRAS in pancreatic tumor development and progression. *Gastroenterology*. 2013;144(6):1220-1229. doi:10.1053/j.gastro.2013.01.071
5. Lou E, Subramanian S, Steer CJ. Pancreatic Cancer Modulation of KRAS, MicroRNAs, and Intercellular Communication in the Setting of Tumor Heterogeneity. *Pancreas*. 2013;42(8):1218-1226.
6. Farrow B, Albo D, Berger DH. The role of the tumor microenvironment in the progression of pancreatic cancer. *J Surg Res*. 2008;149(2):319-328. doi:10.1016/j.jss.2007.12.757
7. Hingorani SR, Iii EFP, Maitra A, et al. Preinvasive and invasive ductal pancreatic cancer and its early detection in the mouse. *Cancer Cell*. 2003;4(December):437-450.
8. Morris JP, Wang SC, Hebrok M. KRAS, Hedgehog, Wnt and the twisted developmental biology of pancreatic ductal adenocarcinoma. *Nat Rev Cancer*. 2010;10(10):683-695. doi:10.1038/nrc2899

9. Cox AD, Der CJ. Ras history: The saga continues. *Small GTPases*. 2010;1(1):2-27. doi:10.4161/sgtp.1.1.12178

10. Eser S, Schnieke A, Schneider G, Saur D. Oncogenic KRAS signalling in pancreatic cancer. *Br J Cancer*. 2014;111(5):817-822. doi:10.1038/bjc.2014.215

11. Liu J, Ji S, Liang C, et al. Critical role of oncogenic KRAS in pancreatic cancer (Review). *Mol Med Rep*. 2016;13(6):4943-4949. doi:10.3892/mmr.2016.5196

12. Choi M, Bien H, Mofunanya A, Powers S. Challenges in Ras therapeutics in pancreatic cancer. *Semin Cancer Biol*. 2017;(November):0-8. doi:10.1016/j.semcancer.2017.11.015

13. Rucki AA, Foley K, Zhang P, et al. Heterogeneous stromal signaling within the tumor microenvironment controls the metastasis of pancreatic cancer. *Cancer Res*. 2017;77(1):41-52. doi:10.1158/0008-5472.CAN-16-1383

14. Principe DR, DeCant B, Mascariñas E, et al. TGFβ signaling in the pancreatic tumor microenvironment promotes fibrosis and immune evasion to facilitate tumorigenesis. *Cancer Res*. 2016;76(9):2525-2539. doi:10.1158/0008-5472.CAN-15-1293

15. Herrera M, Islam ABMMK, Herrera A, et al. Functional heterogeneity of cancer-associated fibroblasts from human colon tumors shows specific prognostic gene expression signature. *Clin Cancer Res*. 2013;19(21):5914-5926. doi:10.1158/1078-0432.CCR-13-0694

16. Xouri G, Christian S. Origin and function of tumor stroma fibroblasts. *Semin*

Cell Dev Biol. 2010;21(1):40-46. doi:10.1016/j.semcdb.2009.11.017

17. Xia Q, Zhang F-F, Geng F, et al. Anti-tumor effects of DNA vaccine targeting human fibroblast activation protein α by producing specific immune responses and altering tumor microenvironment in the 4T1 murine breast cancer model. *Cancer Immunol Immunother*. 2016;65(5):613-624. doi:10.1007/s00262-016-1827-4
18. Wen Y, Wang CT, Ma TT, et al. Immunotherapy targeting fibroblast activation protein inhibits tumor growth and increases survival in a murine colon cancer model. *Cancer Sci*. 2010;101(11):2325-2332. doi:10.1111/j.1349-7006.2010.01695.x
19. Von Ahrens D, Bhagat TD, Nagrath D, Maitra A, Verma A. The role of stromal cancer-associated fibroblasts in pancreatic cancer. *J Hematol Oncol*. 2017;10(1):1-8. doi:10.1186/s13045-017-0448-5
20. Hingorani SR, Wang L, Multani AS, et al. Trp53R172H and KrasG12D cooperate to promote chromosomal instability and widely metastatic pancreatic ductal adenocarcinoma in mice. *Cancer Cell*. 2005;7(5):469-483. doi:10.1016/j.ccr.2005.04.023
21. Rupaimoole R, Slack FJ. MicroRNA therapeutics: Towards a new era for the management of cancer and other diseases. *Nat Rev Drug Discov*. 2017;16(3):203-221. doi:10.1038/nrd.2016.246
22. Taucher V, Mangge H, Haybaeck J. Non-coding RNAs in pancreatic cancer: challenges and opportunities for clinical application. *Cell Oncol*. 2016;39(4):295-318. doi:10.1007/s13402-016-0275-7

23. Lin S, Gregory RI. MicroRNA biogenesis pathways in cancer. *Nat Rev Cancer*. 2015;15(6):321-333. doi:10.1038/nrc3932

24. Lewis BP, Shih IH, Jones-Rhoades MW, Bartel DP, Burge CB. Prediction of Mammalian MicroRNA Targets. *Cell*. 2003;115(7):787-798. doi:10.1016/S0092-8674(03)01018-3

25. Nana-Sinkam SP, Croce CM. Clinical Applications for microRNAs in Cancer. *Clin Pharmacol Ther*. 2013;93(1):98-104. doi:10.1038/clpt.2012.192

26. Kim M, Slack FJ. MicroRNA-mediated regulation of KRAS in cancer. *J Hematol Oncol*. 2014;7(1). doi:10.1186/s13045-014-0084-2

27. Fu X, Cui Y, Yang S, Xu Y, Zhang Z. MicroRNA-613 inhibited ovarian cancer cell proliferation and invasion by regulating KRAS. *Tumor Biol*. 2016;37(5):6477-6483. doi:10.1007/s13277-015-4507-7

28. Karmakar S, Kaushik G, Nimmakayala R, Rachagani S, Ponnusamy MP, Batra SK. MicroRNA regulation of K-Ras in pancreatic cancer and opportunities for therapeutic intervention. *Semin Cancer Biol*. 2017;(November):0-1. doi:10.1016/j.semcancer.2017.11.020

29. Pang W, Su J, Wang Y, et al. Pancreatic cancer-secreted miR-155 implicates in the conversion from normal fibroblasts to cancer-associated fibroblasts. *Cancer Sci*. 2015;106(10):1362-1369. doi:10.1111/cas.12747

30. Ali S, Suresh R, Banerjee S, et al. Contribution of microRNAs in understanding the pancreatic tumor microenvironment involving cancer associated stellate and fibroblast cells. *Am J Cancer Res*. 2015;5(3):1251-

1264. http://www.pubmedcentral.nih.gov/articlerender.fcgi?artid=4449452&tool=pmcentrez&rendertype=abstract.

31. Liu G, Friggeri A, Yang Y, et al. miR-21 mediates fibrogenic activation of pulmonary fibroblasts and lung fibrosis. *J Exp Med*. 2010;207(8):1589-1597. doi:10.1084/jem.20100035

32. Li Q, Zhang D, Wang Y, et al. MiR-21/Smad 7 signaling determines TGF-β1-induced CAF formation. *Sci Rep*. 2013;3. doi:10.1038/srep02038

33. Li Y, Sarkar FH. MicroRNA targeted therapeutic approach for pancreatic cancer. *Int J Biol Sci*. 2016;12(3):326-337. doi:10.7150/ijbs.15017

34. Hao J, Zhang S, Zhou Y, Hu X, Shao C. MicroRNA 483-3p suppresses the expression of DPC4/Smad4 in pancreatic cancer. *FEBS Lett*. 2011;585(1):207-213. doi:10.1016/j.febslet.2010.11.039

35. Kwon JJ, Nabinger SC, Vega Z, et al. Pathophysiological role of microRNA-29 in pancreatic cancer stroma. *Sci Rep*. 2015;5(March):1-15. doi:10.1038/srep11450

36. Schwarzenbach H, Nishida N, Calin G a, Pantel K. Clinical relevance of circulating cell-free microRNAs in cancer. *Nat Rev Clin Oncol*. 2014;11(3):145-156. doi:10.1038/nrclinonc.2014.5

37. Cheng G. Circulating miRNAs: Roles in cancer diagnosis, prognosis and therapy. *Adv Drug Deliv Rev*. September 2014. doi:10.1016/j.addr.2014.09.001

38. Allegra A, Alonci A, Campo S, et al. Circulating microRNAs: new

biomarkers in diagnosis, prognosis and treatment of cancer (review). *Int J Oncol*. 2012;41(6):1897-1912. doi:10.3892/ijo.2012.1647

39. Jones K, Nourse JP, Keane C, Bhatnagar A, Gandhi MK. Plasma microRNA are disease response biomarkers in classical Hodgkin lymphoma. *Clin Cancer Res*. 2014;20(1):253-264. doi:10.1158/1078-0432.CCR-13-1024
40. Sita-Lumsden a, Dart D a, Waxman J, Bevan CL. Circulating microRNAs as potential new biomarkers for prostate cancer. *Br J Cancer*. 2013;108(10):1925-1930. doi:10.1038/bjc.2013.192
41. Yang I-P, Tsai H-L, Huang C-W, et al. The functional significance of microRNA-29c in patients with colorectal cancer: a potential circulating biomarker for predicting early relapse. *PLoS One*. 2013;8(6):e66842. doi:10.1371/journal.pone.0066842
42. Christodoulatos GS, Dalamaga M. Micro-RNAs as clinical biomarkers and therapeutic targets in breast cancer: Quo vadis? *World J Clin Oncol*. 2014;5(2):71-81. doi:10.5306/wjco.v5.i2.71
43. Chen X, Ba Y, Ma L, et al. Characterization of microRNAs in serum: a novel class of biomarkers for diagnosis of cancer and other diseases. *Cell Res*. 2008;18(10):997-1006. doi:10.1038/cr.2008.282
44. Julich H, Willms A, Lukacs-Kornek V, Kornek M. Extracellular vesicle profiling and their use as potential disease specific biomarker. *Front Immunol*. 2014;5(September):413. doi:10.3389/fimmu.2014.00413
45. Schindelin J, Arganda-Carreras I, Frise E, et al. Fiji: An open-source

platform for biological-image analysis. *Nat Methods*. 2012;9(7):676-682. doi:10.1038/nmeth.2019

46. Klinkhammer BM, Floege J, Boor P. PDGF in organ fibrosis. *Mol Aspects Med*. 2017. doi:10.1016/j.mam.2017.11.008

47. Rhim AD, Mirek ET, Aiello NM, et al. EMT and dissemination precede pancreatic tumor formation. *Cell*. 2012;148(1-2):349-361. doi:10.1016/j.cell.2011.11.025

48. Sheedy FJ. Turning 21: Induction of miR-21 as a key switch in the inflammatory response. *Front Immunol*. 2015;6(JAN):1-9. doi:10.3389/fimmu.2015.00019

49. Cui R, Meng W, Sun H-L, et al. MicroRNA-224 promotes tumor progression in nonsmall cell lung cancer. *Proc Natl Acad Sci*. 2015;112(31):E4288-E4297. doi:10.1073/pnas.1502068112

50. Obernosterer G, Martinez J, Alenius M. Locked nucleic acid-based in situ detection of microRNAs in mouse tissue sections. *Nat Protoc*. 2007;2(6):1508-1514. doi:10.1038/nprot.2007.153

51. Silahtaroglu AN, Nolting D, Dyrskjøt L, et al. Detection of microrna s in frozen tissue sections by fluorescence in situ hybridization using locked nucleic acid probes and tyramide signal amplification. *Nat Protoc*. 2007;2(10):2520-2528. doi:10.1038/nprot.2007.313

52. Mitchell PS, Parkin RK, Kroh EM, et al. Circulating microRNAs as stable blood-based markers for cancer detection. *Proc Natl Acad Sci*. 2008;105(30):10513-10518. doi:10.1073/pnas.0804549105

53. Hamada S, Masamune A, Kanno A, Shimosegawa T. Comprehensive analysis of serum microRNAs in autoimmune pancreatitis. *Digestion*. 2015;91(4):263-271. doi:10.1159/000381283

54. Mishra S, Srivastava AK, Suman S, Kumar V, Shukla Y. Circulating miRNAs revealed as surrogate molecular signatures for the early detection of breast cancer. *Cancer Lett*. 2015;369(1):67-75. doi:10.1016/j.canlet.2015.07.045

55. Cheng G. Circulating miRNAs: Roles in cancer diagnosis, prognosis and therapy. *Adv Drug Deliv Rev*. 2015;81:75-93. doi:10.1016/j.addr.2014.09.001

56. Yu J, Li A, Hong S-M, Hruban RH, Goggins M. MicroRNA alterations of pancreatic intraepithelial neoplasias. *Clin Cancer Res*. 2012;18(4):981-992. doi:10.1158/1078-0432.CCR-11-2347

57. Scisciani C, Vossio S, Guerrieri F, et al. Transcriptional regulation of miR-224 upregulated in human HCCs by NF j B inflammatory pathways. *J Hepatol*. 2012;56(4):855-861. doi:10.1016/j.jhep.2011.11.017

58. Zheng B, Ohuchida K, Chijiiwa Y, et al. CD146 attenuation in cancer-associated fibroblasts promotes pancreatic cancer progression. *Mol Carcinog*. 2016;55(11):1560-1572. doi:10.1002/mc.22409

59. Wojtowicz ME, Dunn BK, Umar A. Immunologic approaches to cancer prevention - Current status, challenges, and future perspectives. *Semin Oncol*. 2016;43(1):161-172. doi:10.1053/j.seminoncol.2015.11.001

60. Lollini P-L, Nicoletti G, Landuzzi L, et al. Vaccines and Other

Immunological Approaches for Cancer Immunoprevention. *Curr Drug Targets*. 2011;12(13):1957-1973.

61. Tuohy VK, Jaini R. Prophylactic Cancer Vaccination by Targeting Functional Non- Self. *Ann Med*. 2012;43(5):356-365. doi:10.3109/07853890.2011.565065.Prophylactic

62. Weiner LM, Surana R, Murray J. Vaccine prevention of cancer: can endogenous antigens be targeted? *Cancer Prev Res (Phila)*. 2010;3(4):410-415. doi:10.1158/1940-6207.CAPR-10-0040

63. Chu NJ, Armstrong TD, Jaffee EM. Nonviral oncogenic antigens and the inflammatory signals driving early cancer development as targets for cancer immunoprevention. *Clin Cancer Res*. 2015;21(7):1549-1557. doi:10.1158/1078-0432.CCR-14-1186

64. Farkas AM, Finn OJ. Vaccines based on abnormal self-antigens as tumor-associated antigens: Immune regulation. *Semin Immunol*. 2010;22(3):125-131. doi:10.1016/j.smim.2010.03.003

65. Occhipinti S, Sponton L, Rolla S, et al. Chimeric rat/human HER2 efficiently circumvents HER2 tolerance in cancer patients. *Clin Cancer Res*. 2014;20(11):2910-2921. doi:10.1158/1078-0432.CCR-13-2663

66. Pao W, Girard N. New driver mutations in non-small-cell lung cancer. *Lancet Oncol*. 2011;12:175-180.

67. Minuti G, D'Incecco A, Landi L, Cappuzzo F. Protein kinase inhibitors to treat non-small-cell lung cancer. *Expert Opin Pharmacother*. 2014;15:1203-1213.

68. Ghafouri-Fard S, Shamsi R, Seifi-Alan M, Javaheri M, Tabarestani S. Cancer-testis genes as candidates for immunotherapy in breast cancer. *Immunotherapy*. 2014;6(2):165-179. doi:10.2217/imt.13.165

69. Cheever M a, Allison JP, Ferris AS, et al. The prioritization of cancer antigens: a national cancer institute pilot project for the acceleration of translational research. *Clin Cancer Res*. 2009;15(17):5323-5337. doi:10.1158/1078-0432.CCR-09-0737

70. Capello M, Ferri-Borgogno S, Cappello P, Novelli F. α-Enolase: a promising therapeutic and diagnostic tumor target. *FEBS J*. 2011;278(7):1064-1074. doi:10.1111/j.1742-4658.2011.08025.x

71. Cappello P, Rolla S, Chiarle R, et al. Vaccination with ENO1 DNA prolongs survival of genetically engineered mice with pancreatic cancer. *Gastroenterology*. 2013;144(5):1098-1106. doi:10.1053/j.gastro.2013.01.020

72. Zheng L, Xue J, Jaffee EM, Habtezion A. Role of immune cells and immune-based therapies in pancreatitis and pancreatic ductal adenocarcinoma. *Gastroenterology*. 2013;144(6):1230-1240. doi:10.1053/j.gastro.2012.12.042

73. Skelton RA, Javed A, Zheng L, He J. Overcoming the resistance of pancreatic cancer to immune checkpoint inhibitors. *J Surg Oncol*. 2017;116(1):55-62. doi:10.1002/jso.24642

74. Holmer R, Goumas F a, Waetzig GH, Rose-John S, Kalthoff H. Interleukin-6: a villain in the drama of pancreatic cancer development and progression.

Hepatobiliary Pancreat Dis Int. 2014;13(4):371-380. doi:10.1016/S1499-3872(14)60259-9

75. Schupp J, Krebs FK, Zimmer N, Trzeciak E, Schuppan D, Tuettenberg A. Targeting myeloid cells in the tumor sustaining microenvironment. *Cell Immunol*. 2017;(October):0-1. doi:10.1016/j.cellimm.2017.10.013

76. Chanmee T, Ontong P, Konno K, Itano N. Tumor-associated macrophages as major players in the tumor microenvironment. *Cancers (Basel)*. 2014;6(3):1670-1690. doi:10.3390/cancers6031670

77. Curren Smith EW. Macrophage Polarization and Its Role in Cancer. *J Clin Cell Immunol*. 2015;6(4):4-11. doi:10.4172/2155-9899.1000338

78. Keenan BP, Saenger Y, Kafrouni MI, et al. A Listeria Vaccine and Depletion of T-Regulatory Cells Activate Immunity Against Early Stage Pancreatic Intraepithelial Neoplasms and Prolong Survival of Mice. *Gastroenterology*. 2014;146:1784-1794.

79. Zhang J, Wolfgang C, Zheng L. Precision Immuno-Oncology: Prospects of Individualized Immunotherapy for Pancreatic Cancer. *Cancers (Basel)*. 2018;10(2):39. doi:10.3390/cancers10020039

80. Singh R, Paterson Y. Listeria monocytogenes as a vector for tumor-associated antigens for cancer immunotherapy. *Expert Rev Vaccines*. 2006;5(4):541-552. doi:10.1586/14760584.5.4.541

81. Brockstedt DG, Giedlin M a, Leong ML, et al. Listeria-based cancer vaccines that segregate immunogenicity from toxicity. *Proc Natl Acad Sci U S A*. 2004;101(38):13832-13837. doi:10.1073/pnas.0406035101

82. Le DT, Brockstedt DG, Nir-Paz R, et al. A live-attenuated listeria vaccine (ANZ-100) and a live-attenuated listeria vaccine expressing mesothelin (CRS-207) for advanced cancers: Phase I studies of safety and immune induction. *Clin Cancer Res*. 2012;18(3):858-868. doi:10.1158/1078-0432.CCR-11-2121

83. Ahlmann M, Hempel G. The effect of cyclophosphamide on the immune system: implications for clinical cancer therapy. *Cancer Chemother Pharmacol*. 2016;78(4):661-671. doi:10.1007/s00280-016-3152-1

84. Sakaguchi S. Naturally arising Foxp3-expressing CD25+ CD4+ regulatory T cells in immunological tolerance to self and non-self. *Nat Immunol*. 2005;6(4):345-352. doi:10.1038/ni1178

85. Ward-Hartstonge KA, Kemp RA. Regulatory T-cell heterogeneity and the cancer immune response. *Clin Transl Immunol*. 2017;6(9):e154. doi:10.1038/cti.2017.43

86. Pandiyan P, Zheng L, Ishihara S, Reed J, Lenardo MJ. CD4+CD25+Foxp3+ regulatory T cells induce cytokine deprivation–mediated apoptosis of effector CD4+ T cells. *Nat Immunol*. 2007;8(12):1353-1362. doi:10.1038/ni1536

87. Ghiringhelli F, Larmonier N, Schmitt E, et al. CD4+CD25+ regulatory T cells suppress tumor immunity but are sensitive to cyclophosphamide which allows immunotherapy of established tumors to be curative. *Eur J Immunol*. 2004;34(2):336-344. doi:10.1002/eji.200324181

88. Setiady YY, Coccia JA, Park PU. In vivo depletion of CD4+FOXP3+ Treg

cells by the PC61 anti-CD25 monoclonal antibody is mediated by FcgammaRIII+ phagocytes. *Eur J Immunol*. 2010;40(3):780-786. doi:10.1002/eji.200939613

89. Ito A, Kondo S, Tada K, Kitano S. Clinical Development of Immune Checkpoint Inhibitors. *Biomed Res Int*. 2015;2015:1-12. doi:10.1155/2015/605478

90. Seo YD, Pillarisetty VG. T-cell programming in pancreatic adenocarcinoma: A review. *Cancer Gene Ther*. 2017;24(3):106-113. doi:10.1038/cgt.2016.66

91. Simpson TR, Li F, Montalvo-Ortiz W, et al. Fc-dependent depletion of tumor-infiltrating regulatory T cells co-defines the efficacy of anti–CTLA-4 therapy against melanoma. *J Exp Med*. 2013;210(9):1695-1710. doi:10.1084/jem.20130579

92. Peggs KS, Quezada SA, Chambers CA, Korman AJ, Allison JP. Blockade of CTLA-4 on both effector and regulatory T cell compartments contributes to the antitumor activity of anti–CTLA-4 antibodies. *J Exp Med*. 2009;206(8):1717-1725. doi:10.1084/jem.20082492

93. Romano E, Kusio-Kobialka M, Foukas PG, et al. Ipilimumab-dependent cell-mediated cytotoxicity of regulatory T cells ex vivo by nonclassical monocytes in melanoma patients. *Proc Natl Acad Sci*. 2015;112(19):6140-6145. doi:10.1073/pnas.1417320112

94. Foley K, Kim V, Jaffee E, Zheng L. Current progress in immunotherapy for pancreatic cancer. *Cancer Lett*. 2016;381(1):244-251.

doi:10.1016/j.canlet.2015.12.020

95. Royal RE, Levy C, Turner K, et al. Phase 2 trial of single agent ipilimumab (Anti-CTLA-4) for locally advanced or metastatic pancreatic adenocarcinoma. *J Immunother*. 2010;33(8):828-833. doi:10.1097/CJI.0b013e3181eec14c

96. Leao IC, Ganesan P, Armstrong TD, Jaffee EM. Effective depletion of regulatory T cells allows the recruitment of mesothelin-specific CD8 T cells to the antitumor immune response against a mesothelin-expressing mouse pancreatic adenocarcinoma. *Clin Transl Sci*. 2008;1(3):228-239. doi:10.1111/j.1752-8062.2008.00070.x

97. Li J, Figueira SK, Vrazo ACA, et al. Real-Time Detection of CTL Function Reveals Distinct Patterns of Caspase Activation Mediated by Fas versus Granzyme B. *J Immunol*. 2014;193(2):519-528. doi:10.4049/jimmunol.1301668

98. Borsig L. Selectins in cancer immunity. *Glycobiology*. 2017;(February):1-8. doi:10.1093/glycob/cwx105

99. Lutz ER, Wu AA, Bigelow E, et al. Immunotherapy Converts Nonimmunogenic Pancreatic Tumors into Immunogenic Foci of Immune Regulation. *Cancer Immunol Res*. 2014;2(7):616-631. doi:10.1158/2326-6066.CIR-14-0027

100. Perret R, Sierro SR, Botelho NK, Corgnac S, Donda A, Romero P. Adjuvants that improve the ratio of antigen-specific effector to regulatory T cells enhance tumor immunity. *Cancer Res*. 2013;73(22):6597-6608.

doi:10.1158/0008-5472.CAN-13-0875

101. Shen Z, Zhou S, Wang Y, et al. Higher intratumoral infiltrated Foxp3+ Treg numbers and Foxp3+/CD8+ ratio are associated with adverse prognosis in resectable gastric cancer. *J Cancer Res Clin Oncol*. 2010;136(10):1585-1595. doi:10.1007/s00432-010-0816-9
102. Sinicrope FA, Rego RL, Ansell SM, Knutson KL, Foster NR, Sargent DJ. Intraepithelial Effector (CD3+)/Regulatory (FoxP3+) T-Cell Ratio Predicts a Clinical Outcome of Human Colon Carcinoma. *Gastroenterology*. 2009;137(4):1270-1279. doi:10.1053/j.gastro.2009.06.053
103. Pan J, Zhang Q, Sei S, et al. Immunoprevention of KRAS-driven lung adenocarcinoma by a multipeptide vaccine. *Oncotarget*. 2017;8(47):82689-82699.
104. Grosso JF, Kelleher CC, Harris TJ, et al. LAG-3 regulates CD8+ T cell accumulation and effector function in murine selfand tumor-tolerance systems. *J Clin Invest*. 2007;117(11):3383-3392. doi:10.1172/JCI31184DS1
105. Li X, Hu W, Zheng X, et al. Emerging immune checkpoints for cancer therapy. *Acta Oncol (Madr)*. 2015;54(10):1706-1713. doi:10.3109/0284186X.2015.1071918
106. Kouo T, Huang L, Pucsek AB, et al. Galectin-3 Shapes Antitumor Immune Responses by Suppressing CD8+ T Cells via LAG-3 and Inhibiting Expansion of Plasmacytoid Dendritic Cells. *Cancer Immunol Res*. 2015;3(4):412-423. doi:10.1158/2326-6066.CIR-14-0150

107. Demotte N, Wieërs G, Van Der Smissen P, et al. A galectin-3 ligand corrects the impaired function of human CD4 and CD8 tumor-infiltrating lymphocytes and favors tumor rejection in mice. *Cancer Res*. 2010;70(19):7476-7488. doi:10.1158/0008-5472.CAN-10-0761

NINA J. CHU

Department of Oncology, Sidney Kimmel Comprehensive Cancer Center
The Johns Hopkins University School of Medicine
1650 Orleans Street, Cancer Research Building 1, Room 422, Baltimore, Maryland, 21287
(626) 715-5445
nchu6@jhmi.edu

SUMMARY OF QUALIFICATIONS

PhD candidate interested in basic and translational cancer research focusing on early stage prevention and late stage therapies. Experienced in designing and implementing experiments that investigate the mechanistic development and propagation of the early inflammatory tumor-microenvironment (TME) of solid malignancies, specifically pancreatic cancer. Discovered novel molecular targets via high-throughput screening, constructed both in-tissue and circulating developmental profiles of novel molecular targets for biomarker discovery, validated targets utilizing multiple *in vitro* assays to assess altered functionalities, designed *in vivo* treatment regimens to assess ability of targeted therapies to intercept cancer development and progression. Designed vaccine based treatment regimen in combination with immunomodulatory agents that successfully delays cancer development in mouse models. Collected pre-clinical data served as basis for initiation of a multi-center clinical trial. Has strong collaborative, leadership, and teaching skills exemplified by multiple peer-reviewed publications, several conference attendances, and many student mentees.

EDUCATION

THE JOHNS HOPKINS UNIVERSITY SCHOOL OF MEDICINE, Baltimore, MD
2012-present
PhD in Pharmacology and Molecular Sciences

UNIVERSITY OF CALIFORNIA LOS ANGELES, Los Angeles, CA
2003-2007
B.S. in Biochemistry

RESEARCH EXPERIENCE

PhD CANDIDATE: Sidney Kimmel Comprehensive Cancer Center
Jan. 2013-present
Johns Hopkins University School of Medicine, Baltimore, MD

P.I: Dr. Elizabeth M. Jaffee, MD
Early interception of pancreatic ductal adenocarcinoma (PDA) by targeting the dynamic TME: modulation of novel miRNA targets and utilization of combination immunotherapy.

- Constructed a developmental miRNA profile of key dysregulated miRNAs over PDA progression utilizing Taqman OpenArrays miRNA microarray screen
- Established primary cell lines of PDA TME using fluorescence activated cell sorting (FACS) for *in vitro* functional studies. Performed subsequent phenotypic confirmation
- Examined endogenous spatial expression of key dysregulated miRNAs throughout early TME progression using miRNA fluorescence *in situ* hybridization (miR-FISH)
- Stably inhibited and overexpressed key miRNAs using lentiviral transduction of primary PDA TME cell populations to assess modulation of proliferative, migratory, and invasive capacities
- Constructed a profile of circulating miRNAs in serum to assess the potential of utilizing miRNAs as early diagnostic biomarkers for non-invasive PDA screening
- Designed and executed a vaccine regimen that targets driver mutation $Kras^{G12D}$ in combination with immunomodulatory agents that delays premalignant lesion progression in mice. A clinical trial has been initiated based on this pre-clinical data.
- Assess ability of combination immunotherapy to reprogram immune profiles using flow cytometry of tumor infiltrating lymphocytes

PhD CANDIDATE: Pharmacology and Molecular Sciences
Aug. 2012-Dec. 2012
Johns Hopkins University School of Medicine, Baltimore, MD
P.I: Dr. Jin Zhang, PhD
Developed various FRET-based indicators of activated transcription factors phosphorylated by Protein Kinase A (PKA)

- Developed three FRET biosensors to optimally detect transcription factor activation
- Utilized optimal FRET biosensor to validate the cAMP-PKA-Ca^{2+} oscillatory circuit critical in activating transcription factors
- Performed spatial-temporal imaging of cAMP-PKA-Ca^{2+} oscillatory circuit in MIN6 beta cells and HEK293 cells utilizing fluorescent imaging, construct generation, and cellular transfection

LABORATORY MANAGER: Center for Perinatal Biology
Jan. 2009-July 2012
Loma Linda University School of Medicine, Loma Linda, CA
P.I: Dr. Lawrence D. Longo, MD

Investigated the signal transduction mechanisms in smooth muscle cells that lead to cerebral arterial contraction in fetus and adult life utilizing a developmental sheep model

- Utilized various small molecule and pharmacological agonists (serotonin, phenylephrine, and PDBu) to dissect developmental differences in PKC-mediated contractility
- Elucidated the functional differences that α_1-adrenergic receptor subtypes have on myogenic tone due to maturation
- Investigated the affects that long-term hypoxia acclimatization has on the cellular pathways and tissue ultrastructure that are responsible for cerebral arterial contractility
- Managed the lab and trained several medical students, graduate students, technicians, and research fellows

RESEARCH ASSISTANT: Cedars-Sinai Division of Infectious Disease
Oct. 2007-Dec. 2008
Cedars-Sinai Medical Center, Los Angeles, CA
P.I: Dr. W. David Hardy, MD
Investigated the mechanisms of the recombinant foamy virus, which elucidated the functions of the analogous HIV retrovirus

- Quantified foamy viral message and protein expression levels of p24 antigen, an HIV-1 gag protein, in various cell lines
- Isolated and preserved peripheral blood mononuclear cells from HIV positive individuals for clinical trials performed at the University of California Davis
- Served as a translator between mandarin-speaking senior scientist and PI

PUBLICATIONS

1. Pelosof L, Yerram S, Armstrong T, **Chu N**, Danilova L, Yanagisawa B, Hidalgo M, Azad N, Herman JG. GPX3 promoter methylation predicts platinum sensitivity in colorectal cancer. *Epigenetics* 12(7):540-550 (2017)
2. **Chu NJ**, Armstrong TD, Jaffee EM. Nonviral oncogenic antigens and the inflammatory signals driving early cancer development as targets for cancer immunoprevention. *Clin Cancer Res* 21(7):1549-57 (2015)
3. Goyal R, Goyal D, **Chu N**, Van Wickle J, Longo LD. Cerebral artery alpha-1 AR subtypes: high altitude long-term acclimatization responses. *PLoS One* 9(11):e112784 (2014)
4. Goyal R, Henderson DA, **Chu N**, Longo LD. Ovine middle cerebral artery characterization and quantification of ultrastructure and other features: changes with development. *Am J Physiol Regul Integr Comp Physiol* 302(4):R433-45 (2012)
5. Goyal R, Mittal A, **Chu N**, Arthur RA, Zhang L, Longo LD. Maturation and long-term hypoxia-induced acclimatization responses in PKC-mediated

signaling pathways in ovine cerebral arterial contractility. *Am J Physiol Regul Integr Comp Physiol* 299(5):R1377-86 (2010)

6. Goyal R, Mittal A, **Chu N**, Zhang L, Longo LD. alpha(1)-Adrenergic receptor subtype function in fetal and adult cerebral arteries. *Am J Physiol Heart Circ Physiol* 298(6):H1797-806 (2010)
7. Goyal R, Mittal A, **Chu N**, Shi L, Zhang L, Longo LD. Maturation and the role of PKC-mediated contractility in ovine cerebral arteries. *Am J Physiol Heart Circ Physiol* 297(6):H2242-52 (2009)

MANUSCRIPTS IN PROGRESS

1. **Chu NJ**, Anders R, Cao M, Jaffee EM. Novel miRNA regulation in an early progression model of pancreatic ductal adenocarcinoma.
   Status: In preparation
2. **Chu NJ**, Popovic A, Anders R, Thompson E, Armstrong TD, Jaffee EM. Combination immunotherapy intercepts murine pancreatic cancer progression.
   Status: In preparation
3. **Chu NJ**, Cao M, Anders R, Jaffee EM. Serum miRNA signatures for the early detection of premalignant lesions in a developmental model of pancreatic ductal adenocarcinoma.
   Status: In preparation

HONORS AND AWARDS

WOMEN IN CANCER RESEARCH SCHOLAR AWARD
April 2018
American Association for Cancer Research Annual Meeting 2018, Chicago, IL

1ST PLACE WINNER, BASIC RESEARCH CATEGORY
SKCCC Fellow Research Day
May 2017
Sidney Kimmel Comprehensive Cancer Center, Baltimore, MD

YOUNG INVESTIGATOR TRAVEL FELLOWSHIP AWARD
Oct. 2014
Symposia on Cancer Research 2014, Illuminating Genomic Dark Matter “ncRNA in Disease and Cancer” MD Anderson Cancer Center, Houston, TX

PRESENTATIONS AND CONFERENCES

1. Oral Presentation: American Association for Cancer Research Annual Meeting 2018. April 2018. Chicago, IL

Chu NJ, Jaffee EM. Novel miRNA regulation in an early progression model of pancreatic ductal adenocarcinoma.

2. Poster: Keystone Symposia Cancer Immunotherapy: Combinations (C5). March 2018. Montreal, Québec Canada
   Chu NJ, Jaffee EM. Novel miRNA regulation in an early progression model of pancreatic ductal adenocarcinoma.
3. Poster: Bloomberg-Kimmel Institute for Cancer Immunotherapy Scientific Retreat. June 2017. Baltimore, MD
   Chu NJ, Armstrong TD, Jaffee EM. Novel miRNA regulation in an early progression model of pancreatic ductal adenocarcinoma.
4. Poster: SKCCC Fellow Research Day. May 2017. Baltimore, MD
   Chu NJ, Armstrong TD, Jaffee EM. Novel miRNA regulation in an early progression model of pancreatic ductal adenocarcinoma.
5. Poster: American Association for Cancer Research Annual Meeting 2017. April 2017. Washington, DC
   Chu NJ, Armstrong TD, Jaffee EM. Novel miRNA regulation in an early progression model of PDA.
6. Poster: Keystone Symposia Tumor Immunology: Multidisciplinary Science Driving Combination Therapy (J7). Feb. 2015. Banff, Alberta Canada
   Chu NJ, Armstrong TD, Jaffee EM. Novel miRNA regulation in an early progression model of PDA.
7. Poster: MD Anderson Cancer Center Symposia on Cancer Research 2014: Illuminating Genomic Dark Matter “ncRNA in Disease and Cancer” Oct. 2014. Houston, TX
   Chu NJ, Armstrong TD, Jaffee EM. Novel miRNA Regulation in an Early Progression Model of PDA.
8. Poster: Experimental Biology 2010. April 2010. Anaheim, CA
   Chu N, Goyal R, Goyal D, Longo LD. Maturation and Differential Role of PKC Isoforms in Serotonergic and Phorbol Ester-mediated Cerebral Artery Contractility.

PROFESSIONAL AFFILIATIONS

American Association for the Advancement of Science
American Association for Cancer Research
Women in Cancer Research

LEADERSHIP EXPERIENCE

FOUNDING MEMBER: Pharmacology Student Initiative March 2015-present
Johns Hopkins University School of Medicine, Pharmacology Department, Baltimore, MD

- Leads a student-run departmental organization that aims to: enhance student-faculty relations, facilitate better student camaraderie, increase

student involvement in departmental events, represent pharmacology student interests to the faculty and vice-versa
- Lead annual departmental recruitment resulting in 60-70% confirmation of desired applicants within 5 days of admission offer
- Organized, executed, and publicized departmental social events, annual departmental retreat, new-student orientation, professional development workshops, alumni events, diversity initiatives, community service opportunities, and student forums

COUNSELOR: UCLA Unicamp Jan. 2007-July 2007
University of California Los Angeles, Los Angeles, CA
- Mentored 13-year-old girls from low-income families as part of UCLA Unicamp, the university's official student non-profit organization
- Led activities that emphasized responsibility, cooperation, and positivity with the goal of empowering children at UCLA's outdoor summer camp
- Fundraised to provide all costs of attending camp for both my campers and myself

MEMBER: Bruin Leaders Project Sept. 2003-June 2007
University of California Los Angeles, Los Angeles, CA
- Participated in this hands-on, seminar-based leadership development program that strives to make its participants better students, better leaders, and better citizens
- Engaged in programs that focused on social change, diversity, ethics, public speaking, and conflict management

COMMUNICATIONS COMMISSIONER: On Campus Housing Council
University of California Los Angeles, Los Angeles, CA Sept. 2004-June 2005
- Programmed, produced, and publicized events for all students living on campus
- Wrote monthly informational newsletters concerning campus wide events.
- Worked dynamically with a group of student leaders to represent the concerns of the student body to housing professionals and to serve as a liaison between on-campus housing and other UCLA entities.

AREAS OF EXPERTISE

- Molecular biology: construct generation, transfection, transformation, transduction, qPCR, western blot, monoclonal antibody production and purification
- Cellular/Tissue imaging and analysis: IF, FISH, IHC, multi-color flow cytometry, FACS, proliferation/migration/invasion assays, confocal microscopy, laser capture micro-dissection, pathological grading of

premalignant lesions and PDA tissue, fluorescent Ca^{2+} imaging, measurement and quantification of smooth muscle arterial contractility
- Establishment and maintenance of primary cell lines
- *In vivo* modeling: syngeneic mouse models, drug efficacy studies, drug formulations and dosing (PO, IP, IV, SC), blood and tissue collection, maintenance and propagation of mouse colonies
- Analysis and interpretation of microarray data
- Software: GraphPad Prism, ImageJ, ExpressionSuite, FlowJo, HALO, STATA, Microsoft Office
- Strong ability to work in a collaborative, dynamic, and multi-disciplinary environment